EXPERIENCE DEPENDENT CROSS-MODAL REGULATION OF CORTICAL CIRCUITRY

by

Emily Petrus

A dissertation submitted to Johns Hopkins University in conformity with the requirements for the degree of Doctor of Philosophy

Baltimore, MD

May, 2014

Abstract

Sensory experience is essential not only for the formation and maintenance of cortical circuits during development but also throughout life. Neural networks within the brain regulate activity based on experience, using both synapse specific (Hebbian) and global (homeostatic) mechanisms to achieve optimal signal processing without compromising their overall excitability. The loss of one sense can trigger compensation of spared sensory modalities, which is called cross-modal plasticity. These behavioral enhancements are realized through both Hebbian and homeostatic mechanisms to compensate for the loss of one sense, processing spared senses with heightened sensitivity via alterations in cortical circuit strengths. Specifically, spared cortex enhances the feed-forward signal arriving from the thalamus while deprived cortex remains unchanged, regardless of sensory modality. Loss of vision induces enhanced feed-forward signal propagation throughout layer 4 of auditory cortex and up to layer 2/3. In layer 2/3, Hebbian strengthening of feed-forward signals combine with homeostatic scaling down of spontaneous events and weakened lateral inputs to enhance the signal to noise ratio in auditory cortex after loss of sight. These changes in excitation are complemented by alterations in inhibitory transmission, with an increase in spontaneous event frequency in superficial layers, and an increase in parvalbumin mediated evoked inhibition in layer 4. An increase in spontaneous inhibitory synaptic transmission in layer 2/3 may dampen excitable inputs, allowing only the strong and salient signals to impact the network, while stronger evoked inhibition in layer 4 may serve to sharpen tuning as the signal arrives to auditory cortex. Both cross-modal and uni-modal (within the modality) plasticity require similar molecular mechanisms, as the scaling down of

spontaneous events in superficial auditory cortex is abolished without the presence of Arc, an activity regulated protein which is known to regulate synaptic AMPA receptor localization. Arc's involvement with activity regulated production of amyloid beta (Aβ) indicates that Aβ may play a role in normal physiological maintenance of homeostasis in the network. Here we observed an inability of visual cortex layer 2/3 neurons to homeostatically adapt to loss of vision in mice lacking the main enzyme necessary to produce Aβ. Together these results indicate that cross-modal and uni-modal plasticity may use similar molecular mechanisms to homeostatically adapt to changes in sensory environment. The brain's ability to undergo cross-modal regulation of synaptic strength in response to loss of a sensory modality extends well beyond the classical critical period, and in some cases may be more readily recruited after uni-modal sensory perturbations. The critical period may reflect an optimal balance of excitation and inhibition, which may be reopened throughout life to enable an organism to adapt to their surroundings.

Acknowledgements

I would like to thank my family for supporting me in this fantastic journey

In particular:

Ionel Petrus for his patience

Ginger Babcock, Randy Babcock and Ava Elicker for always stepping up so I can squeeze in a few more experiments

My brother Dale Babcock and son Gabriel Petrus and for reminding me of the joy of discovery

I would also like to thank my advisor Hey-Kyoung Lee for her unwavering support of my career, emotional stability, and making a healthy work-life balance possible. Thank you for being such a powerful role model.

Thank you to the Lee/Kirkwood lab members who helped to guide this project, especially my big sister Kaiwen He, who makes being brilliant look effortless!

Thanks to my committee members Patrick Kanold, Kristina Nielsen and Marshall Shuler for being so supportive and for all of your intellectual commentary.

Table of Contents

Chapter 1: Introduction

Outline:

1. Cortical Circuitry – Primary Sensory Cortex
    a. Thalamus and Cortex
    b. Cortex
        I. V1
        II. A1
2. Hebbian & Homeostatic Plasticity
    a. Experience Dependent Regulation of Excitatory Synapses
    b. Experience-dependent homeostatic adaptation of inhibitory synapses
    c. *In vivo* functions of experience-dependent homeostatic synaptic plasticity
3. Cross-modal Plasticity
    a. System's Level Adaptations
    b. Synaptic Circuit Changes
4. Conclusions

Introduction

Experience dictates not only developmental wiring of the central nervous system, but also the maintenance of these circuits throughout life. Synapse specific strengthening has long been studied as the cellular correlate of memory, as proposed by Donald Hebb (Hebb, 1949). This form of plasticity is balanced by homoeostatic plasticity, which is necessary to adjust the synaptic strengths of entire circuits in response to large scale changes in inputs (Turrigiano, 2008), which would serve to maintain homeostasis in a system. The study of synaptic plasticity has been largely focused on the critical period, a period of time during development which demonstrates heightened sensitivity of an organism or cortical circuit to changes in experience. Lack of experience can result in irreversible changes in sensory processing, hence the critical nature of this time period. We and others have re-examined the notion of an aplastic adult brain, which is resistant to alterations after the prescribed critical period. Instead of the time in life being vital to dictating plasticity, other factors may come into play, such as the balance of excitation

and inhibition (Hensch, 2005). In addition, an organism may alter specific synaptic components of a circuit in response to the current sensory requirements, which may be mediated by attention or neuromodulators (Jitsuki et al., 2011). Each step in primary sensory cortex has unique processing functions which help the organism interpret sensory experience (Douglas and Martin, 2004). In the case of cross-modal plasticity, the loss of one sense results in functional enhancements of the remaining senses (Bavelier and Neville, 2002). Altering synaptic strengths within a cortical circuit depending on experience but also the organism's requirements may mediate the enhancement of spared senses after the loss of one sensory modality.

The goal of this project was to elucidate the effects of sensory deprivation on deprived but also spared sensory cortex. An investigation into how cortical circuits and synaptic strengths were altered in spared cortex allowed for a potential mechanism behind the observed enhancement of spared senses in cross-modal plasticity. The effects were experience dependent and age independent, thus we have provided insight into how cortex can be re-wired in a homeostatic and synapse specific way throughout life.

1. Cortical Circuitry – Primary Sensory Cortex

Sensory cortex is characterized as having 6 layers of morphologically distinct cell types, each of which plays a unique role in afferent and efferent sensory processing. Within each layer and between sensory cortices there is some variability, but from the first attempts to characterize the cortex (Economo, 1927), it was observed that at least this laminar organization was constant between areas (Creutzfeldt, 1977). Layer 1 is characterized as being close to the pia (external surface) of the brain, while layer 6 is

located near the white matter on the inner-most region of cortex. The location of cell bodies dictates their dendritic distribution, and thus what information they receive. Primary sensory cortex receives inputs from thalamus and then sends information out to higher order sensory cortices (for example, from V1 to V2, V4 etc.), but this first cortical input step for sensory information also does quite a bit of processing within itself. In addition, the reciprocal connections it maintains with subcortical and thalamic nuclei help further modify sensory signals.

a. Thalamus and Cortex

Thalamus to Cortex

Much of what is known about canonical cortical circuitry comes from exhaustive studies of primary visual cortex (V1), originally performed in cats (Hubel, 1963; Creutzfeldt, 1977). Most primary sensory cortical areas such as V1 and primary auditory cortex (A1), receive monosynaptic excitatory inputs from thalamocortical (TC) projections, originate from their specific "relay" nuclei. These provide strong feed-forward excitatory inputs to layer 4 (L4) cortical cells, which drive processing of sensory information. Many cortical and thalamic areas preserve an organized representation of the external world. For example in the visual system, retinotopy is seen in both the primary visual thalamic nucleus, the dorsal lateral geniculate nucleus (dLGN), and also in V1 (Hubel and Wiesel, 1970; Kaas et al., 1972; Kaas, 1997). Similarly, tonotopy has been observed in cat auditory thalamus, the medial geniculate body (MGB), (Reale and Imig, 1980; Imig and Morel, 1985) and also loosely in A1 (Rose and Woolsey, 1949; Reale and

Imig, 1980; Morel et al., 1993; Kaas and Hackett, 2000). Whisker inputs first arrive to thalamic barreloids located in the ventrobasal complex (Simons and Carvell, 1989), and then pass information to primary somatosensory cortex (S1). Once in S1 inputs arrange into a barrel field representation of rodent whiskers, with one whisker corresponding to one "barrel" of neurons (Woolsey and Van der Loos, 1970; Kerr et al., 2007). External representations mapped onto sensory thalamic nuclei and cortical structures indicate that neural networks may be constructed to process incoming information in an organized fashion.

Cortex to Thalamus

Layer 6 (L6) pyramidal cells and inter-neurons also receive direct but weaker TC projections, which is part of the cortico-thalamic feedback loop (Singer et al., 1975; Ito et al., 1977; Zarrinpar and Callaway, 2006). L6 sends reciprocal projections back to the thalamus (Sherman and Koch 1986), which target primary thalamic nuclei, the thalamic reticular complex and higher order thalamic nuclei (Bourassa and Deschenes, 1995). In addition, higher order thalamic nuclei receive cortical inputs from layer 5 (L5), which may play a role in cortico-thalamo-cortical connections (Guillery, 1995). These feedback projections from L6 may be involved in modulating thalamic processing of sensory input (McClurkin and Marrocco, 1984; Marrocco et al., 1996; de Labra et al., 2007; Briggs and Usrey, 2009) and may enhance visual processing in the case of the LGN (Murphy, 1999; Thomson, 2010).

Higher order (or association) thalamic nuclei, such as the visual pulvinar, also play an important role in TC sensory processing. These nuclei do not receive direct

afferent sensory inputs; their inputs arrive from L5 (and also L6) of primary sensory cortex (Abramson and Chalupa, 1985; Ojima, 1994; Bourassa and Deschenes, 1995). These cortical inputs drive the response properties of these associative nuclei, as cortical inactivation results in a loss of response to sensory stimuli (Bender, 1983; Diamond et al., 1992). These nuclei have been implicated in multi-sensory integration, as their efferents project to secondary sensory cortices (Guillery, 1995). Other thalamic areas are involved in multisensory integration, for example the visual superior colliculus projects to supragranular (SG) nucleus, which then projects to secondary auditory areas (Kimura et al., 2003). This provides an anatomical pathway to integrate audio/visual inputs; in fact, the dMGB and SG integrate visual information in reward based learning tasks (Komura et al., 2001). It is apparent that the thalamus and cortex co-operate to process both uni and multimodal sensation, thus these projections do not merely "relay" the information, but further process it along the way.

b. Cortex

Although there are many similarities between the visual and auditory cortical areas, there are many key differences in how these sensory cortices process information. This is most likely due to differences in peripheral sensory organs, the type of incoming information (i.e. frequency or intensity differences), and what this information means to the organism. In a canonical circuit of primary sensory cortex, information arrives from the periphery via the thalamus, which sends excitatory inputs to L4. The TC inputs to L4 are segregated into columns or groups of neurons which are linked by similar response

characteristics to specific sensory properties (Mountcastle, 1957; Hubel, 1963), which is preserved in the feed-forward projections to L2/3. L4 neurons form strong feed-forward synapses onto neurons in layer 2/3 (L2/3), but also have dense recurrent excitatory synapses within L4, which may be one way the less numerous TC inputs drive activity in cortex.

In sensory cortex, L2/3 neurons receive strong excitatory feed-forward projections from L4. Once information arrives to L2/3, short and long range lateral processing occurs before information is sent to "higher" cortical areas, where sensation and past experience combines to enhance the perception of sensory experience (Douglas and Martin, 2004). In this way, each of the cortical layers are important for interpreting sensory signals arriving to the first stage of cortical processing. This is a general description of canonical cortical circuits; however the unique features of V1 and A1 are described in detail below.

I. Visual Cortex (V1)

Cats and primates have well established V1 organization which is thought to enhance visual information processing by grouping like-afferents together into orientation and ocular dominance columns (Casagrande and Kaas, 1994; Ohki et al., 2006). Rodents have less complex segregations of visual cortex, with one large monocular and a smaller binocular area per hemisphere. The monocular zone receives input from the contralateral eye, while a large portion of the binocular area is devoted to the area in front of the animal where the eyes' visual fields overlap (Adams and Forrester,

1968). Despite their differences, both rodent and higher order mammals have provided much insight into how V1 organization shapes visual function.

Thalamic inputs to V1

V1 L4 neurons receive strong feed-forward excitatory input from the lateral geniculate nucleus (LGN), the visual thalamus. These inputs represent less than 10% of excitatory synaptic input (Ahmed et al., 1994), yet play a dominant role in driving cortical responses. TC synapses do not appear to be significantly stronger than other excitatory synapses; rather, LGN's ability to drive cortical responses may lie in the strong recurrent lateral excitatory connections between L4 neurons (Douglas et al., 1989).

Layer 4

Spiny stellate cells dominate L4 in V1 of primates and carnivores, and are thus named from their star-like appearance. They confine their dendritic arbor within L4, which allows these neurons to specialize in the reception of TC and within L4 inputs (Gilbert, 1983; Callaway, 1998). Cat V1 L4 is also home to pyramidal neurons (Smith and Populin, 2001), which are also present in rodent V1 L4. L4 of rodent S1 contains a majority (58%) of spiny stellate cells, but is also home to 25% star pyramids and 17% pyramidal neurons (Staiger et al., 2004), so the variety of cell types in rodent V1 L4 may also reflect this diversity, although an extensive within cortical area analysis has not yet been performed in rodent V1. Most L4 neurons in V1 have simple receptive fields (RFs) which help guide orientation selectivity (Gilbert and Wiesel T.N., 1979), which result from the preceding thalamic inputs to this layer (Miller et al., 2001a). Lateral inputs between V1 L4 neurons have recently been shown with glutamate uncaging, but may

include some connections from L4 to deep L3 and superficial L5 (Callaway, 2003). Cells in V1 L4 also receive information from long range lateral inputs within L4 and from L6, which may aid the cortex in orientation selectivity tuning at least in cat V1 (Ahmed et al., 1994; Douglas et al., 1995; Somers et al., 1995). The recurrent excitatory loop in V1 L4 can create a larger response through amplification (Douglas et al., 1989), which in cat occurs within 1 mm from the recipient neuron (Douglas et al., 1995). Proximal excitatory connections between cat V1 L4 cells occur between cells with similar orientation selectivity, while long range lateral excitatory connections link iso and hetero-tuned cells (Crook et al., 1998; Yousef et al., 1999), so a simple "like connects to like" model is not the only way to characterize these networks.

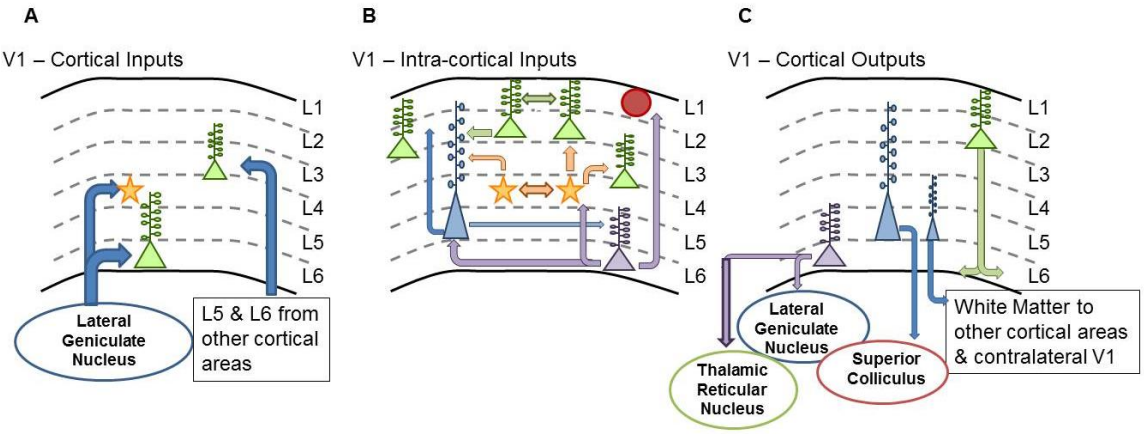

Figure 1.1: Primary visual cortex (V1) excitatory connectivity with afferents **A**, intracortical connections **B**, and efferents **C**. Citations for **A**: Ito et al. 1977, Singer et al. 1975, Zarrinpar & Callaway 1995, Ahmed et al. 1994, Rockland & Pandya 1989, **B**: Callaway et al. 2002, Douglas & Martin 2004, Miller et al. 2001, Burkhalter et al. 1989, Gilbert & Wiesel 1979, Lund et al. 1979, Ferrer et al. 1986, **C**: Sherman & Koch 1986, Bourassa & Desches 1995, Briggs & Usrey 2009, Hallman et al. 1988.

Thus L4 neurons seem to be primarily tasked with receiving TC inputs, but they also do a fair amount of processing between neighbors. The most extensively studied lateral inputs in V1 occur in L2/3, the next step up in the cortical processing pathway.

Layer 2/3

Excitatory neurons in L2/3 are characterized as being pyramidal in shape with apical dendrites pointing toward the pia and a vertical axon projecting downward in the direction of the white matter (Gilbert, 1983). V1 L2/3 neurons receive strong feed forward excitatory input from L4 neurons, but lateral connections represent the numerical majority of inputs (Binzegger et al., 2004; Douglas and Martin, 2004). Superficial injections of tracers depict a "patchy" type of connectivity in cat and macaque V1, demonstrating that lateral connections are grouped together (Gilbert and Wiesel, 1989; Lund et al., 1993), although this pattern is not consistently observed in rats (Burkhalter, 1989; Burkhalter and Charles, 1990). These anatomical connections likely have a physiological relevance, as the connected patches have reciprocal connections (Livingstone and Hubel, 1984), co-tuned orientation (Yoshioka et al., 1996) and ocular dominance preference (Malach et al., 1993). One possible function of the L2/3 lateral connections within V1 would be to form excitatory connections onto local inhibitory networks of hetero-tuned columns (Fitzpatrick, 2000). By linking superficial V1 layers, groups of neurons could work together to integrate contextual information, which would then facilitate their responses to important stimuli. V1 L2/3 neurons also have long range lateral connections to cortical areas outside of V1, which terminate in L4 (Gilbert and Wiesel, 1983). Feedback lateral connections arriving to L2/3 originate in L5 and L6 of distant cortical areas (Rockland and Pandya, 1979). These long range lateral connections are thought to play a role in integrating contextual information from other cortical areas, which would help in visual processing, although their exact functions remain to be proven (Douglas and Martin, 2004).

Layers 5 & 6

L5 receives processed intracortical inputs from L2/3. L5 neurons are characterized as having large somas and a long apical dendrite with tufts at the pia (Gilbert and Wiesel T.N., 1979). These larger neurons with tufted dendrites in L1 are thought to project to the superior colliculus, while smaller L5 neurons with shorter non-tufted apical dendrites are thought to project to contralateral V1 (Hallman et al., 1988). Layer 5 also sends outputs to L2/3 and L6 (Lund et al., 1993). These widespread connections and morphological variety indicate that L5 neurons may have multiple functions in cortico-cortical and cortico-thalamic communication.

L6 contains a broad array of cell types, inputs and outputs. L6 excitatory neurons have been broadly grouped into short and tall neuron types, which target L4 and L1 + L5, respectively (Ferrer et al., 1986). Tall L6 cells also project laterally to other L6 neurons (Ferrer et al., 1986). Because L6 neurons receive TC inputs, but also intracortical inputs (Burkhalter, 1989; Binzegger et al., 2004; Zarrinpar and Callaway, 2006), and send outputs back to the LGN, thalamic reticular nucleus (Bourassa and Deschenes, 1995), other L6 neurons (Katz, 1987) and L4 neurons, they are situated to play a major role in cortical and thalamocortical processing (Briggs, 2010).

Inhibition in V1

The diversity of GABAergic neurons has long been a subject of intense interest, with many distinct varieties in the cortex (Kawaguchi and Kubota, 1997; Chang et al., 2010). These neurons differ morphologically, biochemically and electrophysiologically. Interneurons can be categorized by shape: basket cells, chandelier cells, and Martinotti

cells, by biochemical marker expression: parvalbumin, somatostatin, vasoactive intestinal peptide, or electrophysiological characteristics: fast spiking, regular spiking (Kawaguchi and Kubota, 1997; Issacson and Scanziani, 2012). One study in macaque area 17 (V1) revealed that only 14% of GABAergic neurons are calretenin positive, implying parvalbumin positive neurons represent the majority (Meskenaite, 1997). A recent study demonstrated an organized connectivity pattern between three of the most prevalent interneurons in mice, which demonstrates that although interneurons in V1 are many and varied, they have specific targets which may influence inhibitory tuning in V1 (Pfeffer et al., 2013).

Feed-forward excitation from the thalamus is considered a dominant excitatory input, but inhibition driven by TC inputs (feed-forward inhibition) can shut down V1 L4 neurons when electrical stimulation is applied to LGN, which simultaneously activates both excitation and inhibition (Ferster and Jagadeesh, 1992). Feed-forward processing to L4 via the LGN plays a large role in orientation preference, as cooling visual cortex yields smaller but identical tuning (Ferster et al., 1996). However, lateral inhibition in V1 L4 plays a critical role in shaping responses and regulating their output to higher cortical layers (Miller et al., 2001a). For example, when inhibition is temporarily silenced, cells in cat V1 L4 have broader orientation tuning (Crook and Eysel, 1992). Sharpening of L4 receptive fields may be mediated by feed-forward inhibition (Krukowski and Miller, 2001) and antiphase inhibition (Troyer et al., 1998), which involves inhibition of neurons responding to opposite phase, but increased excitation of neurons tuned to the same phase (Miller et al., 2001a). In sum, L4 of V1 receives a

strong feed forward excitatory and inhibitory input, which plays a large role in orientation selectivity at this first cortical processing step.

Inhibition is known to sharpen receptive fields in within V1. For example, inhibitory neurons receive feed-forward (FF) excitatory inputs which are co-tuned to local excitatory neurons (Buzsaki, 1984; Liu et al., 2010). Lateral inhibition has been proposed to strongly influence tuning in the organized columnar cat V1 (Adesnik and Scanziani, 2010), but rodent networks are hypothesized to experience this on the single-cell level, as precise retinotopy is less obvious (Ohki et al., 2005). Additionally, although inhibition and excitation are co-tuned to stimulus, the broader tuning of inhibitory interneurons contributes to narrower tuning of excitatory neuronal responses. The tuning of interneurons may be a result of their local network; for example, co-tuned GABAergic and excitatory neurons can be found in homogenous systems such as cat V1 L4 where neurons have similar response characteristics as their neighbors (Cardin et al., 2007), while more broadly tuned inhibitory neurons can be found in more heterogeneous cortical areas such as mouse V1 L2/3 (Liu et al., 2009; Kameyama et al., 2010). Finally, inhibition consistently registers onto excitatory neurons with a synaptic delay of a few milliseconds (Liu et al., 2010). This creates a window of excitatory opportunity for neurons to integrate excitatory inputs and produce spike outputs (Pouille and Scanziani, 2001).

Inhibition levels are thought to regulate the critical period throughout cortical areas, but perhaps the most studied is the influence of inhibition on ocular dominance plasticity (ODP) (Hensch, 2005; Sale et al., 2010). As age and visual experience progress, inhibition is thought to mature gradually until reaching a plateau, which stops

ocular dominance plasticity and signals the end of the critical period. New evidence suggests that by altering the balance of excitation and inhibition in V1, ODP and other forms of plasticity can be re-activated. For example, environmental enrichment results in a reduction of GABAergic transmission, which may mediate the observed recovery of ODP, visual acuity and recruitment of LTP from white matter to L2/3 (Sale et al., 2007). Similar results were seen with pharmacological blockade of GABA via picrotoxin, which restored ODP after monocular deprivation, and again rescued LTP from white matter to L2/3 (Harauzov et al., 2010). Finally, dark exposure (DE) has been shown to reduce GABAergic transmission in adult V1 (Morales et al., 2002), which can help recover ODP (He et al., 2006, 2007), which may be mediated by various neuromodulators (Huang et al., 1999; Jiang et al., 2010). Although some of these parameters may be specific to V1 or ODP, overall these results demonstrate the importance of inhibition in regulating cortical plasticity beyond the critical period.

II. Auditory Cortex (A1)

Sounds are characterized by their frequency and intensity, making auditory signals and the neurons that encode this information largely concerned with the time domain. Neurons in A1 are usually tuned to specific frequencies and sound intensity, and are organized tonotopically reflecting the cochlear representation in mouse (Stiebler et al., 1997), rat (Horikawa et al. 1998), cat (Merzenich and Linn, 1975), and primates including humans (Merzenich and Brugge, 1973; Formisano et al., 2003). This broad scale tonotopy has recently been challenged when experimenters use finer scale techniques such as *in vivo* 2-photon calcium imaging (Bandyopadhyay et al., 2010; Castro and Kandler, 2010), but at least on the broad scale, tonotopy is preserved through

the ascending pathway to A1. Like other cortical areas, auditory cortical neurons are organized into columns which enable simultaneous serial and parallel processing (Schreiner et al., 2000; Winer et al., 2005).

Thalamic inputs to A1

Auditory thalamus has strong excitatory projections to L4 (Romanski and LeDoux, 1993), with weaker innervation arriving to L6 in parallel (Cruikshank et al., 2002; Barbour and Callaway, 2008), and interestingly also sends projections of unknown function to layer 1 (Mitani et al., 1985; Huang and Winer, 2000). The ventral medial geniculate body (vMGB) projects preferentially to L4 and lower L3 of A1, while the dorsal MGB projects to secondary auditory areas (Smith et al., 2012). One interesting aspect of auditory thalamocortical (TC) projections is the temporal slowing of auditory signal, which about halves the followed frequency fidelity between thalamic and A1 neurons (Miller et al., 2002). Combined with the fact that thalamic neurons are more broadly tuned than A1 L4 neurons (Miller et al., 2001b), these facts indicate that there is substantial TC signal transformation occurring between these synaptic connections.

Layer 4

The diversity of A1 L4 neurons has been studied in great detail. A1 L4 is home to small, medium and large vertically projecting tufted neurons, spiny stellate neurons, bipolar neurons and double bouquet neurons, most of which project intracortically within columns but presumably not to other cortical areas (Winer, 1984). Winer et al. did not observe many pyramidal neurons but others do report their presence in cat A1, although

they represent a minority of excitatory neurons (Smith and Populin, 2001). L4 neurons have multiple maps which overlay each other, and serve to integrate intensity threshold, binaural interaction, onset latency, spectral integration and cochleotopy (Schreiner et al., 2000). A1 L4 neurons respond to characteristic frequencies (CFs) dictated initially by their TC afferents, however the sharpening of their tuning may be mediated by excitatory and inhibitory intracortical inputs (Suga et al., 1997; Liu et al., 2007). Others have proposed that this may be accomplished by linearly amplifying the excitatory TC inputs. This is supported by the fact that CF responses remain unchanged when the cortex is inhibited by optogenetic activation of PV^+ neurons in A1 (Li et al., 2013).

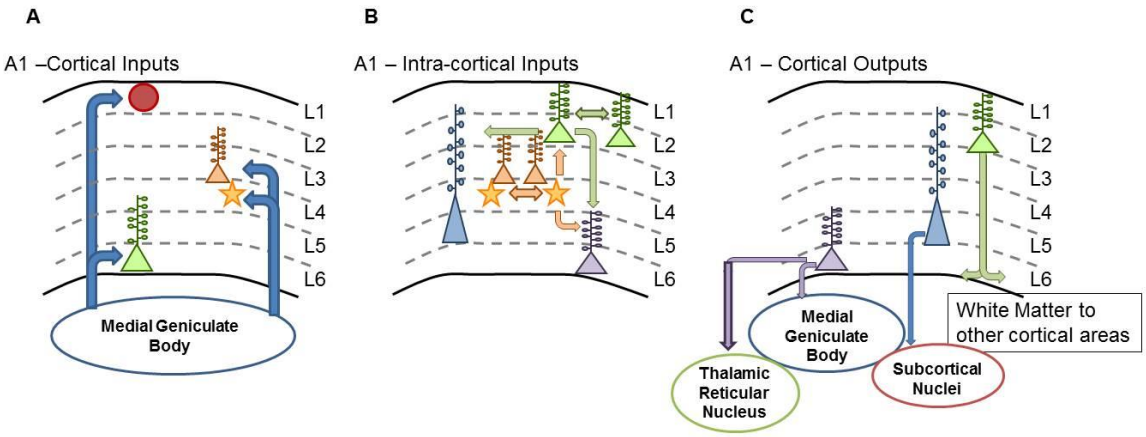

Figure 1.2: Primary auditory cortex (A1) excitatory connectivity with afferents (**A**), within the circuit (**B**), and efferents (**C**). Citations for **A**: Mitani et al. 1985, Huang & Winer 2000, Barbour & Callaway 2008, **B**: Lund et al. 1993, Read et al. 2001, Winer & Prieto 2001, Ojima et al. 1994, **C**: Barbour & Callaway 2008, Winer & Prieto 2001, Ojima et al. 1991.

Layer 2/3

L4 sends strong feed-forward projections to pyramidal neurons in L2/3, which transmit auditory signals to other cortical areas via lateral projections from L2/3 cells, and occasionally through L5a pyramidal cells (Lund et al., 1993). L2/3 lateral

projections are aligned by frequency, which link columns aligned to other similar functions, such as spectral bandwidth (Read et al., 2001), which may be useful for sound processing relevant to the organism. These superficial lateral connections have also been shown to have different connection probabilities, which also may play a role in processing different aspects of sound (Atzori et al., 2001). Recently, it has been shown that supragranular neurons in A1 have a heterogeneous tonotopy (Bandyopadhyay et al., 2010), but also respond differently depending on the sound characteristics, combining suprathreshold spiking with subthreshold inputs (Chen et al., 2011). This represents a unique characteristic of L2/3 neurons in A1, which may be responding to long range projections carrying multiple frequency inputs (Schreiner et al., 2012).

Layers 5 & 6

Layer 5 pyramidal neurons are large and have long apical dendrites, which receive integrated signals from L2/3. This layer's output is thought to modulate subcortical nuclei activity (Winer and Prieto, 2001). L6 receives direct thalamic innervation, but also cortical excitatory input. This means L6 is in an optimal position to integrate TC and intracortical (IC) inputs, so that when it provides feedback connections to the thalamus (Villa et al., 1991) it represents an integrated signal of global A1 function (Ojima, 1994; Prieto and Winer, 1999). These cortico-thalamic projections from L6 to MGB are hypothesized to gate auditory plasticity, yet most L6 neurons are not directly activated by auditory stimuli (Tsumoto and Suda, 1980); in fact, auditory stimuli suppresses spiking in L6 (Zhou et al., 2010). This may be due to the fact that although also disynaptic, inhibition in L6 is driven by the thalamus with shorter latencies than the excitation from L4 and within L6. This latency would ensure that excitation arrives post-

inhibition, which would allow L6 output only when TC driven inhibition is reduced (Zhou et al., 2010). The roles L5 and L6 neurons play in auditory processing are complex and important. Because they both play a role in providing feedback to thalamus and subthalamic nuclei, obviously these neurons are important for modulating auditory stimuli as it arrives to A1, which then will produce effects further along in the processing stream.

Inhibition in A1

Studying inhibition has long been a complicated field for many reasons. Inhibitory neurons have a wide variety of subtypes which vary morphologically and biochemically in other parts of neocortex (Gonchar and Burkhalter, 1997; Gupta, 2000). This wide variety indicates that these neurons have multiple roles in balancing and gating cortical output. Traditionally, excitation and inhibition are thought to balance each other, or at least respond similarly to auditory stimuli (Mariño et al., 2005). For example, A1 L4 neurons receive IC and TC excitation, but also IC inhibition. These inhibitory neurons innervate L4 and are driven by excitatory TC inputs, which results in co-activation of L4 excitatory and inhibitory cells. Inhibition arrives with a small delay of 2-4 ms (Wu et al., 2006), but has similar receptive fields (Wehr and Zador, 2003; Zhang et al., 2003) and amplitude responses (Wehr and Zador, 2003). A balanced excitatory/inhibitory system is integral in cortical processing, however the timing of inhibition and broader tuning may have an even bigger role in sharpening frequency tuning and allowing only the strongest signals to pass (Tan et al., 2007; Wu et al., 2008). For example, A1 inhibitory neurons are known to have broader tuning to characteristic frequency (Tan et al., 2012), which generates an "iceberg effect", favoring inhibition in

all areas except at the point of the tuning curve, where excitation is visible as the tip of this iceberg (Wu et al., 2011a). This broader tuning of inhibition may be in part thanks to the heterogenous nature of neuron placement in A1 (Bandyopadhyay et al., 2010; Rothschild et al., 2010), as inhibitory neurons may receive a wide variety of excitatory inputs.

Unique Features of A1

Many of these aspects of A1 circuitry are conserved throughout other sensory cortices; however there are a few unique features of A1, which represent a divergence from what is usually observed in V1. One unique property of auditory inputs arriving to A1 is that information arising from two ears integrates at the subcortical nuclei and thus is binaural in nature. In contrast, V1 usually represents the first step in binocular convergence of inputs from each eye. This difference may reflect the very nature of auditory input, such that spatial information is processed differently than temporal characteristics in auditory processing (Clarey et al. 1992, Ehret, 1997). A unique connectivity observed in A1 is the feedback projections from L2/3 to L4 neurons, which then can send out long range projections to other cortical areas (Barbour and Callaway, 2008). Perhaps most importantly, differences in inhibitory synaptic physiology in A1 have been documented, including faster inhibitory response kinetics (Hefti and Smith, 2003) and a novel neuron type which displays strong outward rectification after initial spiking, which halts future spiking (Metherate and Aramakis, 1999). Because sound occurs on the microsecond timescale (Carr, 1993), audition may require faster inhibitory responses than vision (Karmarkar and Buonomano, 2007).

A1 circuitry has many unique characteristics, likely a consequence of specializations particular to processing sound stimuli. Although unique aspects exist, it is important to recognize that A1 does share many similarities to other sensory cortices. These similarities are not just morphological, but can be at the level of functional processing of sensory inputs. It has been shown that rewiring auditory TC pathways together with retinal inputs (Sur et al., 1986; Angelucci et al., 1998) can cause A1 neurons to process visual information in a manner similar to their processing in V1. This processing includes direction selectivity, simple/complex RFs, and orientation tuning (Roe et al., 1990; Sharma et al., 2000). These examples demonstrate the ever plastic nature of the brain. In the absence of their main inputs, sensory cortices can be used to process other sensory information. In the next subsection, I will discuss different types of synaptic plasticity mechanisms that can alter cortical circuits with changes in sensory experience.

2. Hebbian and Homeostatic Plasticity

** Components of this subsection are reproduced with journal's permission: (Whitt et al., 2013)

Hebbian plasticity, such as long-term potentiation (LTP) and long-term depression (LTD), is essential to strengthen or weaken specific connections within neuronal circuits to store information as relative differences in the gain between competing inputs. However, for proper functioning of the nervous system neuronal firing must be maintained within a desired "target range" of activity, but Hebbian plasticity

alone is insufficient to provide such stability. To the contrary, Hebbian plasticity has an innate positive feedback, which destabilizes neural firing. For example, LTP of inputs would increase the firing of the postsynaptic neuron, which could further potentiate other inputs to the cell by increasing the probability of pre- and postsynaptic spike correlation. Therefore, there has to be additional mechanism(s) in place that can provide stability to neuronal firing. This ensures that neurons remain flexible and plastic to changing inputs, but also maintain a physiologically relevant range of firing to avoid excitotoxicity caused by hyperexcitability and to prevent the loss of valuable information after a sustained period of quiescence. The term "homeostatic plasticity" is used to describe changes that allow neurons to adjust their activity and compensate for prolonged periods of increased or decreased input activity. There are several ways in which cortical neurons can stabilize their own activity in response to prolonged changes in incoming signals, including altering their intrinsic excitability or changing the relative strength of excitatory and inhibitory inputs [reviewed in (Turrigiano and Nelson, 2004)] as well as adapting their plasticity mechanisms in accordance to the "sliding threshold" model (Bienenstock et al., 1982; Bear et al., 1987; Bear, 1995). Homeostatic plasticity allows for the adjustment of overall neuronal activity while preserving the relative strength of individual synapses, and therefore is particularly important to maintain physiological functions in situations of chronic alterations in neuronal drive, as would happen with the loss of a sensory modality or when changes in network activity are triggered by various neurological conditions. In this review, we will focus on experience-driven homeostatic changes that occur in sensory cortical areas. It is especially critical for the sensory cortices to adequately adapt

to prolonged periods of sensory deprivation or overstimulation because it impacts the organism's ability to survive in a changing environment.

a. Experience-dependent homeostatic regulation of excitatory synapses

Homeostatic plasticity was initially demonstrated *in vitro* as a scaling of quantal amplitude of α-amino-3-hydroxy-5-methyl-4-isoxazolepropionic acid receptor (AMPAR)-mediated synaptic responses to alterations in activity of cultured neurons, such that chronic inactivity produces larger miniature excitatory postsynaptic currents (mEPSCs) while a prolonged increase in activity decreases the amplitude of mEPSCs (O'Brien et al., 1998; Turrigiano et al., 1998). Since this initial proposal of a mechanism by which neurons homeostatically regulate activity, numerous studies have followed up to examine the molecular mechanisms as well as *in vivo* counterparts [reviewed in (Turrigiano, 2008; Lee, 2012)]. One of the initial models used to demonstrate homeostatic synaptic plasticity *in vivo* is the visual cortex, which has long been used as a model for studying various forms of experience-dependent plasticity. To manipulate neural activity *in vivo* that can result in homeostatic adaptation of visual cortical neurons, various visual deprivation paradigms have been used including dark rearing (DR), dark exposure (DE), monocular or binocular lid suture, binocular enucleation, and monocular tetrodotoxin (TTX) injections. While all of these manipulations should alter incoming sensory information to V1 to a varying degree, their effects on cortical neurons vary. For example, several days of intraocular TTX injections, DR from birth, several days of DE,

or binocular enucleation all homeostatically scale up AMPAR-mEPSC amplitudes in V1 L2/3 pyramidal neurons (Desai et al., 2002; Goel et al., 2006, 2011; Goel and Lee, 2007; Gao et al., 2010; He et al., 2012), while lid suture either decreases (Maffei and Turrigiano, 2008) or does not change the average mEPSC amplitude (He et al., 2012) in the same neurons. These discrepancies probably result from the different sensory deprivation paradigms used. It is known that diffuse light penetrating through the eyelids produces some degree of cortical activation (Blais et al., 2008), which may prevent homeostatic plasticity or even produce LTD (Rittenhouse et al., 1999). Collectively the visual deprivation experiments suggest that a complete lack of visually driven cortical activity is needed to elicit homeostatic synaptic plasticity in L2/3 of V1.

It is pertinent to mention that monocular deprivation (MD) paradigms have traditionally been used in the context of studying Hebbian synaptic changes related to ocular dominance plasticity (ODP) (Hubel and Wiesel, 1970; Gordon and Styker, 1996; Sawtell et al., 2003; Frenkel and Bear, 2004). Specifically, MD using monocular lid suture initially decreases the strength of the closed eye inputs and later strengthens the open eye inputs to V1 neurons, phenomena which respectively mimic LTD and LTP (Rittenhouse et al., 1999; Sawtell et al., 2003; Frenkel and Bear, 2004; Yoon et al., 2009). Though the initial weakening of the deprived eye inputs may seem to contradict studies reporting homeostatic scaling up of mEPSCs following monocular deprivation paradigms, there are some key differences in experimental design when considering these findings. Studies reporting homeostatic scaling up of mEPSCs following MD were observed in the contralateral monocular zone of V1, which receives only the deprived eye inputs (Desai et al., 2002; Maffei et al., 2004; Maffei and Turrigiano, 2008). Furthermore,

these studies utilize intraocular TTX injection, which completely silences all retinal activity. Therefore, in these studies the postsynaptic neuron experiences a total reduction or absence of visually driven activity. It is also known that MD-induced weakening of the deprived eye inputs are far less effective with intraocular TTX-injection method of monocular inactivation than monocular lid suture or monocular blurring (Rittenhouse et al., 1999, 2006; Frenkel and Bear, 2004). It is of interest to note that while intraocular TTX injection can abolish all retinal activity (both visually-driven and spontaneous), it paradoxically produces rhythmic oscillatory firing of thalamic neurons in the lateral geniculate nucleus (LGN) (Linden et al., 2009). Furthermore, intraocular TTX injection increases, while monocular lid suture decreases, the correlative firing between two LGN neurons when compared to recordings from normal controls (Linden et al., 2009). Therefore, the quality and pattern of neural activity arriving to V1 likely varies across different modes of visual deprivation.

While the exact alterations in neural activity arriving at V1 remain unclear for each visual deprivation paradigm, the consensus is that a prolonged absence of visually driven activity (as opposed to spontaneous activity) produces homeostatic scaling up of mEPSC amplitudes, while uncorrelated visually driven activity triggers LTD-type of synaptic weakening. In support of the idea that lacking visually driven activity produces homeostatic synaptic changes, specifically removing visually driven activity, while leaving spontaneous retinal activity intact with DE, globally scales up synapses in L2/3 of V1 (Goel et al., 2006, 2011; Goel and Lee, 2007; Gao et al., 2010). DE-induced homeostatic changes are reversible, because re-exposing DE animals to light reduces the amplitude of mEPSCs in L2/3 neurons of V1 to match that of normal animals (Goel et al.,

2006, 2011; Goel and Lee, 2007; Gao et al., 2010). In contrast to intraocular TTX injection or DE paradigms, MD via lid-suture initially weakens the deprived eye inputs to the binocular zone of V1 contralateral to the deprived eye (Rittenhouse et al., 1999; Sawtell et al., 2003; Frenkel and Bear, 2004; Yoon et al., 2009). The binocular zone receives input from both eyes, hence there is visually driven activity from the open eye, albeit this is weaker in rodents due to a large contralateral bias. In addition, as mentioned above, there is also visually driven activity arising from diffuse light across the closed lid of the dominant contralateral eye. Therefore, the lid-suture paradigm does not eliminate all visually driven activity. The uncorrelated visually driven activity arising from the closed eye then triggers LTD-type of Hebbian synaptic weakening (Rittenhouse et al., 1999, 2006; Frenkel and Bear, 2004). It is thought that the overall reduction in neural activity caused by the initial depression of the deprived eye inputs then either slides down the synaptic modification threshold to promote LTP at the open eye inputs (Frenkel and Bear, 2004; Ranson et al., 2012) or initiates a global scaling up of excitatory inputs (Mrsic-Flogel et al., 2007a) to manifest the delayed open eye input potentiation.

Laminar specificity of homeostatic changes

It is clear that there are laminar differences in homeostatic synaptic plasticity in V1 following visual deprivation (**Fig. 1.3**). For instance, Desai et al. (2002) reported that L2/3 and L4 neurons of the mouse visual cortex have distinct windows of "critical period", during which modulation of visual activity can affect synaptic gain. For example, L4 has an early and narrow critical period for homeostatic synaptic plasticity (Desai et al., 2002), which opens at postnatal day 16 (P16) and closes by P21. In L2/3, homeostatic plasticity is elicited at a later age (by P21) (Desai et al., 2002; Goel and Lee,

2007) and persists at least through P90 (Goel and Lee, 2007). L6 appears to have a unique response to visual deprivation in that there is an age-dependent reversal in the polarity of synaptic change between P16 and P21 (Petrus et al., 2011). In L6 pyramidal neurons, DE initiated at P16 increases, while DE initiated at P21 decreases, in the average amplitude of mEPSCs. This suggests that either there is a developmental change in the cortical activity in L6 circuit after DE, or that there is a change in the mechanism by which L6 neurons adapt to DE with synaptic scaling-like mechanism at younger ages and LTD-type of plasticity later on (Petrus et al., 2011, Chapter 3).

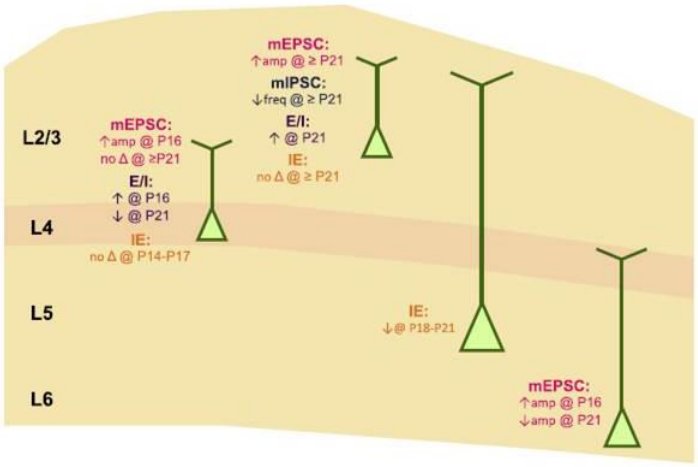

Figure 1.3: Lamina-specific homeostatic adaptation to visual deprivation in V1. Principle neurons of different lamina are shown, and their known modes of homeostatic adaptation at different ages are noted. Results for visual deprivation leading to complete loss of visually driven activity is shown, except for L5 neurons wehrewhere lid suture was used. Note that there is a switch in the polarity of synaptic changes in L4 and L6 during the course of development, such that homeostatic adaptation occurs only early in development. L2/3 changes are initiated later and persist through adulthood. E/I: excitation/ inhibitory balance. IE: Intrinsic excitability (Whitt et al., 2013).

In either case, the results suggest that experience alters sensory processing differently based on the developmental stage of the cortex. The developmental switch in the polarity of excitatory gain change in L6 is interesting considering a recent finding that

L6 neurons act to bidirectionally modulate the gain of visually evoked activity in other cortical layers independent of its projection back to the LGN (Olsen et al., 2012). While homeostatic synaptic plasticity has not been studied in L5 neurons directly, visual deprivation between P19-P21 is reported to reduce the intrinsic excitability of L5 pyramidal neurons (Nataraj et al., 2010). Therefore, it is clear that cortical neurons adapt to losing visual experience in a laminar-specific manner.

Adding to the complexity, each lamina of cortex has unique inputs and outputs, (Binzegger et al., 2004) hence, there is a possibility that specific inputs may respond differentially to the same change in visual experience. Multiplicative synaptic scaling was observed initially in cortical cultured neurons when activity was deprived pharmacologically with TTX (Turrigiano et al., 1998). Based on this experimental data, it was proposed that multiplicative synaptic scaling reflects a global adaptation of excitatory synaptic gain. This mode of homeostatic adaptation is thought to be critical for preserving information storage at individual synapses while allowing homeostatic adaptation of neuronal firing (Turrigiano and Nelson, 2004; Turrigiano, 2008; Lee, 2012). However, *in vivo* homeostatic adaptation of L2/3 neurons only follows the rules of multiplicative synaptic scaling in early development (Goel and Lee, 2007; Gao et al., 2010; Goel et al., 2011; He et al., 2012), but not when visual deprivation occurs later in life (Goel and Lee, 2007). Furthermore, homeostatic synaptic changes observed during development in L6 are also not multiplicative at any age (Petrus et al., 2011). The non-multiplicative homeostatic synaptic scaling likely reflects changes at a subset of synapses, meaning the average strength may increase or decrease in response to altered inputs, but not all synapses undergo this phenomenon by the same multiplication factor

universally. At this point, it is not known whether the non-multiplicative synaptic scaling of cortical neurons *in vivo* is due to changes in activity of specific inputs, but there is evidence of input-specific synaptic scaling from *in vitro* studies (Kim and Tsien, 2008; Béïque et al., 2011). In particular, inactivating a specific presynaptic axon by expressing inward-rectifying potassium channel (Kir1.4) specifically scales up AMPA receptor function in the opposing dendritic spine without altering the strength of neighboring spines (Béïque et al., 2011). Moreover, there is recent evidence that input-specific homeostatic plasticity operates *in vivo*. In the optic tectum of Xenopus laevis tadpoles, two days of DE produces homeostatic strengthening of visual inputs without changes in the strength of mechanosensory inputs, which converge onto the same tectal neuron (Deeg and Aizenman, 2011).

Such synapse-specific scaling may be especially critical in a complex neural network, which receives diverse inputs with different activity levels as is in the sensory cortices. Thalamorecipient layers of primary sensory cortices (i.e. L4 and L6) receive two main distinct types of inputs: thalamocortical (TC) and intracortical (IC). Although less numerous, TC synapses from the LGN to L4 principal neurons tend to have more release sites and higher probability of release than IC synapses (Stratford et al., 1996; Gil et al., 1999), which is why TC synapses are thought to be the primary driver of these neurons. On the other hand, IC inputs reflect projections from other layers or other cortical areas. Hence, the information content and the activity levels arising from TC and IC inputs are likely to be very different. Thus, input-specific homeostatic synaptic changes may be more beneficial to complex cortical circuits with multiple inputs, in terms of proper adaptation to incoming activity.

Molecular mechanisms of experience-dependent homeostatic synaptic plasticity

Homeostatic synaptic plasticity is mediated at least in part by modulation of the number, subunit composition, and conductance of AMPARs [for a recent review see (Lee, 2012)]. AMPARs exist as tetramers made up of subunits including GluA1, 2, 3, and 4 (or GluR1-4), with GluA1 and GluA2 being more prevalent in most cortical areas [reviewed in (Traynelis et al., 2010)]. Due to RNA editing, GluA2 subunits contain a positively charged arginine residue, which is bulkier than the genetically encoded glutamine, at the pore loop (Sommer et al., 1991; Burnashev et al., 1992). This confers GluA2-containing AMPARs with their hallmark electrophysiological properties. These include impermeability to Ca^{2+}, a linear current-voltage (I-V) relationship, and insensitivity to polyamines [reviewed in (Liu and Zukin, 2007; Traynelis et al., 2010)]. In contrast, AMPARs lacking GluA2 are Ca^{2+} permeable, display inward rectification of current, have larger conductance, and are blocked by polyamines, especially at positive potentials. Though initially described in a subset of interneurons (Bochet et al., 1994; Otis et al., 1995; Isa et al., 1996; Washburn et al., 1997; Mcbain, 1998), recent studies indicate that Ca^{2+}-permeable AMPARs (CP-AMPARs) are present at pyramidal synapses under certain conditions [reviewed in (Isaac et al., 2007; Liu and Zukin, 2007)], including homeostatic adaptation to inactivity [reviewed in (Lee, 2012)].

Sensory experience-dependent homeostatic synaptic plasticity can alter receptor composition, phosphorylation, and conductance of AMPARs at cortical synapses. For example, visual deprivation in the form of DE scales up mEPSCs of L2/3 neurons in V1 and increases the content of GluA1, but not GluA2, at the postsynaptic density (PSD) of V1 (Goel et al., 2006). These changes correlated with the appearance of functional CP-

AMPARs, which are likely GluA1 homomers, at synapses (Goel et al., 2006, 2011). The plasma membrane targeting of GluA1 in V1 requires phosphorylation of GluA1 on the serine 845 (S845) residue (Goel et al., 2011) similar to what has been reported in other brain areas (Esteban et al., 2003; Sun et al., 2005; Oh et al., 2006). GluA1-S845 is phosphorylated by cAMP-dependent protein kinase (PKA) (Roche et al., 1996), and targeted by various neuromodulators linked to the cAMP signaling (Chao et al., 2002; Hu et al., 2007; Seol et al., 2007; Qian et al., 2012). While increasing GluA1-S845 phosphorylation via pharmacological activation of beta-adrenergic receptors is able to increase the amplitude of mEPSCs in L2/3 of V1, the increase did not occur via multiplicative scaling as seen with DE (Goel et al., 2011). This suggests that there are likely other mechanism(s) responsible for providing multiplicative scaling, and that phosphorylation of GluA1-S845 itself is likely a targeting signal for increasing cell surface GluA1 levels. One peculiar aspect of L2/3 synapses in V1 is that both pharmacological phosphorylation of GluA1-S845 and mutation of GluA1-S845 to an alanine residue to prevent phosphorylation increase the amplitude of mEPSCs and synaptic expression of CP-AMPARs (Goel et al., 2011). This is quite distinct from CA1 synapses, where mEPSC amplitude is not affected by these two manipulations (He et al., 2011). This led to a speculation that synaptic expression of CP-AMPARs may be more pervasive at cortical synapses compared to CA1 (He et al., 2011; Lee and Kirkwood, 2011). There is additional evidence that CP-AMPARs expression is relatively tightly controlled at CA1 synapses. For example, CP-AMPARs are located predominantly at perisynaptic locations, and only express at synapses in small quantities following mGluR activation (He et al., 2009) or only transiently after LTP under limited conditions (Plant

et al., 2006; Guire et al., 2008). This contrasts the relatively robust recruitment of synaptic CP-AMPARs following visual deprivation in V1 (Goel et al., 2006, 2011), as well as with single whisker experience in rodent barrel cortex (Clem and Barth, 2006).

In contrast to the proposed role of GluA1 in homeostatic adaptation to visual deprivation (Goel et al., 2006, 2011; He et al., 2012), Gainey et al. (2009) reported that GluA2 rather than GluA1 is critical for scaling synapses in V1. The apparent contradiction may be due to several factors. One difference is that the mode of visual deprivation is different: the studies showing GluA1 dependence were done with DE (Goel et al., 2006, 2011; He et al., 2012), while GluA2 dependence was demonstrated using monocular TTX injection and recording from the monocular zone of V1 (Gainey et al., 2009). As discussed above, these two modes of visual deprivation may produce different degrees of activity changes *in vivo* in V1. Another possibility is that the GluA1 changes may happen in conjunction with GluA2-dependent mechanisms. In a recent study, we showed that DE increases the conductance of synaptic AMPAR without changes in the number of open channels at peak current (He et al., 2012). This idea is consistent with an interpretation that synaptic expression of GluA1 CP-AMPARs may be replacing existing synaptic GluA2 to mediate up-scaling.

Experience-dependent homeostatic plasticity in other cortical areas

Although it is tempting to make the generalization that changes in activity produce uniform results across all brain areas, not all cortices respond in the same manner and their basal synaptic transmission may differ as well. There are many similarities and differences between visual (V1), auditory (A1) and somatosensory (S1)

cortical plasticity. Some of the differences may be due to the distinct qualities of various sensory inputs and processing required for proper sensory perception, but others may be differences arising from studying distinct cell types or laminae (for instance, the mode of visual deprivation is an important determinant, and distinct layers in V1 respond differentially to sensory deprivation (**Fig. 1.3**), as mentioned previously).

Sensory neural hearing loss (SNHL) produced by bilateral cochlear ablation increases the strength of excitatory synapses in L2/3 of A1 (Kotak et al., 2005). SNHL is similar to binocular enucleation, in that it removes both sensory evoked activity as well as spontaneous activity arising in the sensory organ. As mentioned above, binocular enucleation scaled up L2/3 synapses in V1 (He et al., 2012), which highlights the similarity of L2/3 neurons in A1 and V1 when responding to sensory organ damage. However, there are qualitative differences in that mEPSC frequency is reduced in A1 L2/3 neurons following SNHL (Kotak et al., 2005), but unaltered in V1 L2/3 with enucleation (He et al., 2012).

In rodent barrel cortex (S1BF), whisker deprivation studies have revealed dramatic changes in both synaptic function and connectivity [reviewed in (Feldman and Brecht, 2005)]. However, it is pertinent to note that the majority of whisker deprivation studies are done under conditions that promote competition of different whisker inputs, such as depriving a single row of whiskers or a checkerboard deprivation paradigm, which elicit Hebbian plasticity. In contrast, uniform deprivation of all whiskers produces minimal change in synaptic function of S1BF neurons (Finnerty and Connors, 2000; He et al., 2012), unless such deprivation is done from birth (Popescu and Ebner, 2010). In particular, a week of bilateral whisker deprivation initiated later in development does not

alter the average amplitude or frequency of mEPSC in L2/3 S1BF neurons (He et al., 2012). The apparent lack of homeostatic synaptic changes in L2/3 S1BF following bilateral whisker deprivation was suggested to be due to its similarity to bilateral lid suture manipulation, which does not elicit global homeostatic synaptic changes in L2/3 of V1 (He et al., 2012). A recent study reported that unilateral infraorbital nerve resection, which is expected to abolish all tactile driven activity, potentiates thalamocortical inputs to S1BF (Yu et al., 2012). These results further support the idea that a complete loss of sensory driven activity is needed to trigger homeostatic synaptic plasticity in primary sensory cortices.

b. Experience-dependent homeostatic adaptation of inhibitory synapses

There are several aspects of inhibitory transmission in V1 that are affected by periods of visual deprivation, including reduced expression of GABA and the GABA synthesizing enzyme glutamic acid decarboxylase (GAD) (Benevento et al., 1995; Huang et al., 1999; Kreczko et al., 2009) and alterations in the overall maturation of inhibitory circuits (Huang et al., 1999). While there is a relative wealth of knowledge regarding experience-dependent homeostatic changes in excitatory drive in the cortex, there is much less known about adaptation of the inhibitory circuit after altered sensory input. Inhibitory tone in the cortex is a function of several different aspects of inhibitory transmission, including diverse inhibitory cell types, excitatory drive to these inhibitory neurons, and, of course, the way in which the inhibitory neurons affect each other and excitatory neurons in the circuit. It is perhaps not surprising then, that experience does

not alter all classes of inhibitory cells in all layers in the same manner. While maintaining excitatory-to-inhibitory (E/I) balance is thought to be critical for normal cortical functions, in some cases experience driven homeostatic adaptations in cortical inhibitory transmission occur inversely with excitatory changes, yielding a net shift in the E/I balance. Presumably, the shift in E/I balance is an adaptive mechanism to maintain cortical activity within a desired functional range.

Excitatory drive onto inhibitory neurons

The first reports of homeostatic plasticity in culture revealed that excitatory and inhibitory circuits change differently after prolonged changes in activity. Specifically, blocking neuronal activity with TTX causes excitatory synapses onto pyramidal neurons to be scaled up, without changes in excitatory drive onto interneurons (Turrigiano et al., 1998). To the contrary, pharmacologically enhancing activity in neuronal cultures via brain-derived neurotrophic factor (BDNF) (Rutherford et al., 1998) or through addition of $GABA_A$ receptor antagonist bicuculline (Chang et al., 2010) increases the average amplitude of mEPSCs onto GABAergic neurons, suggesting a net increase in inhibition. These data suggest that the excitatory synapses onto inhibitory neurons only adapt to increased activity. Consistent with this idea, sensory experience (which is expected to increase patterned activity in the cortex) is critical for the developmental increase in the strength of excitatory inputs to GABAergic neurons in S1BF. Excitatory thalamic input to feed-forward inhibitory interneurons in L4 of S1BF shows a developmental strengthening, which is attenuated in whisker-trimmed animals (Chittajallu and Issac, 2010). This study was performed during the second postnatal week, an age at which thalamocortical inputs to L4 stellate cells do not respond to sensory deprivation (Feldman

and Brecht, 2005). Thus, the same whisker deprivation does not alter the strength of thalamic input to L4 stellate cells nor the synaptic strength of unitary inhibitory inputs from L4 interneuron to stellate cells (Chittajallu and Issac, 2010). This suggests that the modification of excitatory inputs to L4 interneurons is the main locus of adaptation in L4 S1BF in response to whisker deprivation after the critical period of plasticity for L4 stellate neurons has closed. The net outcome of these changes conforms to the idea that these are homeostatic adaptations, because it is predicted to increase the E/I ratio in response to sensory deprivation. Whether these types of adaptation exist beyond the initial developmental period needs to be tested.

Homeostatic adaptation of inhibitory synapses

Early studies that directly measured inhibitory currents in cultured neocortical neurons revealed that after two days of TTX-induced activity blockade, miniature inhibitory postsynaptic currents (mIPSCs) in pyramidal neurons scale down due to a loss of $GABA_A$ receptors clustered at the synapse and an overall loss of functional inhibitory synapses (Kilman et al., 2002). In contrast, prolonged increase in activity triggers accumulation of postsynaptic $GABA_A$ receptors (Rannals and Kapur, 2012). Both of these studies also report corresponding alterations in presynaptic GABA synthesizing enzyme levels, as well as changes in mIPSC frequency, suggesting that these homeostatic changes involve both pre- and post-synaptic mechanisms. Reduced inhibitory transmission after periods of neuronal inactivity would result in an overall increase in excitability of pyramidal neurons, which would complement homeostatic increase in excitatory transmission to increase the E/I balance in the network.

As discussed above, many sensory deprivation paradigms have been developed over the years to identify experience-dependent alterations in network activity *in vivo*, and different layers of the cortex have distinct critical periods during which experience can shape excitatory synapses. In L4 of V1, 2 days of monocular deprivation from postnatal day 14 to 17 (P14-17) causes a decrease in the amplitude of unitary IPSCs (uIPSCs) from fast-spiking interneurons to principal neurons in the contralateral monocular zone (Maffei et al., 2004). This was accompanied by an increase in the strength of excitatory inputs between principal neurons of L4, which indicates an increase in E/I balance (Maffei et al., 2004). In line with the idea that this is a homeostatic adaptation to inactivity, visual deprivation at this early age increases the spontaneous firing of L4 principal neurons (Maffei et al., 2004). However, this type of homeostatic adaptation in L4 only occurs in early development, and the same visual deprivation paradigm initiated at P18 does not alter the recurrent excitatory connections of the principal neurons in L4, but increases the unitary IPSC amplitude (Maffei et al., 2006). These alterations would decrease the E/I ratio, and are consistent with the finding that spontaneous activity in L4 principal neurons are decreased with visual deprivation at this later age (Maffei et al., 2006). These results illustrate that the mechanisms by which the cortical circuit adapts to changes in sensory inputs may be distinct depending on the developmental age. The opposite regulation of inhibitory inputs to L4 principal neurons by sensory deprivation during different phases of development is reminiscent of the opposite changes in the strength of excitatory inputs to L6 principal neurons (Petrus et al., 2011). These changes would act to increase E/I balance to the principal neurons during early development, but decrease this at a later age. L4 and L6 are the major

thalamorecipient layers, and whether the developmental change in how they adapt to sensory deprivation reflects any specific nature of thalamocortical inputs is unclear at this point. It is interesting to note that the developmental switch seems to coincide with the transition from pre-critical to critical period for cortical plasticity (Feller and Scanziani, 2005).

In L2/3 of V1 changes in the E/I balance seem dependent on the mode of visual deprivation. For instance, 2 days of monocular TTX injection leads to an increase, while the same duration of monocular lid suture decreases, the E/I ratio of L2/3 pyramidal neurons in the monocular zone of V1 (Maffei and Turrigiano, 2008). Using a minimal stimulation paradigm, it was shown that the changes in E/I ratio with intraocular TTX injection are due to an increase in L4 to L2/3 excitatory inputs and a concomitant decrease in the inhibitory inputs, but monocular lid suture only decreased the amplitude of excitatory inputs (Maffei and Turrigiano, 2008). This conforms to the idea that V1 L2/3 neurons differentially adapt their inhibitory network to distinct visual deprivation paradigms. This parallels the effect of various modes of binocular deprivation on homeostatic regulation of mEPSCs in L2/3 V1 neurons. Distinct from monocular deprivation paradigms and *in vitro* studies, a week of DE does not alter the amplitude, but decreases the frequency, of mIPSCs recorded from L2/3 V1 neurons (Gao et al., 2011). These changes were not accompanied by alterations in presynaptic parameters of evoked IPSCs (eIPSCs) or the density of inhibitory synapses as measured by GAD-65 puncta density (Gao et al., 2011). These data suggest that experience driven homeostatic plasticity can selectively modify spontaneous inhibitory transmission while leaving evoked inhibitory transmission unaltered, perhaps allowing experience to set the overall

inhibitory “tone” or “background noise” in sensory systems while preserving the temporal response properties of cortical neurons which critically depend on action potential evoked inhibition (Zhang et al., 2011).

c. *In vivo* functions of experience-dependent homeostatic synaptic plasticity

There is emerging evidence that ocular dominance plasticity (ODP) is orchestrated by the coordinated recruitment of Hebbian and homeostatic synaptic plasticity. It is well documented that brief MD functionally disconnects the deprived eye inputs to V1 (Wiesel and Hubel, 1965a, 1965b; Hubel and Wiesel, 1970). The basic cellular mechanisms underlying ODP have been extensively studied in rodents. The main idea emerging from many studies is that there are two phases to ODP: an initial depression of the closed eye inputs followed by a delay potentiation of the open eye inputs. Evidence suggests that the former is mediated by LTD-like Hebbian plasticity, while the latter is mediated by homeostatic synaptic plasticity (either sliding threshold or synaptic plasticity). After a brief period of MD, V1 neurons decrease responsiveness to the closed eye, which is then followed by an increase in response to the open eye (Frenkel and Bear, 2004) resulting in a preferential responsiveness to the remaining open eye (Gordon and Styker, 1996). There is clear evidence that the initial weakening of the closed eye inputs is due to LTD of excitatory synapses (Rittenhouse et al., 1999; Heynen et al., 2003), which is mainly due to the degradation of the quality of the visual input rather than a general reduction in retinal illumination (Rittenhouse et al., 2006). The delayed potentiation of the open eye inputs was initially proposed to be due to the sliding down of LTP induction threshold by the loss of the closed eye inputs, which promotes potentiation of synapses serving the open eye inputs (Bienenstock et al., 1982; Frenkel

and Bear, 2004). Later this idea was challenged and it was suggested that the open eye potentiation is due to homeostatic synaptic scaling triggered by losing the closed eye inputs. This proposal was based on the observation that both the open eye and closed eye inputs display a delayed potentiation (Mrsic-Flogel et al., 2007b). The latter idea was further supported by the demonstration that the delayed potentiation of the open eye inputs following MD does not occur in the TNFalpha knockout mouse (Kaneko et al., 2008), which specifically lack up-scaling of excitatory synapses by inactivity (Stellwagen and Malenka, 2006). However, a recent study showed that synaptic scaling based potentiation of the open eye inputs only occur in young mice, but not in adults (Ranson et al., 2012). TNFα knockouts lack the delayed potentiation of the open eye inputs during the critical period (Kaneko et al., 2008), but display normal delayed potentiation in adults (Ranson et al., 2012). On the other hand, mice specifically lacking LTP (i.e. CaMKIIα-T286A mutant) display normal open eye potentiation when young, but lack this in adults (Ranson et al., 2012). These results indicate that the mechanisms of the delayed open eye potentiation seen following MD changes with age, and fits nicely with data showing that V1 L2/3 neurons exhibit multiplicative synaptic scaling only during early development, but not in adults (Goel and Lee, 2007). In adults, the non-multiplicative increase in mEPSC amplitude suggests that only a subset of synapses remain plastic (Goel and Lee, 2007) consistent with recruitment of input-specific plasticity mechanisms such as LTP. It is possible that MD in adults slides down the LTP threshold such that spontaneous cortical activity may be sufficient to produce LTP at a subset of active synapses, which would result in the delayed potentiation of the open eye inputs following MD (Bienenstock et al., 1982; Sawtell et al., 2003; Ranson et al., 2012).

Homeostatic mechanisms of maintaining optimal synaptic performance need not be limited to sensory experience. Sleep is hypothesized to maintain the integrity of neuronal circuits via homeostatic mechanisms [reviewed in (Tononi and Cirelli, 2003)]. During wakefulness synapses are actively processing information, including but not limited to sensory experience, which may increase overall excitability in the system. Sleep has been hypothesized to homeostatically down-regulate cortical excitability in order to normalize the synaptic strength, which then facilitates memory consolidation and enhance performance on a variety of motor and procedural tasks [reviewed in (Stickgold et al., 2001)]. In support of this hypothesis, molecular markers of LTP increase during the wake cycle, while markers of LTD increase during sleep (Vyazovskiy et al., 2008). However, whether sleep associated synaptic depression is truly mediated by synaptic scaling type of global homeostatic synaptic plasticity is unclear at this point. At least in V1, sleep induced consolidation of ODP is mediated in part by facilitation of LTP-like mechanisms that enhance the open eye inputs (Aton et al., 2009).

It is pertinent to point out that deciphering whether synaptic change is due to synaptic scaling or Hebbian LTP/LTD-type of mechanism is often difficult. For example, neuromodulators linked to cAMP signaling, which promote LTP (Seol et al., 2007), produce apparent global scaling up of mEPSCs in L2/3 of V1 (Huang et al., 2012). On the other hand, neuromodulators linked to phospholipase C (PLC) enhance LTD globally to scale down synapses (Huang et al., 2012). A surprising aspect of this particular study is that the same visual experience either triggers global LTP or global LTD depending on the neuromodulator present (Huang et al., 2012). This study underscores the difficulty in distinguishing synaptic scaling from Hebbian plasticity *in vivo*, where the exact nature of

change in activity following sensory manipulation or the neuromodulatory tone is often unknown.

3. Cross-modal Plasticity

In addition to synaptic plasticity of sensory cortical circuits responding to changes in primary sensory inputs, there are also cross-modal cortical changes. It is well documented that losing a sense produces compensation of the remaining senses in a phenomenon coined as "cross-modal plasticity" [reviewed in (Bavelier and Neville, 2002)]. Studies aimed at understanding sensory compensation at the system's level are widespread, but experiments addressing the synaptic basis for this phenomenon are just beginning to surface.

a. Systems Level Adaptations

It is has been well established that the loss of one sense can result in enhancement of the remaining senses, for example blind people may have improved auditory pitch discrimination and sound localization performances (Lessard et al., 1998; Roder et al., 1999; Gougoux et al., 2004; Voss et al., 2004). Blind individuals also experience enhanced fine tactile discrimination (Goldreich and Kanics, 2003; Alary et al., 2008, 2009) and speech processing (Röder et al., 2001; Amedi et al., 2003). This enhancement of the remaining senses is not limited to blind individuals, as deaf patients also experience heightened tactile sensitivity (Levänen and Hamdorf, 2001), facial emotional

expression comprehension (McCullough and Emmorey, 1997; Arnold and Murray, 1998), and performance on visual tasks specifically targeting peripheral vision (Neville and Lawson, 1987; Bavelier et al., 2000; Dye et al., 2009). This boost in performance in audio/visual compensation especially in the peripheral field of the spared sense may be one mechanism by which blind and deaf patients navigate the world and lower their detection threshold for events that the lost sense may have helped detect.

The enhancement of the remaining senses may be possible due to recruitment of the deprived cortical space to mediate these changes. For example, visual cortex of blind patients is activated by braille reading (Sadato et al., 1996, 1998; Büchel, 1998; Burton et al., 2002) and auditory tasks (Voss et al., 2008), while deaf patients experience auditory cortex activation during visual or tactile tasks (Levanen, 1998; Auer et al., 2007). The cross-modal activation of these primary sensory cortices reflect functional adaptations, because deactivating visual cortex via repetitive transcranial magnetic stimulation (rTMS) renders blind patients unable to read Braille (Cohen et al., 1997), and a blind individual suffering a visual cortex stroke was unable to comprehend sign language (Hickok et al., 1995). In addition, cooling auditory cortex renders blind cats no better than their sighted peers on peripheral visual tasks, on which moments before they had demonstrated a significant advantage (Lomber et al., 2011).

Many of these studies were performed in patients with early sensory loss, however cross-modal benefits and cortical recruitment can occur very quickly even in adults. For example, only a week of blindfolding rendered normally sighted adults better at Braille reading, which was negated by inactivation of visual cortex via rTMS (Merabet et al., 2008). It should be noted that this enhancement occurred with intensive Braille

comprehension training, although both sighted and blindfolded individuals received the same training exercises. However, this includes a clue into how cross-modal reorganization can be recruited: the necessity of the organism to pay attention to, or use a sense may mediate these changes at least in adults. For example, rats reared in a low frequency environment usually re-organize their auditory cortex and renders them unable to detect a variety of frequencies, which was ameliorated with intensive training (Zhou and Merzenich, 2007, 2009). In addition, neuromodulators may play a role in cross-modal plasticity, which indicates higher level processing may influence how these systems level changes occur (Jitsuki et al., 2011; Zheng et al., 2014).

Although compensation of spared sensory modalities generally is perceived as advantageous to individuals, this cross-modal reorganization can be maladaptive. The degree of cross-modal reorganization of deprived cortices also may predict the success of peripheral surgical remedies. For example, deaf patients with high levels of cross-modal reorganization of auditory cortex experience more difficulty learning to use a cochlear implant (Lee et al., 2001; Giraud and Lee, 2007). Additionally, after surgical repair of vision (via cataract removal for example) some patients experience difficulty with visual tasks (Senden, 1960; Gregory, 2003). However, after restoring auditory input to previously deaf auditory cortex via cochlear implant, there is an increase in audio-visual interactions between these sensory modalities (Giraud et al., 2001). Interestingly, even after language acquisition from years of use, recipients of cochlear implants still have better lip-reading performance than hearing peers, indicating they still may benefit from these multimodal interactions (Rouger et al., 2007).

The use of multimodal training paradigms may be beneficial or even essential to helping people regain function once the periphery is fixed via neural prosthetics. These paradigms may work in one or both of the following ways: 1) the deprived sense can make use of the multimodal interactions to understand previously absent information, for example seeing a bird and hearing one for the first time would help a recent cochlear implant user identify the auditory cue of bird song which matches the image they already know. The other scenario that could be helpful is depriving the individual of a sense they previously heavily relied upon. For example, a cochlear implant user struggling to use the new device could be deprived of vision, thus forcing the brain to use previously nonexistent auditory inputs. Regardless of how patients re-learn to use a sense, or learn to navigate their world minus one sense, it is important to understand the synaptic and molecular mechanisms, which underlie these phenomena.

b. Synaptic Circuit Changes

also contains part of the Whitt, Petrus, Lee 2013 review

Cross-modal changes in excitatory synaptic strength were first observed in L2/3 of S1 and A1 of visually deprived mice (Goel et al., 2006; He et al., 2012) (Figure 1.4). Depriving vision via a week of DE decreases the average amplitude of mEPSCs, which is reversed by subsequent visual experience. The cross-modal synaptic changes follow the rules of multiplicative synaptic scaling, at least in juveniles (Goel et al., 2006; He et al., 2012), which suggests global adaptation in synaptic strength. Interestingly, cross-modal synaptic changes require a longer duration of DE than unimodal changes (He et al.,

2012). Furthermore, while a milder form of vision loss (i.e. lid suture) can trigger a cross-modal decrease in mEPSC amplitudes in S1BF, the unimodal increase in mEPSCs requires a complete loss of visually driven activity (He et al., 2012). Despite the difference in the sensory requirement, at the molecular level cross-modal homeostatic synaptic adaptation employs the same mechanisms as unimodal changes observed in V1 (**Fig. 1.4**). For instance, in S1 the cross-modal scaling down of mEPSCs by visual deprivation is accompanied by removal of synaptic AMPARs (He et al., 2012), including

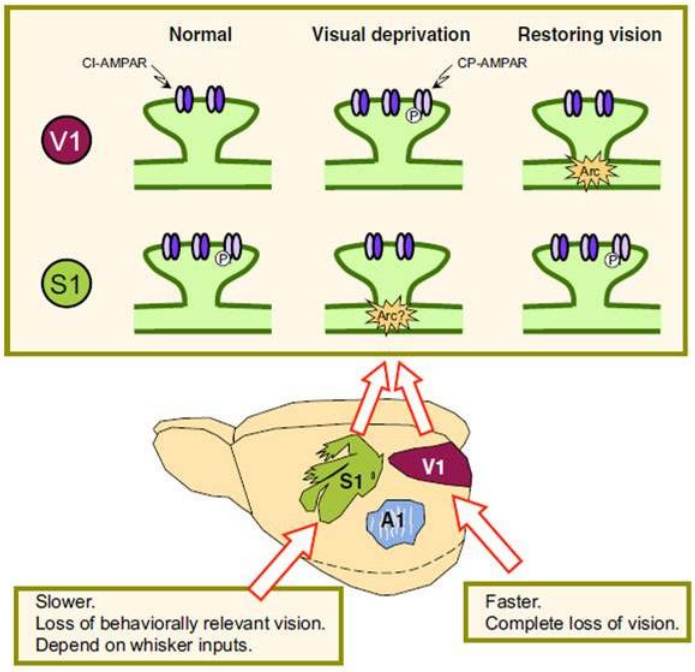

Figure 1.4: Visual deprivation induced unimodal and cross-modal homeostatic synaptic plasticity. Unimodal changes in V1 and cross-modal changes in S1 require distinct sensory requirements. At the cellular level, unimodal and cross-modal changes occur in opposite directions at excitatory synapses and follows the rules of multiplicative synaptic scaling. The underlying molecular mechanisms are covered, such that scaling up of synapses in both cortical areas involve synaptic expression of CP-AMPARs, and scaling down depends on immediate early gene Arc and removal of synaptic AMPARs (Whitt et al., 2013).

CP-AMPARs (Goel et al., 2006), while scaling up of mEPSCs by re-exposure to light recruits CP-AMPARs to synapses (Goel et al., 2006). In addition to homeostatic synaptic

plasticity, cross-modal plasticity can also occur via Hebbian mechanisms. It was demonstrated that 3 days of bilateral lid suture potentiates L4 inputs to L2/3 neurons in S1BF by transiently driving GluA1 containing AMPARs to synapses (Jitsuki et al., 2011). This LTP-like cross-modal change was accompanied by sharpening of whisker maps, measured as a decrease in the response to surround whiskers in the visually deprived mice (Jitsuki et al., 2011). This study attributed the sharpened whisker maps to LTP of the L4 inputs to L2/3 neurons, which is expected to increase the impact of feedforward sensory information arising from the principal whisker. However, a global scaling down of mEPSCs in L2/3 of S1BF following visual deprivation (Goel et al., 2006) could also explain the sharper whisker map by reducing the strength of previously weak inputs (such as those from surround whiskers) below the action potential threshold. This in essence would sharpen the receptive field (RF) of L2/3 neurons in S1BF. There is evidence that global scaling down of cortical excitatory synapses may sharpen neuronal RFs. For example, orientation selectivity is broadened in Arc knockout mice (Wang et al., 2006), which lack down scaling of mEPSCs by visual experience (Gao et al., 2010).

In addition to the changes observed in excitatory synaptic circuitry, cross-modal cortical reorganization has also been shown to induce changes in inhibition. For example, after unilateral olfactory epithelium injury, a significant increase in GABAergic neurons was observed in S1BF ipsilateral to the lesion site. This resulted in an upregulation of whisker sensitivity (Ni et al., 2010), which indicates GABAergic neurons play an integral role not only in regulating sensitivity, but can be regulated cross-modally as well. Interesting work has been performed in hamsters enucleated at birth, which show changes in PV^+ distribution induced by cross-modal sensory deprivation. At least in

hamsters, V1 typically has high density of PV^+ neurons in L4, while PV^+ neurons in A1 are concentrated in L5 (Desgent et al., 2005). However hamsters deprived of vision from birth assume a PV^+ distribution in V1 that mimics A1 (Desgent et al., 2010; Desgent and Ptito, 2012). Although this could be a product of altered V1 development due to altered input activity, there is a possibility that the demands of processing auditory information may require inhibitory circuits in V1 to develop similar to A1. Alternatively, the higher distribution of PV^+ neurons now in L5 of V1 could have implications for modulation of the cortico-thalamo-cortical loop, as more inhibition in L5 could result in less excitatory output of V1 L5 to subthalamic nuclei (Callaway, 2004).

Conclusions

The cortex is organized in a way to efficiently process information. The laminar distribution of neurons in the primary sensory cortex allows for serial and horizontal excitation and inhibition to work together as information arrives from the thalamus, is processed, and sent out to higher order cortical areas. Sensory experience is necessary for the correct initial wiring, but also can cause changes once these circuits are developed. As sensory experience changes, the cortex responds in a variety of ways to ensure information is efficiently processed, through Hebbian and/or homeostatic mechanisms. The mechanisms synaptic circuits employ may depend on the type of experience, for example a global response may be appropriate for a global reduction or increase in activity, or a targeted increase in synaptic strength may be beneficial for increasing an important signal for better readout. These differences may be partially due to age of the organism, as mature mice rarely undergo global multiplicative synaptic scaling compared to young mice or in culture (Turrigiano et al., 1998; Desai et al., 2002;

Goel and Lee, 2007), but it also may depend on what the spared vs. deprived cortex is required to do for adaptation to a new set of experiences. The loss of one sense can cause compensatory changes in spared sensory modalities, and the changes in deprived and spared cortex can follow both Hebbian and homeostatic mechanisms.

Chapter 2: Methods

The aim of this thesis was to determine the functional changes in cortical circuits experienced by spared and deprived sensory cortex in adult mice. Electrophysiological analysis of post synaptic responses of principle neurons to excitatory and inhibitiroy inputs were determined using whole cell electrophysiology. Isolated spontaneous and/or evoked events mediated by AMPA or GABA receptors were recorded and compared between normally reared (NR) control animals, versus dark exposed (DE) and light exposed (LE) groups. Evoked events were mediated by light activation of channel rhodopsin (ChR2) which was restricted to specific neuron populations or via targeted electrical stimulation. Another aim of this project was to identify if certain activity induced molecules may play a role in cross-modal or uni-modal plasticity. Arc and BACE1 were both explored as important regulators of homeostatic plasticity in cross-modal (Arc) regulation of auditory neurons after DE, and BACE1 was identified as being required for V1's homeostatic response to visual deprivation.

Wild Type Animals

Male and female C57BL/6J mice (Jackson Laboratories) were raised in 12-hr light/ 12-hr dark conditions. At post natal day 90 (P90) mice (2-3 mice from established litters) were dark exposed (DE) for 7 days. Age-matched controls remained in normal light conditions (NR). DE animals were cared for using infrared vision goggles with dim infrared light. Some mice were returned to normal light conditions for 7 days to study the effect of light re-exposure (LE). CBA/CaJ (CBA) mice were obtained from Jackson Laboratories and were DE or NR at P90. Experiments isolating inhibitory currents used

only male mice between P39-P45. All experiments were approved by the Institutional Animal Care and Use Committees (IACUCs) of Johns Hopkins University and University of Maryland and followed the guidelines of the Animal Welfare Act.

Transgenic Animals

BACE1 WT/KO Animals

Male mice were derived from heterozygous breeders and identified as $BACE1^{-/-}$ (KO) or $BACE1^{+/+}$ (WT) via polymerase chain reaction (PCR) analysis as described previously (Laird et al., 2005). Mice were raised in 12-hour light/12-hour dark cycle until postnatal day 22-26 (P22-P26), at which point some mice were dark exposed (DE) for 2 days while others remained in a normal lighted environment (normal reared, NR). DE animals were cared for using infrared vision goggles with dim infrared light. Some DE mice were returned to normal light conditions for 2 hours to study the effect of light re-exposure (LE).

Arc WT/KO Animals

Male and female Arc/Arg3.1 WT and KO mice were raised in a 12-hour light/12-hour dark cycle until P21. Recruitment of cross-modal plasticity requires 7 days of sensory manipulation, therefore a group of mice were dark exposed (DE) for 7 days while age matched controls remained in normal lighted environments. A subset of DE animals were returned to light exposure (LE) for 7 days.

Cre-recombinase Expressing Animals

Layer 4-cre mice (B6;C3-Tg(Scnn1a-cre)1Aibs/J, Jackson Laboratories) or male PV^{+} cre mice (B6;129P2-*Pvalb*$^{tm1(cre)Arbr}$/J, Jackson Laboratories) were also used, with

Layer 4-cre mice experiencing 7 days of DE at P90, while only male PV^+-cre mice were DE between P35-P38.

Thalamic Channelrhodopsin-2 (ChR2) Viral Transfection

P21 mice were anesthetized with 1-3% isoflurane mixed with O_2 and transcranially injected bilaterally with 1.5 µl adeno-associated virus containing channelrhodopsin-2 and yellow fluorescence protein as a marker (AAV2/9.hSynapsin.hChR2(H134R)-EYFP.WPRE.hGH, Addgene26973, Penn Vector Core) into MGB (auditory) thalamus at coordinates: Bregma 1.8, Lateral 2.9, Depth 3.25 or dorsal LGN (visual) thalamus at coordinates: Bregma 2.3, Lateral 2.0, Depth 2.42. Mice recovered on a heated surface and were returned to the animal colony, where they remained for 6-8 weeks to produce optimal ChR2 expression before experimental paradigms were initiated.

Cortical Channelrhodopsin-2 (ChR2) Viral Transfection

Layer 4 cre mice (B6;C3-Tg(Scnn1a-cre)1Aibs/J, Jackson Laboratories) or PV^+ cre mice (B6;129P2-*Pvalb*$^{tm1(cre)Arbr}$/J, Jackson Laboratories) were bilaterally injected with double floxed ChR2 (AAV9.EF1.dflox.hChR2(H134R)-mCherry.WPRE.hGH, Penn Vector Core, University of Pennsylvania) using the same surgical techniques listed above. Primary auditory cortex layer 4 (A1L4) was targeted with coordinates: Bregma 2.92, Lateral 3.6, Depth 0.8, while primary visual cortex layer 4 (V1L4) was found using coordinates: Bregma -3.6, Lateral 2.5, Depth 0.43. Layer 4 cre mice required 6-8 weeks post transfection incubation, while PV+ cre mice required only 10-14 days prior to

experimental use. Both species were injected between P21-P25 and were maintained 2-3 same sex mice per cage. For PV+ cre experiments only male mice were used.

Cortical Slice Preparation

Mice were anesthetized using isoflurane vapors, after the disappearance of the corneal reflex the brain was quickly dissected and immersed in ice-cold dissection buffer (in mM: 212.7 sucrose, 10 dextrose, 3 $MgCl_2$, 1 $CaCl_2$, 2.6 KCl, 1.23 $NaH_2PO_4 \cdot H_2O$, 26 $NaHCO_3$) which was bubbled with a 95% O_2/5% CO_2 gas mixture. Brain blocks containing primary visual and auditory cortices were dissected and coronally sectioned into 300 μm thick slices using a Vibratome 3000 plus microslicer (Ted Pella, Redding, CA). Slices were then maintained in the dark at room temperature for 1 hour in a holding chamber containing artificial cerebrospinal fluid (ACSF, in mM: 124 NaCl, 5 KCl, 1.25 $NaH_2PO_4 \cdot H_2O$, 26 $NaHCO_3$, 10 dextrose, 2.5 $CaCl_2$ 1.5 $MgCl_2$, bubbled with 95% O_2/5% CO_2).

Light-evoked Sr^{2+}-mEPSCs

Slices were transferred to a submersion-type recording chamber mounted on the fixed stage of an upright microscope (E600 FN; Nikon, Tokyo, Japan) with oblique infrared (IR) illumination. AMPA receptor-mediated excitatory postsynaptic currents were isolated pharmacologically with 20 μM bicuculline and 100 μM DL-2-amino-5 phosphonopentanoic acid (DL-APV). These agents were added to modified ACSF containing 4 mM $MgCl_2$ and 4 mM $SrCl_2$ with 0 mM $CaCl_2$, which was bubbled with 95% O_2/5% CO_2, maintained at 30 ± 1 °C, and continually perfused at a rate of 2 ml/min. Slices were allowed to incubate in this solution for a minimum of 30 minutes prior to

recording. Pyramidal neurons were identified visually in L4 and patched using a whole-cell patch pipette with a tip resistance between 3-5 MΩ, which was filled with internal solution containing in mM: 130 Cs-gluconate, 8 KCl, 1 EGTA, 10 HEPES, 4 ATP, 5 QX-314; pH 7.4, 285-295 mOsm). Biocytin (1 mg/ml) was added to the internal solution for post-hoc cell identification. ChR2 was activated using a 455-nm light emitting diode (LED) (ThorLabs DC2100) illuminated through a 40x objective lens, and controlled by a digital stimulator (Cygnus DG4000A). The minimal light intensity to elicit a reliable response was determined on a cell-by-cell basis with a 5-ms duration remaining constant. Cells were held at -80 mV and recorded for a minimum of 10 minutes; event analysis was performed using mini analysis software (see below). Data was acquired every 10 seconds for a duration of 1200 ms, which included a seal test pulse (100-ms duration), a 500-ms duration before LED illumination, and a 500-ms duration after LED illumination. A 400-ms window before LED was used for quantifying spontaneous desynchronized events (preLED), and a 400-ms window following a 50-ms delay from LED onset was used for quantifying LED-evoked desynchronized events (postLED). 50 subsequent events were obtained from each of the pre and post-LED time window to analyze light-evoked Sr^{2+}-mEPSCs kinetics. Cells were excluded from analysis if they had less than 2Hz increase from the pre LED to post LED analysis. To calculate the amplitude of LEv-Sr^{2+}-mEPSCs corresponding to LED evoked desynchronized events without spontaneous desynchronized events, we used the following equation: [(postLED amplitude x postLED frequency) – (preLED amplitude x preLED frequency)]/ (postLED frequency – preLED frequency). Sr^{2+}-mEPSCs were analyzed using a constant 30 traces equaling 15,000 ms

pre LED window and 12,000 ms post LED time window, with all events occurring during these windows being selected for analysis.

Light-evoked Sr^{2+}-mIPSCs

These events were recorded in a similar experimental setup to light evoked Sr^{2+} mEPSCs with the following differences. The bath contained normal ACSF (described above) with 4 mM Sr^{2+} and Mg^{2+}, but contained the following drugs: 100 µM D,L-APV and 10 µM NBQX. The internal solution contained in mM: 130 Cs-gluconate, 8 KCl, 1 EGTA, 10 HEPES, 4 ATP, 5 QX-314; pH 7.4, 285-295 mOsm. Cells were held at -80 mV for a minimum of 10 minutes, and LED activated responses were recorded using the minimal stimulation to produce a visible desynchronized release of vesicles, with analysis windows the same as used for the Sr^{2+} mEPSCs experiments. The threshold for event detection was set at 3 times the RMS noise and cells were excluded from analysis if they had less than a 2-Hz increase from the pre LED to the post LED analysis windows. Sr^{2+}-mIPSCs were analyzed using a constant 30 traces equaling 15,000 ms pre LED window and 12,000 ms post LED time window, with all events occurring during these windows being selected for analysis.

Recording of mEPSCs

AMPA receptor-mediated miniature excitatory postsynaptic currents were isolated pharmacologically with 1 µM tetrodotoxin (TTX), 20 µM bicuculline, and 100 µM DL-2-amino-5 phosphonopentanoic acid (DL-APV). These agents were added to ACSF bubbled with 95% O_2/5% CO_2 and maintained at 30 ± 1 °C, which was continually perfused at a rate of 2 ml/min. Cells in L2/3 were identified by their pyramidal-shaped

soma and apical dendrite pointing towards the pia. Principle neurons in L4 were patched based on their location within the granular layer of cortex. Neurons were patched using a whole-cell patch pipette with a tip resistance between 3-5 MΩ, which was filled with internal solution containing in mM: 130 Cs-gluconate, 8 KCl, 1 EGTA, 10 HEPES, 4 ATP, 5 QX-314; pH 7.4, 285-295 mOsm). Recordings were initiated 2-3 minutes after cell break-in. Biocytin (1 mg/ml) was included in the internal solution to confirm morphology and location of recorded cells. Axon patch-clamp amplifier 700B (Molecular Devices, Union City, CA) was used for voltage-clamp recordings. Cells were held at -80mV and the recorded mEPSC data was digitized at 10 kHz by a data acquisition board (National Instruments, Austin, TX) and acquired through Igor Pro software (WaveMetrics, Lake Oswego, OR). Recordings were excluded from analysis if the RMS noise was >2, series resistance > 25MΩ, and input resistance <100 MΩ. We also excluded all mEPSCs with a rise time >3 ms, and those showing a negative correlation between amplitude and rise time. 200 consecutive mEPSCs were analyzed from each cell, and the data is expressed as mean ± standard error of the mean.

Recording of mIPSCs

mIPSCs were recorded in layers 2/3 and 4 of primary auditory cortex (A1) in the presence of 1μM TTX, 100 μM D,L-APV, and 10 μM NBQX, which were then analyzed using the same Mini Analysis program (Synaptosoft). The intracellular solution used contained in mM: 140 CsCl, 8 KCl, 10 EGTA, 10 HEPES, and 10 QX-314, pH of 7.3 and 280-300 mOsm. Cells were held at -80mV, and the threshold for mIPSC detection was set at 3 times the RMS noise. 300 consecutive mIPSCs from each cell were selected for analysis, but bursts (characterized as more than 2 events with an inter-event interval of

less than 10ms) were excluded from amplitude measurements. As for mEPSCs, cells with a negative correlation between rise time and amplitude, a series resistance higher than 25 MΩ, and input resistance lower than 100 MΩ were excluded from analysis. Cells with RMS noise higher than 4 and events with rise times longer than 5ms were also excluded.

Data Analysis

Acquired mEPSCs and mIPSCs were analyzed with a Mini Analysis program (Synaptosoft, Decatur, GA), with a detection threshold set at 3 times the root mean square (RMS) noise level. One factor analysis of variance (ANOVA) was used to analyze data across multiple groups, Student's t-test was used for two-group comparisons, and Kolmogorov-Smirnov test was used for cumulative probabilities. For all tests $P < 0.05$ was considered statistically significant.

Biocytin Processing

300 µm thick cortical slices were fixed in 4% paraformaldehyde (PFA) overnight at 4°C. Slices were rinsed 2 x 10 minutes in 0.1 M phosphate buffer (PB) in mM: 19 $NaH_2PO_4 \cdot H_2O$, 81 Na_2HPO_4) at room temperature and permeabilized in 2% Triton X-100 in 0.1 mM PB for one hour. Slices were then incubated in avidin-AlexaFluor 633 or 488 conjugate diluted 1:2000 in 1% Triton X-100/0.1 M PB overnight at 4°C in the dark. After the incubation, slices were washed 2 x 10 minutes in 0.1 M PB and mounted on glass slides and allowed to dry overnight in the dark. Slides were cover-slipped with Prolong™ Anti-fade (Invitrogen) mounting media and sealed with nail polish. Images were taken using a Zeiss LSM 510 META confocal microscope.

Vocalizations

** These procedures were performed in collaboration with Kanold lab at University of Maryland, College Park (UMD CP). Half of the recordings were performed at Johns Hopkins, the other half of recordings and analysis were performed at UMD CP by Krystyna Orzechowski and Amal Isaiah respectively.

We measured ambient sound levels with a calibrated sound meter and vocalizations with an ultrasonic microphone (Avisoft UltraSoundGate 116H with Avisoft CM16; sampling rate of 150kHz and for approximately 20 hours in each condition). Ambient sound levels (40-43dB) were similar under both rearing conditions. Vocalizations were manually tagged in spectrograms using criteria previously established (Grimsley et al., 2011). Peak frequencies and durations were measured after 5 main types of calls were isolated in recordings (**Fig. 4.6A**; upgoing, downgoing, chevron, flat/harmonic and unstructured). A total of 971 calls were analyzed (428 in DE and 543 in NR condition). There were no significant differences either in durations of these calls or peak frequencies (**Fig. 4.6B-C**, duration; $F_{1,969} = 2.36$, $P = 0.13$ and frequency; $F_{1,969} = 0.53$, $P = 0.47$, ANOVA). The slopes of linear functions plotted for frequency vs. duration also were not significantly different (**Fig. 4.6D**, $F_{1,967} = 0.58$, $P = 0.45$).

Deafening

Experimental mice were initially anesthetized with isofluorane vapors (3%), after which a moderate plane of anesthesia was maintained (1.5% flow). Mice were placed in a stereotaxic apparatus (David Kopf Instruments, California) and rotated to their side so the ear faced up. The external pinnae were removed and incisions were made to the ventral

surface to enhance visualization of ear anatomy. Using a dissection microscope the tympanic membrane was lanced using a blunted 30 gauge needle. Ossicles were moved to the side to visualize the round window. 50 µl kanamycin solution (175 mg/ml saline) was infused into the inner ear, and a small piece of gel foam (Pfizer) soaked in kanamycin solution was placed in the inner ear. Incisions were sutured (PDS II: Ethicon) closed and animals were allowed to recover on a warm heat pad and returned to their cage after full consciousness was observed. Animals were kept no more than 3 per cage, and were sacrificed between 6-8 days post procedure. Deafening procedures were verified by observing startle response and hair cell ablation. One mouse was removed from the experiment due to unsuccessful deafening procedures.

Confirmation of Deafening Procedure Efficacy

Whole cochlea were removed from experimental animals and submerged in cold 4% PFA for 2 hours. 0.5 ml of 4% PFA were injected through the round window to ensure complete fixation. Cochlea were washed 3 times in 0.1 M PB and decalcified in 5% EDTA overnight. The samples were then sunk in 30% sucrose overnight and sectioned on a sliding microtome (Microtome HM400, Midwest Lab Equipment, Florida) at 60-µm thickness. Slices were permeabilized in 0.2% Triton in 0.1M PB for 1 hour, followed by staining with Alexa Fluor 488-phalloidin (Invitrogen) at 1:200 dilution for 2 hours. Slices were also counterstained for DAPI at 1:5000 dilution (Invitrogen). Cochlear slices were mounted to glass slides and cover-slipped using ProLong Gold antifade reagent (Life Technologies). Confocal z-stacks were obtained using a Zeiss LSM510 Meta confocal microscope. Destruction of hair cells was verified for all

deafened animals, and the presence of intact hair cells was verified for all control animals (**Fig. 4.4**).

To test hearing, mice were brought to a quiet isolation room 30 minutes prior to observation. Pairs of control and deaf animals were placed in individual clean cages with bedding for a 10-minute habituation period. Animals were observed with a webcam (Logitech) suspended 1 meter above the cages. Video clips were obtained with 3 seconds pre and 5 seconds post sound exposure to observe the startle response to 90dB sounds played twice at random intervals over a 5 minute period. A naïve observer scored the videos. All (6/6) control animals showed startle responses while only 1/5 deafened animals showed a partial response (i.e. startled for 1 of 2 repeats).

Chapter 3: Developmental switch in the polarity of experience-dependent synaptic changes in layer 6 of mouse visual cortex.

** Reproduced with journal's permission from: (Petrus et al., 2011).

Abstract

Layer 6 (L6) of primary sensory corticex is distinct from other layers in that it provides a major cortical input to primary sensory thalamic nuclei. L6 pyramidal neurons in the primary visual cortex (V1) send projections to the lateral geniculate nucleus (LGN) as well as to the thalamic reticular nucleus and higher order thalamic nuclei. Although L6 neurons are proposed to modulate the activity of thalamic relay neurons, how sensory experience regulates L6 neurons is largely unknown. Several days of visual deprivation homeostatically adjusts excitatory synapses in L4 and L2/3 of V1 depending on the developmental age. For instance, L4 exhibits an early critical period during which visual deprivation homeostatically scales up excitatory synaptic transmission. On the other hand, homeostatic changes in L2/3 excitatory synapses are delayed and persist into adulthood. In the present study we examined how visual deprivation affects excitatory synapses on L6 pyramidal neurons. We found that L6 pyramidal neurons homeostaticaly increase the strength of excitatory synapses following 2 days of dark exposure (DE), which was readily reversed by 1 day of light exposure. This effect was restricted to an early critical period, similar to that reported for L4 neurons. However, at a later developmental age, a longer duration of DE (1 wk) decreased the strength of excitatory synapses, which reversed to normal levels with light exposure. These changes are

opposite to what is predicted from the homeostatic plasticity theory. Our results suggest that L6 neurons differentially adjust their excitatory synaptic strength to visual deprivation depending on the age of the animals.

Introduction

Experience-dependent synaptic plasticity in sensory cortices is widely accepted to be essential for developmental fine-tuning and adaptation of cortical circuits to ongoing changes in the neural circuit that is constantly being adjusted to the environment. One form of homeostatic plasticity is global homeostatic synaptic scaling (Turrigiano et al., 1998; Turrigiano and Nelson, 2004), in which a period of inactivity results in scaling up of excitatory synaptic strength, whereas increased activity scales it down. Several studies showed that visual deprivation scales up excitatory synapses in primary visual cortex (V1), but such changes happen at distinct periods during postnatal development depending on the lamina. For instance, layer 4 (L4) neurons show an early critical period for synaptic scaling, which starts a few days after eye opening at around postnatal day 16 (P16) and ends within a few days, by P21 (Desai et al., 2002). On the other hand, in L2/3 neurons, homeostatic synaptic scaling starts later at around P21 (Desai et al., 2002) and persists into adulthood (Goel and Lee, 2007). A recent study showed that in L5, visual deprivation suppresses intrinsic excitability of pyramidal neurons and promotes high-frequency firing-induced LTP of intrinsic excitability (Nataraj et al., 2010). This contrasts a lack of change in intrinsic excitability of L4 neurons (Maffei et al., 2004). Collectively, these results suggest that principle neurons in different layers of V1 undergo distinct

homeostatic regulation with visual deprivation. In this study, we examined whether and how visual experience alters excitatory synapses on L6 pyramidal neurons.

In a canonical circuit of V1, L6 is similar to L4 in that it receives direct thalamocortical inputs as well as processed intracortical inputs (Ribak and Peters, 1975; Levay and Gilbert, 1976; Burkhalter, 1989; Binzegger et al., 2004; Zarrinpar and Callaway, 2006; da Costa and Martin, 2009). However, L6 differs from L4 in that one of its outputs targets the dorsal lateral geniculate nucleus (dLGN), often with collaterals innervating the thalamic reticular complex, and a subset of its neurons targets higher order thalamic nuclei (Bourassa and Deschenes, 1995). There is evidence that corticogeniculate inputs originating from L6 modulate sensory processing of LGN neurons in diverse species (McClurkin and Marrocco, 1984; Marrocco et al., 1996; de Labra et al., 2007; Briggs and Usrey, 2009). Despite their proposed role in shaping visual processing in LGN (Thomson, 2010), there is little information as to how L6 neurons alter their synapses following alterations in visual experience. Here we report that the changes in visual experience lead to differential regulation of excitatory synapses of L6 pyramidal neurons depending on the developmental age of the animal.

Results

Visual deprivation scales up excitatory synapses in L2/3 and L4 of V1, but with distinct critical periods. Synaptic scaling in L4 has an early critical period that closes by P21, while in L2/3 it starts by P21 (Desai et al., 2002) and persists into adulthood (Goel and Lee, 2007). To determine whether L6 neurons undergo homeostatic synaptic

changes during a defined critical period, we dark-exposed (DE) mice for a few days (2 or 7 days) starting at different ages (P16 or P21), and measured AMPAR-mediated miniature excitatory postsynaptic currents (mESPCs) in visually identified L6 pyramidal neurons. A subset of the cells was filled with biocytin to confirm their location in L6 and identify the pyramidal shaped morphology of their soma (**Fig. 3.1A**).

Dark-exposure increases AMPA receptor-mediated mEPSC amplitude in L6 of P16 mice

DE for 2 days starting at P16 significantly increased the average mEPSC amplitude in L6 pyramidal neurons, which was reversed with 1 day of light exposure [P16 normal-reared (NR), 13.5 ± 1.4 pA, n = 10; DE, 21 ± 1.7 pA, n = 10; light exposure (LE), 13.9 ± 0.8 pA, n = 9; ANOVA, $F_{(2,26)} = 9.98$, $p < 0.001$] (**Fig. 3.1B-D**). The decrease in mEPSC amplitude in the 1-day light exposure group was accompanied by a significant increase in mEPSC decay kinetics (Table 1), which suggests changes in AMPAR function (Mosbacher et al., 1994). On the other hand, there was no significant difference either in the average mEPSC frequency (P16 NR, 1.4 ± 0.5 Hz, n = 10; DE, 2.1 ± 0.8 Hz, n = 10; LE, 0.5 ± 0.07 Hz, n = 9; ANOVA, $F_{(2,26)} = 2.04$, $p > 0.15$) (**Fig. 3.1E**) or in the general cell properties (Table 2.1 - appendix) among the three groups.

Previously, we reported that in L2/3 neurons the DE-induced scaling up of mEPSCs follows the rules of multiplicative synaptic scaling (Goel et al., 2006; Goel and Lee, 2007; Gao et al., 2010). The interesting property of multiplicative synaptic scaling is that it allows preservation of relative differences in synaptic strength across synapses despite global changes across all synapses (Turrigiano et al., 1998; Turrigiano and Nelson, 2004). To test whether the DE-induced scaling in L6 is multiplicative, we

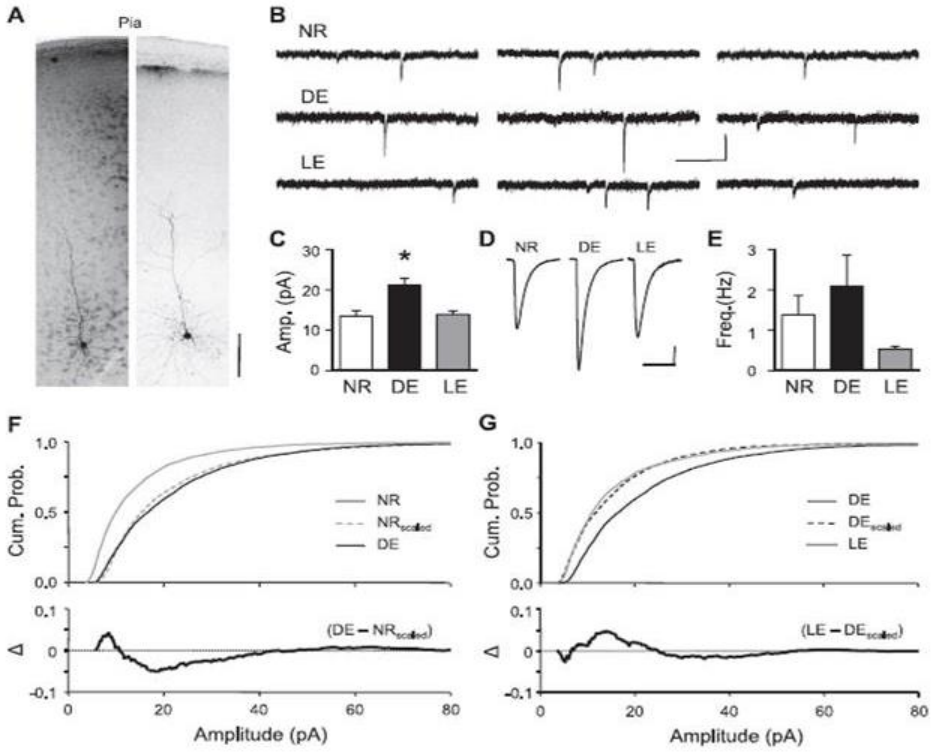

Figure 3.1: Brief manipulations of visual experience homeostatically regulate miniature excitatory postsynaptic currents (mESPCs) of L6 neurons of postnatal day 16 (P16) mice. **A.** examples of biocytin-filled L6 pyramidal neurons in V1. Fluorescent images of processed V1 slices are shown in inverted grayscale for better visualization of the filled neurons. The images are projected images of z-stacks (40 stacks at 3-µm intervals). Scale bar: 100 µm. **B.** Representative mEPSC traces from a normal-reared (NR; 3 traces at top), a dark=exposed (DE; 3 traces at middle), and a light-exposed (L#; 3 traces at bottom). Each traces is 1 sec in duration. Scale bars: 20 pA, 250 ms. **C.** Average mEPSC amplitude increased with 2 days of DE and reversed after 1 day of LE. * $P < 0.001$ [1-way ANOVA followed by Fisher's protected least significant difference (PLSD) post hoc test, $P < 0.002$]. **D.** average mEPSC traces. Scale bars: 3 pA, 15 ms. **E.** Average mEPSC frequency was not significantly changed **F.** top: cumulative probability graph showing mEPSCs of NR (solid gray line) are smaller than those of DE (solid black line). NR_{scaled} (dashed gray line) reprsents NR mEPSCs scaled up by a scaling factor of 1.54 to match the average mEPSC amplitude to that of DE. Note that the cumulative probability curves of NR_{scaled} and DE are significantly different (Kolmogorov-Smirnov test, $P < 0.005$), which suggests that the change sis not multiplicative. Bottom: subtraction of cumulative probability graphs of DE and NR_{scaled}; to illustrate the nonmultiplicative change (Δ = DE - NR_{scaled}). **G.** Top: cumulative probability graph demonstrating that 1 day of LE (gray line) decreased mEPSC amplitudes compared with DE (black line) levels. Scaling factor is 0.71 for the De_{scaled} (dashed line). The cumulative probability curves of DE_{scaled} and LE are significantly different (Kolmogorov-Smirnov test, $P < 0.02$). Bottom: subtraction of cumulative probability graphs of LE and DE_{scaled} (Δ = LE - DE_{scaled}). Amp., amplitude; Freq., frequency; Cum. Prob., cumulative probability.

compared the cumulative probability curve of mEPSC amplitude of DE with that of NR mEPSCs scaled up by multiplying with a factor of 1.54 (NR_{scaled}) to match the average mEPSC to that of DE. We found that the cumulative probability of mEPSCs from DE and NR_{scaled} are significantly different (Kolmogorov-Smirnov test, $p < 0.001$) suggesting that the change is not multiplicative (**Fig. 3.1F**). This was also the case for DE and LE groups (DE_{scaled}: scaling factor 0.71; Kolmogorov-Smirnov test, $p < 0.001$) (**Fig. 3.1G**). These results suggest that visual experience-dependent homeostatic plasticity does not affect all synapses in L6 neurons equally.

Lack of homeostatic synaptic plasticity in L6 of p21 mice

Next, we determined whether DE-induced changes in L6 neurons are restricted to an early critical period, as in L4 (Desai et al., 2002). To test this, mice were dark-exposed for 2 days from P21 to P23. In contrast to younger mice, at this later age 2 days of DE did not significantly change either the average amplitude of the mEPSCs (P23 NR, 13.1 ± 0.9 pA, n = 10; DE, 13.8 ± 1.1 pA, n = 10; t-test, $p > 0.59$) (**Fig. 3.2A-C**) or their average frequency (P23 NR, 1.8 ± 0.3 Hz, n = 10; DE, 1.3 ± 0.2 Hz, n = 10; t-test, $p > 0.19$) (**Fig. 3.2D**). Interestingly however, DE significantly altered the amplitude distribution of the mEPSC amplitudes (Kolmogorov-Smirnov test, $p < 0.0001$) (**Fig 3.2E** top). Interestingly, however, DE significantly altered the amplitude distribution of the mEPSC amplitudes (Kolmogorov-Smirnov test, $p < 0.0001$) **(Fig. 3.2E, top**). In particular, there was an increase in the fraction of smaller and larger mEPSCs at the expense of medium sized mEPSCs in the DE group compared to NR (**Fig. 3.2E**, bottom). This suggests that excitatory synapses on L6 neurons are malleable with visual deprivation at this later age, but the direction and magnitude of changes across all the synapses cancel each other such

that there is no net alteration in average synaptic weight. In any case, our results support the idea that L6 and L4 share similarities of having an early critical period for homeostatic synaptic plasticity with brief duration of DE.

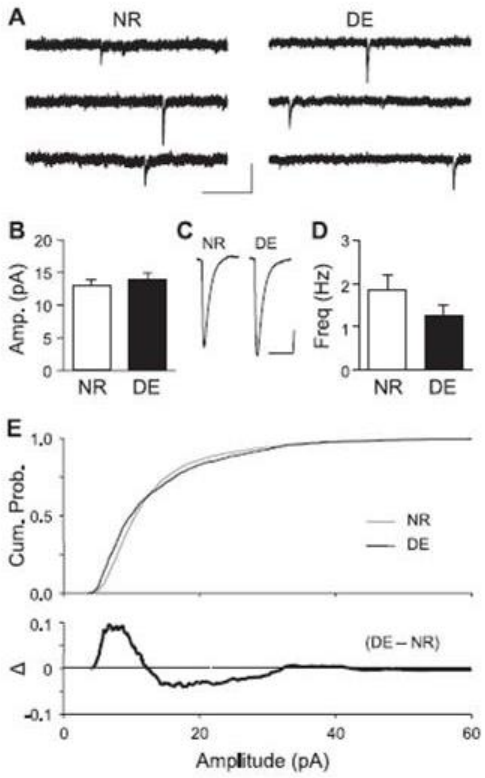

Figure 3.2: Two days of DE initiated at p21 fails to change the average mEPSC amplitude in L6 neurons. **A.** representative mEPSC traces from NR (3 traces at left) and DE cells (3 traces at right). Scale bars: 20pA, 250 ms. **B.** no significant change in average mEPSC amplitudes of NR and 2-day DE. **C**/ average mEPSC traces. Scale bars: 3pA, 15 ms. **D.** no significant change in average mEPSC frequency between NR and 2-day DE. **E.** top: comparison of mEPSC cumulative probability of NR (gray line) and DE (black line). The cumulative probability curves of NR and **D** are significantly different (Kolmogorov-Smirnov test, $P < 0.0001$. Bottom: subtraction of cumulative probability graphs of DE and NR (Δ = DE – NR).

A longer duration of DE decreases L6 mEPSCs in p21 mice

To determine whether the absence of homeostatic synaptic plasticity in L6 at later ages is due to a complete termination of the plasticity mechanisms or due to a requirement of a longer duration of visual deprivation, we repeated the study using 7 days

of DE (7d-DE) initiated at P21. Surprisingly, we found that the longer duration of DE now decreased the average mEPSC amplitude in L6 neurons, which reversed back to normal levels with 1 day of light exposure (P28 NR, 12.5 ± 0.8 pA, n = 12; DE, 10.6 ± 0.6 pA, n = 14; LE, 13.4 ± 0.9, n = 13; ANOVA $F_{(2,36)} = 3.382$, $p < 0.05$) (**Fig. 3.3A-C**). There was no significant change in mEPSC frequency (P28 NR, 1.0 ± 0.2 Hz, n = 12; DE, 1.6 ± 0.3 Hz, n = 14; 1d-LE, 1.4 ± 0.4, n = 13; ANOVA $F_{(2,36)} = 1.105$, $p > 0.34$) (**Fig. 3.3D**), suggesting a postsynaptic change. The 7d-DE group showed an increase in the mEPSC decay time constant (τ), which reversed back to NR levels with 1-day of light exposure (Table 3.1 - appendix). This further corroborates postsynaptic regulation of AMPAR function. The decrease in mEPSC amplitude following 7d-DE was not multiplicative in nature, because the cumulative probability curve of mEPSCs of NR scaled down with a scaling factor of 0.85 (NR_{scaled}) was significantly different from that of DE (Kolmogorov-Smirnov test, $p < 0.001$) (**Fig. 3.3E**). Re-exposure to light for 1 day after 7d-DE was sufficient to increase the mEPSC amplitude to NR levels with a scaling factor of 1.26, but again in a non-multiplicative manner (Kolmogorov-Smirnov test, $p < 0.001$) (**Fig. 3.3F**). These data suggest that later in development L6 neurons respond to a longer duration of visual deprivation by decreasing the strength of their excitatory synapses, but this novel form of synaptic plasticity is in an opposite direction to what is predicted from the homeostatic synaptic scaling hypothesis.

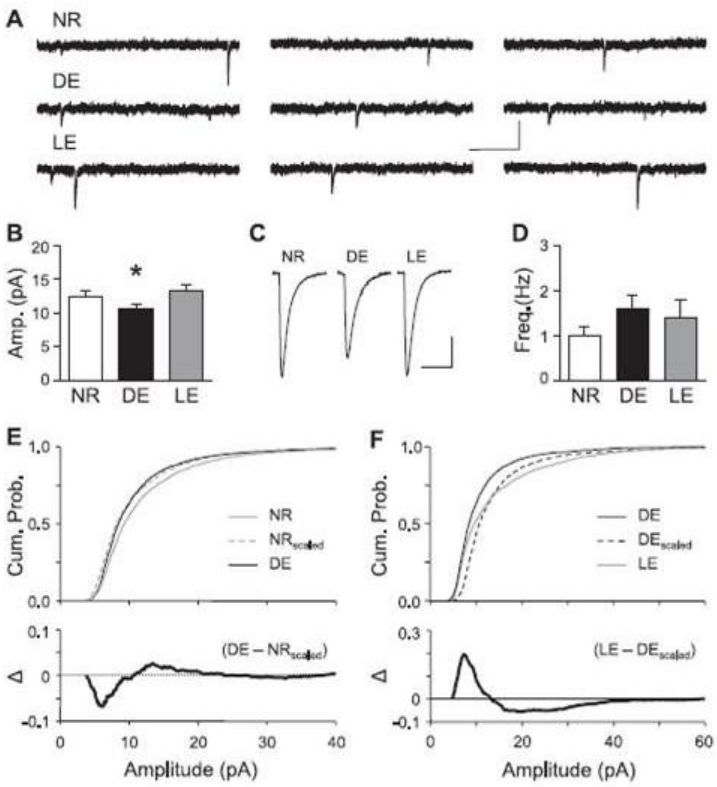

Figure 3.3: L6 neurons undergo nonhomeostatic regulation of mEPSCs with 7 days of DE initiated at p21. **A.** Representative mEPSC traces from NR (3 traces at top), DE (3 traces at middle) and LE cells (3 traces at bottom). Scale bars: 20pA, 250 ms. **B.** Average mEPSC amplitude significantly decreased with 7 days DE, which reversed with 1 day of LE. * $P < 0.05$ (1-way ANOVA, followed by Fisher's PLSD post hoc test, $P < 0.002$). **C.** average mEPSC traces. Scale bars: 3 pA, 15 ms. **D.** No significant change in mEPSC frequency across NR, 7-day DE, and 1-day LE. **E.** Top: cumulative probability of mEPSC amplitudes from NR (solid gray line) and 7-day DE (solid black line) groups. The curve for NR_{scaled} (dashed gray line) represents mEPSCs of NR that were scaled down by a scaling factor of 0.84 to match the average mEPSC amplitude to that of DE. There was a significant difference between NR_{scaled} and DE (Kolmogorov-Smirnov test, $P < 0.0001$), suggesting a nonmultiplicative change sin synaptic strength. Bottom: subtraction of cumulative probability graphs of DE and NR_{scaled} (Δ = DE - NR_{scaled}). **F.** top: cumulative probability of mEPSC amplitudes of 7-day DE (solid black line), 1-day LE (solid gray line) and DE_{scaled} (dashed black line). mEPSC amplitudes of DE were multiplied by a scaling factor of 1.37 to obtain DE_{scaled}, which matched in average mEPSC amplitude to that of LE. There was a statistically significant difference between LE and DE_{scaled} (Kolmogorov-Smirnov test, $P < 0.0001$). Bottom: subtraction of cumulative probability graphs of LE and DE_{scaled} (Δ = LE – De_{scaled}).

Discussion

We demonstrated that L6 neurons share similarities with L4 neurons in that they display an early critical period for homeostatic synaptic plasticity with a brief duration of DE. The homeostatic increase in mEPSC amplitude of L6 neurons triggered by 2 days of DE was rapidly reversed by 1 day of light exposure. While 2 days of DE initiated later in life (at P21) was ineffective at causing a net change in the average mEPSC amplitude, a longer duration of DE decreased the average mEPSC amplitude (**Fig. 3.4A**). The visual experience-induced changes in mEPSC amplitude at both younger and older ages did not accompany alterations in mEPSC frequency, but was associated with changes in mEPSC decay kinetics, which suggest that they occur via postsynaptic regulation of AMPARs.

Our observation that L6 neurons of young mice homeostatically increase their excitatory synapses with brief DE only early in development is similar to observations made in L4 (Desai et al., 2002). These results corroborate the idea that thalamic recipient layers are highly plastic during an early critical period. While the direction of change in mEPSCs with 2 days of DE is consistent with what is expected of a homeostatic adaptation, it did not occur via a multiplicative synaptic scaling mechanism. This is qualitatively different from multiplicative synaptic scaling observed in L2/3 at a later developmental time point (i.e. P21-P28 range) (Goel et al., 2006; Goel and Lee, 2007; Gao et al., 2010). Whether the L4 neurons scale multiplicatively with DE was not determined in a previous study (Desai et al., 2002). The non-multiplicative changes in L6 mEPSCs could be due to many factors. One possibility is that the changes triggered by DE are restricted to a subset of synapses. L6 neurons not only receive direct geniculocortical inputs (Ribak and Peters, 1975; Levay and Gilbert, 1976), like L4, but

they also receive diverse sets of inputs as shown from synaptic responses elicited in response to uncaging glutamate in L2/3, L4, L5, and L6 (Zarrinpar and Callaway, 2006). It is interesting to note that L6 receives less LGN inputs than L4 (Ribak and Peters, 1975; Binzegger et al., 2004; da Costa and Martin, 2009). In a recent anatomical study, it was estimated that corticothalamic L6 neurons in cat V1 receive about 20 geniculocortical synapses, mainly onto their basal dendrites (da Costa and Martin, 2009). Collectively, these results would suggest that intracortical inputs are likely highly represented in the recorded mEPSCs. Whether visual experience differentially affects geniculocortical and intracortical inputs or intracortical inputs originating from specific layers would require further studies. As a note of caution, we cannot rule out the possibility that visual experience may have altered the dendritic cable properties, which could have influenced the sampling of a subset of synaptic populations. However, it is unlikely that this could happen at a gross level, because we did not see a correlation between dendritic filtering and experimental manipulations.

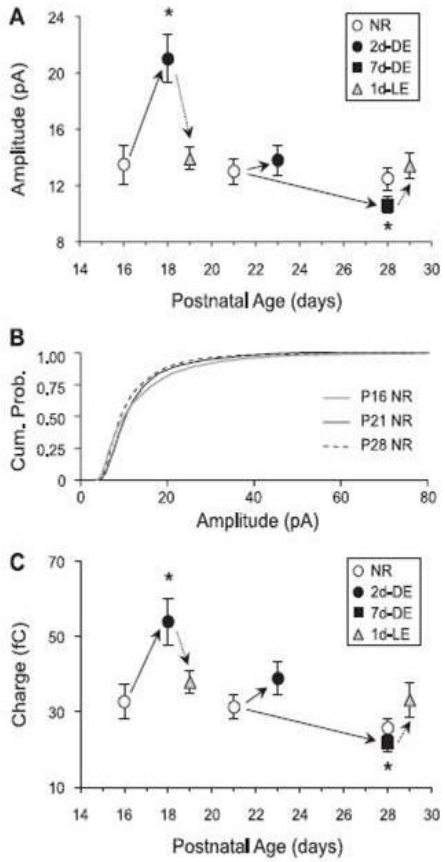

Figure 3.4: A summary of mEPSC amplitude changes in L6 neurons induced by manipulation of visual experience across different ages. **A.** there was no significant changes in the average mEPSC amplitude across ages between p16 and p28 in NR controls (open circles). Two days of DE (solid circles) initiated at p14 increased the average mEPSC amplitude, but when initiated at p21, DE failed to alter the average mEPSC amplitude. However, 7 days of DE (solid squares) initiated at p21 significantly decreased the average mEPSC amplitude. One day of LE (1d-LE; shaded triangles) reversed the changes in mEPSC amplitude caused by DE. *$P < 0.05$ (1-way ANOVA followed by Fisher's PLSD post hoc test). **B.** difference in cumulative probability curves of mEPSC amplitude in p16, p21 and p28 NR groups (Kolmogorov-Smirnov test: $P < 0.0001$ across all groups). Data shown in previous figures are replotted here for direct comparison. **C.** comparison of average charge transfer of mEPSCs. Symbols are the same as in **A**. * $P < 0.05$ (1-way ANOVA followed by Fisher's PLSD post hoc test).

An unexpected finding from our work is that at P21, a short duration (2 days) of DE did not cause a net change, but a longer duration (7 days) of DE decreased the average amplitude of mEPSCs. Even though 2 days of DE did not result in a net change

in the average mEPSC amplitude, there was a significant shift in the distribution of mEPSCs. This suggests that a short duration of DE increases and decreases the strength of individual synapses on L6 neurons, but these cancel each other such that there is no net change in the average (**Fig. 3.2E**, bottom). However, with a longer duration DE, L6 synapses weakened overall. The decrease in mEPSCs with 7 days of DE is contrary to what is expected of a homeostatic adaptive change, which predicts that loss of visually driven activity in V1 would scale up excitatory synapses. Further, it distinguishes L6 plasticity from L2/3 plasticity at this developmental age. We reported previously that the same durations of DE scales up mEPSC amplitude in L2/3 (Goel et al., 2006; Goel and Lee, 2007; Gao et al., 2010). The unexpected decrease in the average mEPSC amplitude of L6 neurons in response to 1 week of DE may reflect adaptation to an increase in input activity from other cortical layers, which project back to L6. However, this is unlikely, considering a recent study showing that visual deprivation decreases the intrinsic excitability of L5 (Nataraj et al., 2010), which provides a major input to L6 (Zarrinpar and Callaway, 2006). Alternatively, the DE-induced decrease in mEPSCs may be a manifestation of a non-homeostatic synaptic plasticity, such as long-term depression (LTD), which is expected from a reduction of input activity to specific sets of synapses. It is known that L6 neurons undergo pairing-induced LTD of intracortical inputs originating from superficial layers, which depends on the activation of metabotropic glutamate receptors (mGluRs) (Rao and Daw, 2004). In any case, the decrease in mEPSC amplitude was not multiplicative, and was readily reversed by 1 day of light exposure. Furthermore, the decrease in mEPSC amplitude with 7 days of DE was associated with a concomitant increase in the mEPSC decay kinetics, which suggests that

the changes are mediated by regulation of postsynaptic AMPAR function. Specifically, our data suggest that the mEPSC amplitude changes may be due to regulation of AMPAR subunit composition, because AMPARs containing the edited form of GluA2 (or GluR2) subunit display slower decay kinetics and lower conductance than GluA2-lacking receptors (Mosbacher et al., 1994). The regulation of GluA2-lacking AMPARs was also observed in L2/3 accompanying multiplicative homeostatic synaptic plasticity (Goel et al., 2006). These results suggest that the regulation of AMPAR subunit composition may be a general mechanism for adjusting synaptic gain in V1 regardless of the mode of synaptic plasticity. While the exact nature of synaptic changes in L6 at older developmental ages would require further investigation, our findings suggest that L6 synapses, at least a subpopulation of them, are capable of undergoing plastic changes with visual deprivation even after the short early critical period for homeostatic synaptic plasticity.

We have shown that visual deprivation leads to two distinct outcomes at L6 excitatory synapses depending on the age of the animal and the duration of visual deprivation. While we did not observe a significant change in the average mEPSC amplitude across the developmental ages examined (**Fig. 3.4A**), we nonetheless found that that distribution of mEPSC amplitudes significantly changed (**Fig. 3.4B**). This suggests that there is considerable adjustment of excitatory synaptic gain during this developmental period, which may alter the rules of experience-dependent synaptic plasticity. Considering that L6 neurons provide cortical input to the LGN, their synaptic regulation with visual deprivation is likely to alter LGN processing of visual information.

Chapter 4: Crossmodal Induction of Thalamocortical Potentiation in the Adult Auditory Cortex

** Reproduced with journal's permission from: (Petrus et al., 2014).

Abstract

Sensory systems do not work in isolation; instead they show interactions that are specifically uncovered during sensory loss. To identify and characterize these interactions, we investigated whether visual deprivation leads to functional enhancement in primary auditory cortex (A1). Here we demonstrate that in adults, visual deprivation strengthens thalamocortical (TC) synapses in A1, but not in primary visual cortex (V1). Because deafening potentiated TC synapses in V1, but not A1, crossmodal TC potentiation seems to be a general property of adult cortex. Our results suggest that adults retain the capability for crossmodal changes whereas such capability is absent within a sensory modality. Thus, multimodal training paradigms might be beneficial in sensory-processing disorders.

Introduction

Early blindness leads to behaviorally-observed cross-modal benefits such as improved frequency discrimination performances (Gougoux et al., 2004) and sound localization abilities (Lessard et al., 1998) which is also observed in late blind individuals (Voss et al., 2004). However, whether and how A1 neuronal responses are altered by

losing vision and the underlying changes in A1 cortical circuitry are unknown. In particular, whether the cross-modal changes are manifested as changes in the thalamorecipient layer, which receives direct feed-forward sensory inputs, is not known.

The connectivity and organization of A1, in particular at the level of thalamocortical (TC) inputs can be modified by auditory experience during an early critical period which occurs between P12-P15 in mice (de Villers-Sidani et al., 2007; Insanally et al., 2009; Sanes and Bao, 2009; Barkat et al., 2011), thus unimodal experience has an influence only during early life. This narrow plastic window observed in TC inputs is also observed in visual cortex (V1) (Katz and Crowley, 2002; Hensch, 2005) indicating that TC inputs may be less plastic later in life. However, recent evidence suggests that TC plasticity can be reactivated later in life following sensory deprivation or in response to peripheral nerve transection (Montey and Quinlan, 2011; Oberlaender et al., 2012; Yu et al., 2012).

Cross-modal plasticity was first observed at the synaptic level as a global reduction in the postsynaptic strength of excitatory synaptic transmission in layers 2/3 (L2/3) of A1 and barrel cortex after visual deprivation (Goel et al., 2006) and has different deprivation requirements than unimodal plasticity (He et al., 2012). The reduction in excitatory synaptic strength was in contrast to a global increase in the strength of excitatory synapses observed in deprived V1, which may indicate a homeostatic adaptation to increased activity in the spared sensory cortices (Whitt et al., 2013). Therefore, we examined whether the feed-forward TC inputs to A1 are altered cross-modally, and how this impacts A1 neuronal properties in the TC recipient layer 4 (L4). Here we report that depriving adult mice of vision for a short period of time causes

potentiation of auditory TC synapses in A1. These cross-modal changes in A1 circuitry may play a role in the enhancement of auditory perception in blind individuals.

Results

We performed visual deprivation after the thalamocortical (TC) critical period for hearing (de Villers-Sidani et al., 2007; Insanally et al., 2009; Sanes and Bao, 2009; Barkat et al., 2011) in A1 by exposing mice (C57/BL6 strain, p90-100) to darkness (DE) for 7 days. Neurons in A1 L4 exhibited enhanced frequency selectivity and heightened sound sensitivity after DE, indicating enhanced hearing capabilities after the loss of vision (Petrus et al., 2014). Cells in A1 L4 receive TC as well as intracortical inputs. To test the hypothesis that these changes were mediated by stronger feed-forward inputs from the thalamus, we examined the cross-modal regulation of these synapses using optogenetics. We injected adeno-associated virus containing channelrhodopsin-2 (AAV-ChR2) into the medial geniculate body (MGB, auditory thalamus) of mice 6-8 weeks prior to experiments after which DE was initiated around P90, with a subset of mice returned to the normal environment for 7 days of light exposure (LE). NR controls were kept in the normal light/dark cycle. A1 slices were made from NR, DE and LE mice and L4 principal neurons were patched for whole-cell recordings. The borders of A1 were well-delineated by yellow fluorescence protein (EYFP) expressed in the transfected TC-terminals (**Fig. 4.1A**).

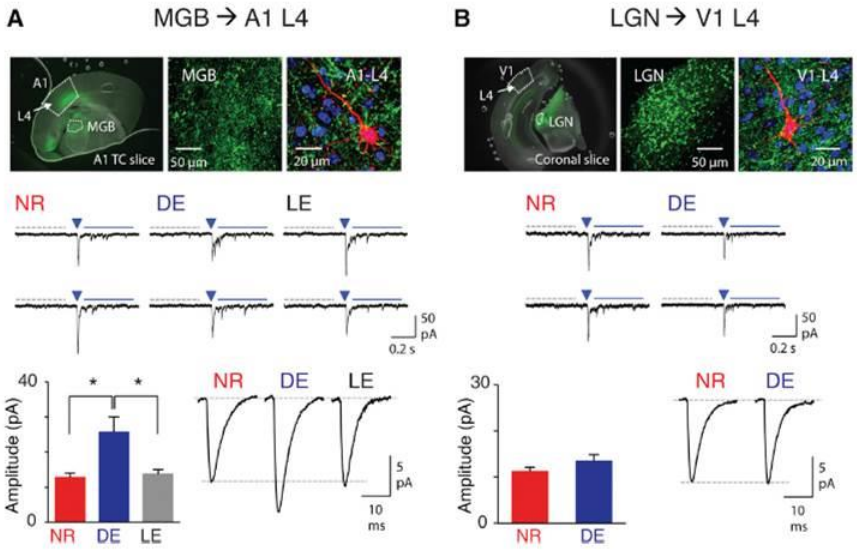

Figure 4.1: Crossmodal Potentiation of TC Synapses in A1 without Changes in V1. **A.** Cross-modal regulation of TC synapses in A1-L4. Top: AAV-ChR2-EYFP injection to MGB. Note expression of EYFP (green) in MGB (left and center panels). Top right: a biocytin-filled A1-L4 neuron (red) with DAPI (blue) and EYFP (green). Middle: Example traces of LEv-Sr^{2+}-mEPSCs from NR, DE, and LE groups. A 5 ms duration LED light was delivered at the arrowhead to activate TC synapses. Spontaneous events were collected during a 400 ms window (gray dotted line) before the LED, and LEv-Sr^{2+}-mEPSCs were measured during a 400ms window 50ms after the LED (blue solid line). Bottom left: average calculated LEv-Sr^{2+}-mEPSCs amplitude of TC inputs. *$p < 0.04$, ANOVA. Bottom right: average raw LEv-Sr^{2+}-mEPSCs traces (without subtracting spontaneous events). **B.** TC synapses in V1-L4. Top: AAV-ChR2-EYFP inection to LGN. Note EYFP (green) in LGN (left and center panels). Top right: a biocytin-filled V1-L4 neuron (red) with DAPI (blue) and YFP (green). Middle: Example traces of LEv-Sr^{2+}-mEPSCs. Marks are the same as in **A**. Bottom left: average calculated LEv-Sr^{2+}-mEPSCs amplitude of TC inputs. Bottom right: average raw LEv-Sr^{2+}-mEPSCs traces. Bar graphs are mean ± SEM.

To quantitatively compare the strength of individual TC-synapses independent of ChR2 expression level, we replaced Ca^{2+} with Sr^{2+} in the bath. Sr^{2+} desynchronizes evoked release, such that individual events reflect single vesicle release which allows determination of quantal synaptic response size (Gil et al., 1999). We then measured the amplitude of light evoked strontium-desynchronized miniature excitatory postsynaptic currents (LEv-Sr^{2+}-mEPSCs) in L4 neurons. Basal spontaneous events were

mathematically subtracted to obtain the amplitude of evoked TC LEv-Sr^{2+}-mEPSCs. We found that DE significantly increased the amplitude of TC LEv-Sr^{2+}-mEPSCs in L4 neurons compared to NR in A1, which reversed with LE **(Fig. 4.1A).** We next determined if changes occurred in TC-synapses in L4 of the primary visual cortex (V1) by injecting AAV-ChR2 into the lateral geniculate nucleus (LGN) and recording in V1 **(Fig. 4.1B)**. In contrast toL4 of A1, TC-synapses in L4 of V1 were unaltered after DE **(Fig. 4.1B)**. This is consistent with a narrow critical period for synaptic scaling and plasticity in V1-L4 following visual deprivation (Desai et al., 2002; Jiang et al., 2007).

Cross-modal potentiation of TC-synapses in A1-L4 after DE was opposite in polarity to the mEPSC changes observed previously in A1-L2/3 of juvenile animals (Goel et al., 2006). We determined that the polarity of cross-modal synaptic changes is laminar-specific, because DE triggers potentiation of excitatory synapses in L4 of A1 regardless of age. In both juveniles (P28) and adults (P90), DE increased mEPSC amplitude in A1-L4, both of which recovered after LE (**Fig. 4.2A, B**).

L4 changes did not occur via multiplicative scaling (**Fig. 4.2C, D**) suggesting that the change is not uniform across the sampled synapses. The most parsimonious explanation is that the change is restricted to a subset of synapses, which may include TC-synapses. The regulation of A1-L4 mEPSC amplitude by DE was not strain-specific, and was also observed in adult CBA mice (**Fig. 4.2E**).

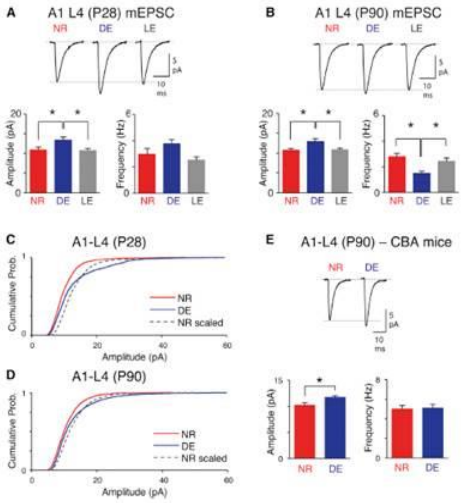

Figure 4.2: Crossmodal Potentiation of A1 L4 mEPSCs is Age-Independent and Nonmultiplicative. **A.** Results from juvenile (P28) mice. DE increase the average mEPSC amplitude of A1 L4 neurons, which reverses with LE (bottom left). Top: average mEPSC traces. Bottom right: average mEPSC frequency. **B.** Results from adult (P90) mice. In A1 L4, DE increases the mEPSC amplitude, which reverses with LE (B, bottom left). Top: average mEPSC traces. Bottom right: average mEPSC frequency. *$p < 0.05$, ANOVA. **C.** DE induces a nonmultiplicative increase in mEPSC amplitude of A1 L4 in young mice. The amplitudes of NR mEPSCs were multiplied by a scaling factor of 1.27 to match the average mEPSC amplitude to that of DE (Kolmogorov-Smirnov test between DE and NR scaled: $p < 0.0001$). **D**. Nonmultiplicative increase in mEPSC amplitude of A1 L4 in p90 mice with DE. Scaling favtor was 1.17 (Kolmogorov-Smirnov test between DE and NR scaled: $p < 0.0001$). **E.** DE increases the average mEPSC amplitude of A1 L4 neurons of CBA mice, which do not undergo age-related hearing loss. Top: average mEPSC amplitude comparison. Bottom left: average mEPSC traces. Bottom right: No change in the average mEPSC frequency. * $p < 0.02$, t-test. Bar graphs are mean ± SEM.

In contrast to A1, mEPSC amplitude did not change with DE in V1-L4 (**Fig. 4.3**), which is consistent with the stability of TC-synapses when within-modality sensory manipulations are performed in adults.

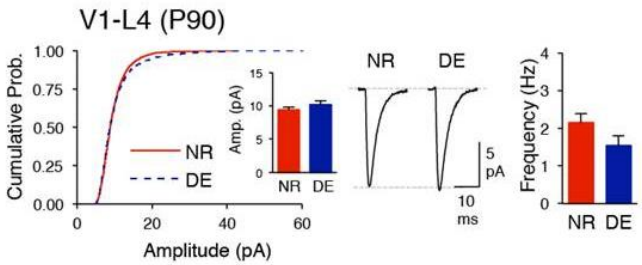

Figure 4.3: Absence of a regulation of mEPSCs in V1 L4 in adults (P90). Left: Cumulative probability of mEPSC amplitudes. Inset: Average mEPSC amplitude. Middle: Average mEPSC traces. Right: Average mEPSC frequency.

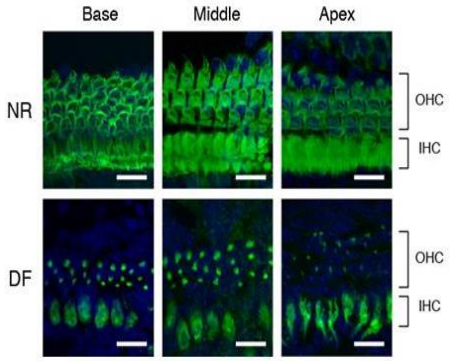

Figure 4.4: Confirmation of cochlear damage by phalloidin staining of hair cells. Alexa488-conjugated phalloidin staining (green) of cochlear hair cells from a normal-reared (NR) mouse (top panels) and a deaf (DF) mouse (bottom panels). Sections were counterstained with DAPI (blue). Sections were taken from the basal, middle, and apical portions of the cochlea. Note abnormal degenerated hair cells in the DF samples. OHC: outer hair cells. IHC: inner hair cells. Scale Bars: 15 µm.

DE-induced potentiation of TC-synapses in A1-L4 without changes in V1-L4 was unexpected, because it suggests that TC-plasticity is more readily recruited *across* sensory modalities than *within* a sensory modality in adults. To determine whether the cross-modal potentiation of TC-synapses is a general feature of the adult sensory cortex, we repeated the study in mice that were deafened by ototoxic lesioning of the cochlea (**Fig. 4.4**). We found that the strength of TC-synapses in L4 of A1, as measured as the amplitude of LEv-Sr^{2+}-mEPSCs after expressing ChR2 into the MGB, did not differ between normal and deaf (DF) adult mice (**Fig. 4.5A**).

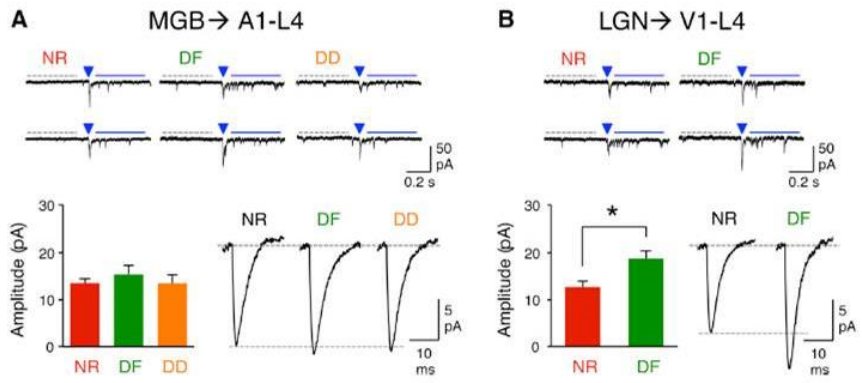

Figure 4.5: Crossmodal Potentiation of TC Synapses is Observed with Deafening and Is Experience Dependent. **A**. Regulation of TC synapses in A1 L4. Top: Example traces of LEv-Sr^{2+}-mEPSCs from NR, deaf (DF) and DE + DF (DD) group. A 5-ms duration LED light was delivered at the arrowhead to activate TC synapses. Marks are the same as in Fig.1. Bottom left: average calculated LEv-Sr^{2+}-mEPSCs amplitude of TC inputs. Bottom right: average raw LEv-Sr^{2+}-mEPSC traces (without subtracting spontaneous events). **B.** Crossmodal potentiation of TC synapses in V1 L4 after deafening. Top: example traces of LEv-Sr^{2+}-mEPSCs. Marks are the same as in Fig.1. Bottom left: average calculated LEv-Sr^{2+}-mEPSCs amplitude of TC inputs. * $p < 0.008$, t-test. Bottom right: average raw LEv-Sr^{2+}-mEPSC traces. Bar graphs plot mean ± SEM.

In contrast, TC-synapses in L4 of V1 were significantly potentiated in adult DF mice (**Fig. 4.5B**). These results demonstrate the generality of our finding that sensory deprivation recruits TC-plasticity in other sensory cortices at an age when it does not modify TC-synapses in its respective primary sensory cortex.

We previously reported that cross-modal regulation of L2/3 synapses in barrel cortex following DE is dependent on whisker inputs without a gross change in whisking frequency (He et al., 2012). This suggests that cross-modal synaptic plasticity in L2/3 requires bottom-up sensory experience without much change in the amount of sensory drive. To determine whether cross-modal TC-potentiation is also experience-dependent, we deafened the visually deprived mice (DD). Deafening prevented the TC-potentiation associated with DE (**Fig. 4.5A**), which suggests that the cross-modal TC-potentiation

requires auditory experience. However, we did not find significant difference in the auditory environment or ultrasonic vocalizations between NR and DE mice (**Fig. 4.6**), which suggests that the bottom-up sensory input is not greatly different between the two conditions.

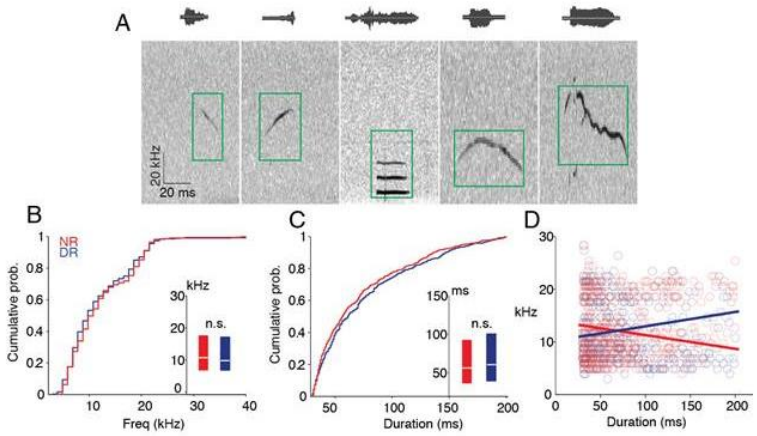

Figure 4.6: Comparisons of vocalizations under each rearing condition. **A.** Spectrograms of detected vocalizations. Green boxes indicate analyzed time window.5 main calls were distinguished upgoing, downgoing, chevron, flat/harmonic and unstructured. **B, C.** Peak frequencies (B) and durations (C) of calls were measured. There were no significant differences either peak frequencies ($F_{1,969} = 2.36$, $P = 0.13$, ANOVA) or durations ($F_{1,969} = 0.53$, $P = 0.47$, ANOVA) of these calls. **D.** The slopes of linear functions plotted for frequency vs. duration also were not significantly different from each other ($F_{1,967} = 0.58$, $P = 0.45$).

Discussion

Here we demonstrate that TC-inputs to A1, which do not modify with deafening, do potentiate following visual deprivation in adults. This, together with visual deprivation-induced cross-modal facilitation of LTP at L4 to L2/3 synapses in somatosensory barrel cortex (S1BF) (Jitsuki et al., 2011), suggests an enhancement of feed-forward sensory processing in spared senses. Recent studies highlight some degree

of TC-plasticity in adult cortices (Heynen and Bear, 2001; Cooke and Bear, 2010; Montey and Quinlan, 2011; Oberlaender et al., 2012; Yu et al., 2012). We propose that TC-plasticity is more effectively recruited *across* sensory modalities than *within* a sensory modality, which may serve as a substrate for sensory compensation throughout life. Furthermore, cross-modal TC-plasticity is likely universal across sensory systems, because we find that deafening also results in TC-potentiation in L4 of V1 in adult mice.

The novelty of our study is that TC-plasticity is recruited in adult primary sensory cortex *across* sensory modality when it is not expressed *within* a sensory modality. Furthermore, we suggest that the cross-modal recruitment of TC-plasticity in A1 may underlie the observed improvement in auditory processing with vision loss. It is known that experience-dependent TC-plasticity in primary sensory cortices is mainly restricted during an early developmental phase (Crair and Malenka, 1995; Fox, 2002; Barkat et al., 2011), which corresponds to the pre-critical period. Recently, studies have highlighted that there is some degree of plasticity at the TC inputs in adults *within* a sensory modality with manipulations such as nerve transection (Yu et al., 2012) or sensory deprivation (Montey and Quinlan, 2011; Oberlaender et al., 2012). Here we show that sensory deprivation in one modality can potentiate TC-inputs *across* sensory modalities, which supports the growing body of evidence that TC-plasticity can be effectively recruited in adults. Blind individuals show perceptual enhancement of hearing in aspects such as improved sound localization (Lessard et al., 1998; Voss et al., 2004), pitch discrimination (Gougoux et al., 2004), and spatial tuning characteristics (Roder et al., 1999). Our results show sharper tuning curves and lower activation thresholds in neurons at the thalamorecipient layer of A1 (Petrus et al., 2014), due to the observed strengthening of

feed-forward inputs. Cross-modal potentiation of TC-inputs to A1 is experience-dependent, as it required intact hearing. Because there was no significant difference in the auditory environment and vocalizations between normal and visually deprived groups, we surmise that there might be cortical and/or subcortical adjustments that allow auditory inputs to more effectively potentiate TC synapses after losing vision. Moreover, since deafening prevented the DE induced plasticity, we have shown that auditory experience is required for this plasticity to occur. The observed potentially beneficial changes in A1 TC-inputs and auditory processing could account for enhanced auditory performance in blind individuals. Moreover, since DE was able to rapidly induce changes in TC recipient neurons in adults and improve auditory processing, multisensory training paradigms may benefit individuals with central processing deficits: e.g. auditory processing disorders. Overall our results here demonstrate rapid and robust cross-modal changes in functional attributes of primary sensory cortices following the loss of a sensory modality.

Chapter 5: Changes in Excitatory and Inhibitory Circuitry in A1and V1 after Visual Deprivation

Abstract

Alterations in sensory experience result in dramatic changes in cortical wiring and synaptic strengths within a sensory modality. Recently it has been observed that the loss of one sense can cause robust changes in spared sensory cortices as well. These changes may underlie the increased sensitivity to spared senses observed clinically and anecdotally. Here we have described the laminar specific changes in evoked and spontaneous excitatory and inhibitory transmission in auditory cortex (A1) after the loss of vision in mice. The changes in circuit strengths reveal a stronger feed-forward (FF) auditory input to the superficial layers of A1 at the expense of lateral and spontaneous events, which may enhance the signal to noise ratio. An increase in evoked inhibitory strength in A1 L4 with an increased frequency of spontaneous events in A1 L2/3 were also observed, which may further enhance auditory tuning and dampen subthreshold inputs respectively. In contrast, FF inputs within V1 were unaltered by loss of vision, while lateral superficial connections were strengthened. These changes reflect distinct responses of deprived and spared sensory cortex after the loss of one sensory modality.

Introduction

The loss of one sense can trigger compensatory changes in other primary sensory processing, which has been called cross-modal plasticity (Bavelier and Neville, 2002). For example, blind individuals have better pitch discrimination and sound localization (Roder et al., 1999; Gougoux et al., 2004), and enhanced braille comprehension is mediated at least in part by recruitment of primary visual cortex (V1) (Cohen et al., 1997). This systems level plasticity likely reflects functional adaptation of cortical circuits, such as cross-modal plasticity of excitatory synapses in the primary sensory cortices following visual deprivation via dark exposure (DE) (Goel et al., 2006; He et al., 2012). Previously, we and others showed that in juveniles DE induces cross-modal synaptic changes in the supragranular layers. These changes include a decrease in AMPA receptor (AMPAR)-mediated miniature excitatory postsynaptic currents (mEPSCs) in primary auditory (A1) and barrel (S1BF) cortices (Goel et al., 2006; He et al., 2012), facilitation of long-term potentiation (LTP) at layer 4 (L4) to L2/3 synapses in S1BF (Jitsuki et al., 2011). Cross-modal alterations in cortical circuitry were not correlated with an increase in external sensory inputs such as from whisking behavior or audition, but do require these bottom up inputs (He et al., 2012; Petrus et al., 2014).

Deprived sensory cortices also undergo changes in lamina specific ways, which may give some insight to how these brain regions respond to sensory deprivation. In post-critical period V1, DE increases mEPSC amplitudes in L2/3 (Goel and Lee, 2007), decreases mEPSC amplitudes in L6 (Petrus et al., 2011), but does not alter L4 mEPSCs after P23 (Desai et al., 2002). Together these results suggest that each cortical lamina plays a unique role in reorganizing synaptic weights, and these changes may underlie the

recruitment of deprived cortex for processing other senses. This could be beneficial for the organism by lowering the action potential threshold in deprived cortex, such that previously subthreshold inputs from other sensory modalities may produce activation. For example, deaf cats perform better on visual tasks by recruiting auditory cortex (Lomber et al., 2011), and even briefly blinded humans use visual cortex to enhanced braille reading abilities (Merabet et al., 2008).

Here we show that visual deprivation leads to stronger feed-forward (FF) processing to superficial neurons in A1 at the expense of lateral inputs to enhance the signal to noise ratio. Neurons in A1 L4 experienced stronger lateral connections, which may boost the signal before it arrives to A1 L2/3. In contrast, FF processing in V1 did not change with visual deprivation, but lateral inputs to V1 L2/3 were strengthened, which may underlie recruitment of deprived cortex for processing other stimuli (Sadato et al., 1996; Merabet et al., 2008; Lomber et al., 2011). Finally, spontaneous and evoked inhibition in A1 is lamina specific, and may work to sharpen auditory tuning and suppress sub-threshold stimuli from activating the re-structured cortical circuit.

Results

Previously we reported a DE induced potentiation of TC inputs from auditory thalamus to A1 L4, which would increase the strength of FF inputs to A1. In order to study if these potentiated FF inputs alter the strength of next sets of FF synapses in A1 circuitry after DE, we took advantage of a L4 Cre (Scnn1a-Cre) mouse line to restrict ChR2 expression in L4 of V1 or A1. To do this we injected adeno-associated virus

(AAV) containing double floxed ChR2 (DIO ChR2) with a mCherry reporter to cortical L4 and verified that the expression was expressed mainly in L4 (**Fig. 5.1B**). In order to determine the strength of excitatory FF inputs from L4 to L2/3 we activated ChR2 expressing L4 neurons using a brief pulse of blue light emitting diode (LED, 455 nm, 5 ms) and recorded in L2/3 pyramidal neurons above the expression area of V1 or A1. To quantitatively compare the strength of L4 to L2/3 synaptic transmission, we desynchronized release at L4 terminals by substituting external Ca^{2+} with strontium (Sr^{2+}) and analyzed the amplitude of desynchronized light-evoked single vesicle excitatory synaptic currents (Sr^{2+}-mEPSCs) between normal reared controls (NR) and animals dark-exposed (DE) for 1 week (see Methods for details).

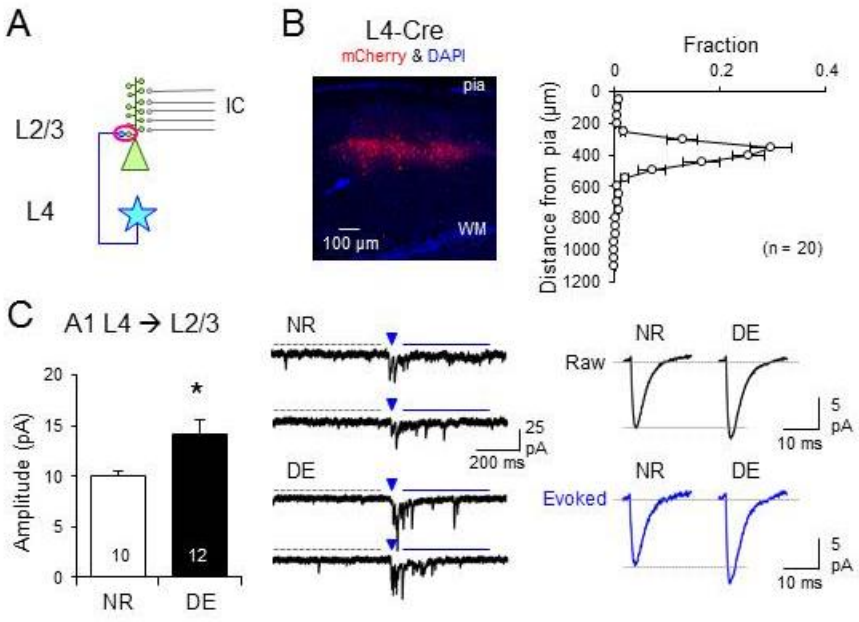

Figure 5.1: A1 L4 synapses to L2/3 are potentiated after DE. **A.** Schematic of experimental setup, isolating feed-forward synaptic inputs from A1 L4 to L2/3. **B.** Confirmation that L4-cre mice injected with floxed ChR2 (red) effectively restrict expression of ChR2 to L4. **C.** Isolated amplitudes of evoked Sr^{2+} -mEPSCs are larger from A1 L4 to L2/3 after DE.

We found that DE for 1 week increased the amplitude of light evoked Sr^{2+} mEPSCs amplitudes of the FF projections from A1 L4 to L2/3 (**Fig. 5.1C**). This result suggests that loss of vision potentiates the feedforward inputs from L4 to L2/3 in A1, which is similar to the potentiation observed at the same inputs in barrel cortex after DE (Jitsuki et al., 2011). However, these results differ from previously reported decrease in mEPSC amplitudes in A1 L2/3 after DE at P28 (Goel et al., 2006) and P90 (**Fig. 5.2A**).

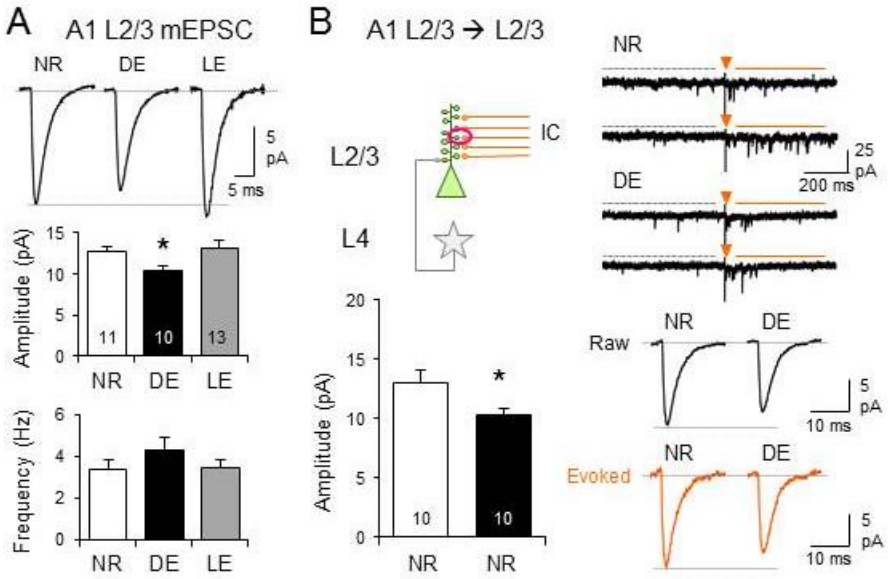

Figure 5.2: A1 L2/3 mEPSCs and laterally projecting synapses are weakened after DE. **A.** mEPSC amplitudes in A1 L2/3 of adult mice reversibly reduce in amplitude after DE, with no significant effect on frequency. **B.** (top) Schematic of experimental setup, isolating lateral synaptic inputs from A1 L2/3 to L2/3. (bottom & right) Isolated amplitudes of evoked Sr^{2+}-mEPSCs are smaller between A1 L2/3 neurons after DE.

Because the fraction of synapses from L4 inputs to L2/3 is estimated to be less than 5% of total synapses on L2/3 (Douglas and Martin, 2004), we determined that the decrease in A1-L2/3 mEPSC amplitudes may be mediated by weaker lateral connections between A1-L2/3 neurons (**Fig. 5.2B**). To test this, we placed a stimulating electrode lateral to the recording site in L2/3 and measured Sr^{2+} desynchronized events of electrically evoked L2/3 lateral inputs. We found that DE decreased the strength of A1 L2/3 lateral inputs

(**Fig. 5.2B**), which mirrors the effects we saw with mEPSC amplitudes (**Fig. 5.2A**). This suggests that mEPSCs recorded from A1 L2/3 mainly reflect lateral inputs to L2/3, which are the majority of synapses. Collectively, our results suggest that DE potentiates feedforward inputs from L4 to L2/3 at the expense of lateral inputs from L2/3.

We previously reported that feedforward input from MGB to A1 L4 is potentiated in DE mice (Petrus et al., 2014). There is evidence that the ability of L4 neurons to drive cortical activity may rely on recurrent excitatory lateral connections within the layer (Douglas et al., 1989).

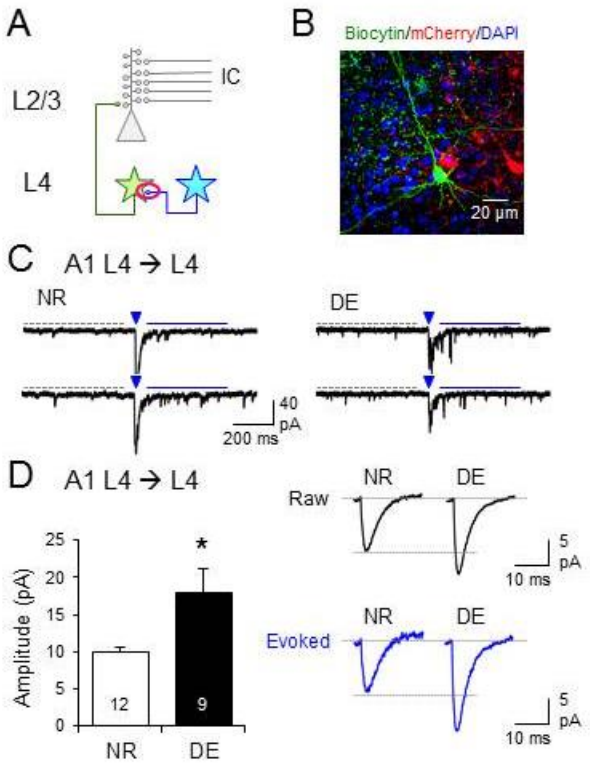

Figure 5.3: A1 L4 lateral inputs are strengthened after DE. **A.** Schematic of experimental setup, isolating lateral synaptic inputs between A1 L4 neurons. **B.** A biocytin (green) filled neuron situated next to ChR2 (red) expressing neurons in A1 L4. The section was counterstained with DAPI (blue) to label nuclei of cells. **C.** Representative traces of Sr^{2+}-mEPSC desynchronized release between A1 L4 neurons. **D.** Isolated amplitudes of evoked Sr^{2+}-mEPSCs are larger between A1 L4 neurons after DE.

To determine whether changes in the L4 recurrent lateral inputs could account for the cross-modal potentiation of L4 to L2/3 inputs in A1, we used the same optogenetics method to express ChR2 specifically in L4 neurons, but recorded from a neighboring non-expressing L4 neuron (**Fig. 5.3A, B**). To assess the strength of L4 inputs to L4 neurons, we quantified the light-evoked Sr^{2+}-mEPSC amplitude. We observed a significant increase in the amplitude of light-evoked Sr^{2+}-mEPSCs arising from A1-L4 lateral connections after DE (**Fig. 5.3D**). This is consistent with an interpretation that there is amplification of signals arriving in L4 prior to its propagation to L2/3.

Unlike A1, we found that visual deprivation failed to increase the strength of feedforward synapses from L4 to L2/3 (**Fig. 5.4A**), which indicates that FF circuitry is unaltered in V1 after DE. We confirmed that the DE induced increase in mEPSC amplitudes occur in L2/3 of V1 in adults (**Fig. 5.4B**), consistent with previous findings (Goel and Lee, 2007). This mainly reflects the potentiation of L2/3 inputs, which we isolated by electrically stimulating the lateral L2/3 inputs to L2/3 pyramidal neurons and isolating Sr^{2+}-mEPSCs (**Fig. 5.4C**). Taken together with our previous results showing no change in thalamocortical synaptic strength in L4 of V1 following DE (Petrus et al., 2014), our results suggest that visual deprivation mainly potentiates intralaminar synapses in L2/3 of V1 without changes in the strength of feedforward connections.

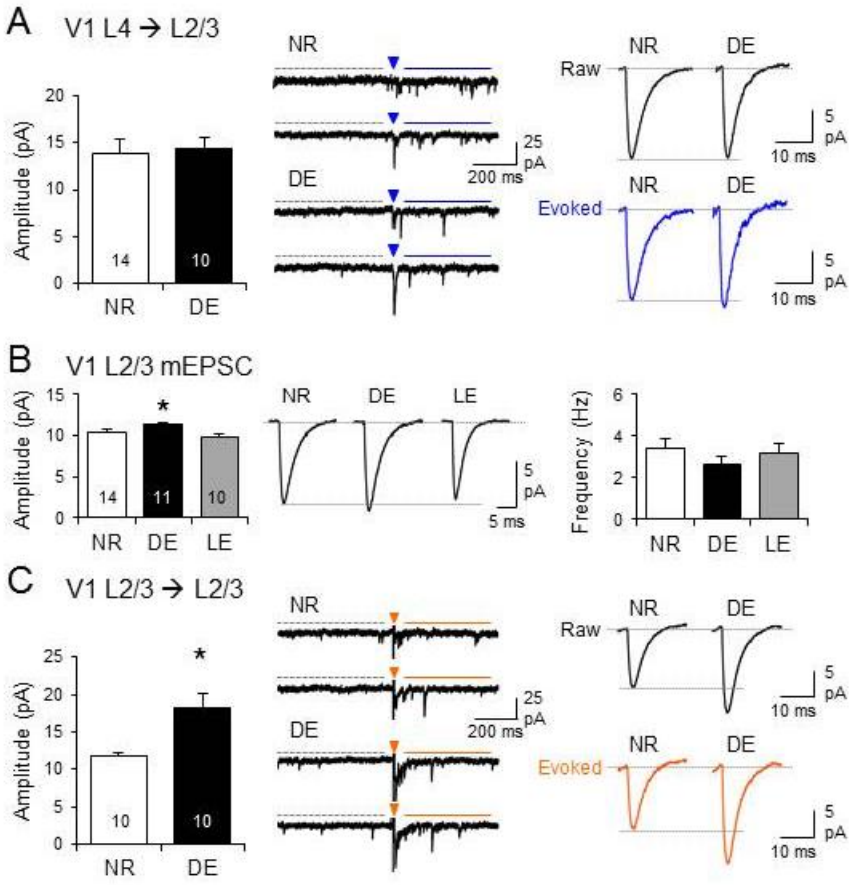

Figure 5.4: Feed-forward inputs to V1 L2/3 neurons are not changed by DE, but lateral inputs and mEPSC amplitudes are reduced after DE in V1 L2/3. **A.** Feed-forward projections from V1 L4 neurons to L2/3 neurons are not significantly different after DE. **B.** mEPSC amplitudes scale up after DE and reverse after light exposure (LE). There was no observed change in mEPSC frequency in V1 L2/3. **C.** Isolated amplitudes of evoked Sr^{2+}-mEPSCs are larger between V1 L2/3 neurons after DE.

Excitation and inhibition are thought to balance input strength to neurons (Wehr and Zador, 2003). In addition, inhibition is thought to sharpen tuning curves in many sensory modalities (Crook et al., 1998; Wu et al., 2008; Liu et al., 2012). Therefore, any enhancements in spared sensory cortex may benefit not only from changes in excitatory circuit strengths, but also inhibition. PV^{+} expressing interneurons are the majority of interneurons in sensory cortex, and provide the strongest inputs to pyramidal neurons at

the soma (Gonchar and Burkhalter, 1997; Pfeffer et al., 2013). Thus we targeted the expression of ChR2 specifically in PV^+ neurons by using a PV^+-Cre line and again injecting DIO-ChR2 with a mCherry reporter in A1. We recorded from a nearby pyramidal neuron in A1 L2/3 or A1 L4 (**Fig. 5.5**) and used Sr^{2+} to desynchronize vesicle release such that the evoked Sr^{2+}-mIPSCs.

We observed an increase in light evoked PV^+ mediated Sr^{2+}-mIPSC amplitudes to A1-L4 principle neurons (**Fig. 5.5A**). Because PV^+ interneurons provide the majority of feedforward inhibition that can sharpen the temporal precision of sensory evoked responses (Yang et al., 2013), the potentiation of PV+ synapses may serve to refine auditory tuning (Suga et al., 1997; Tan et al., 2004; Wu et al., 2008). In contrast, we did not observe significant changes in the amplitude of light evoked Sr^{2+}-mIPSCs from PV^+ interneurons to L2/3 pyramidal neurons (**Fig. 5.5B**). This suggests that DE specifically strengthens evoked inhibition in L4 of A1 without changes in L2/3.

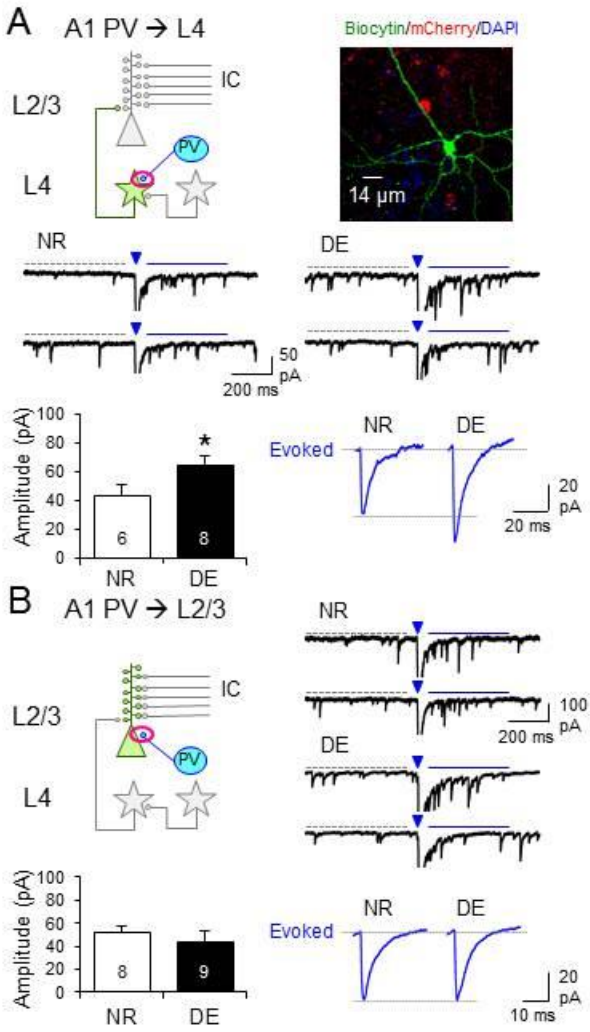

Figure 5.5: DE induces potentiation of Sr^{2+}-mIPSCs evoked from PV^+ interneurons to A1 L4 principal cells, but does not alter their strength to A1 L2/3 pyramidal neurons. **A.** (top left) Schematic demonstrating experimental protocol, isolating PV^+ mediated Sr^{2+}-mIPSCs synaptic strengths onto A1 L4 neurons. (top right) A biocytin filed neuron (green) near PV^+ neurons expressing ChR2 (red), with DAPI labeling nearby nuclei (blue). (bottom) Isolated amplitudes of evoked Sr^{2+}-mIPSCs are larger from PV^+ interneurons to A1 L4 principal neurons. **B.** (top left) Schematic demonstrating experimental protocol, isolating PV^+ mediated Sr^{2+}-mIPSCs synaptic strengths onto A1 L2/3 neurons. (right & bottom) Isolated amplitudes of evoked Sr^{2+}-mIPSCs are unchanged from PV^+ interneurons to A1 L2/3 principal neurons.

There is some evidence that spontaneous miniature inhibitory postsynaptic currents (mIPSCs) may not be co-regulated with evoked inhibition (eIPSCs) (Gao et al., 2011, personal communication Gao and Lee). Spontaneous events also arise from

different vesicular pools than evoked events (Atasoy et al., 2008; Fredj and Burrone, 2009; Xu et al., 2009), and may have functions independent of evoked inhibitory transmission. Thus it is important to study cross-modal regulation of mIPSCs in addition to eIPSCs in A1 after DE.

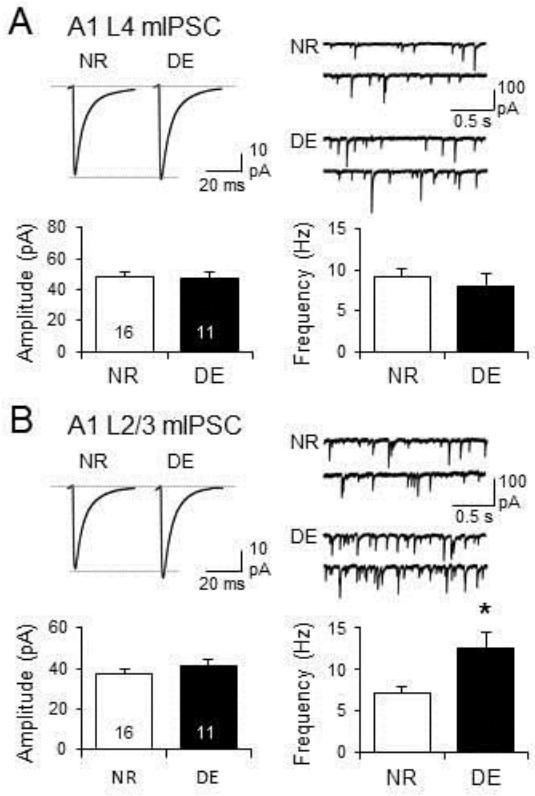

Figure 5.6: DE does not change mIPSC kinetics in A1 L4, but does increase their frequency in A1 L2/3 principal neurons. **A.** No change was observed in A1 L4 mIPSC amplitude or frequency after DE. **B.** mIPSC amplitude was not significantly larger in A1 L2/3 after DE, but an increase in frequency was observed.

In A1 L4 pyramidal neurons, we did not observe significant changes in the frequency, amplitude, or kinetics of spontaneous mIPSCs after DE (**Fig. 5.6A**, supplemental Table 5.1). However, mIPSC frequency increased in A1 L2/3 following DE without changes in amplitude or kinetics (**Fig. 5.6B**, supplemental Table 5.1). These results contrast the observed effects on evoked IPSCs from PV+ interneurons, and suggest that L4 and L2/3

neurons in A1 adapt their inhibition in a distinct manner with vision loss. Our results support the hypothesis that evoked inhibitory synaptic transmission and spontaneous synaptic transmission can be regulated independently.

Discussion

The results here demonstrate that the loss of vision triggers widespread and synapse specific alterations in excitatory and inhibitory inputs to A1 neurons. Previously we reported a DE-induced potentiation of feed-forward excitatory inputs from auditory thalamus (**Chapter 4**), which is amplified via lateral connections within A1 L4. The FF signal is again potentiated in A1 from L4 to L2/3, indicating a stronger FF auditory signal through the A1 circuit after the loss of vision. This stronger FF signal to L2/3 is at the expense of A1 L2/3 lateral inputs, which are weakened after DE, which reflects the reduction in mEPSC amplitudes in A1 L2/3. In contrast, DE did not alter FF inputs to V1 from the thalamus (**Chapter 4**) or from L4 to L2/3. However, mEPSC amplitudes increased and lateral inputs in V1 L2/3 were potentiated after DE. The changes in excitatory transmission A1 after DE were accompanied by laminar specific changes in evoked and spontaneous inhibition, such that evoked inhibition via Sr^{2+}-mIPSCs were stronger in A1 L4, but there were no observed changes in mIPSC parameters. Conversely, an increase in the frequency of mIPSCs in L2/3 was accompanied by no change in evoked Sr^{2+} -mIPSCs, which indicates evoked and spontaneous inhibition are not co-regulated and may be specifically regulated in a laminar dependent.

While stronger lateral connections in A1 L4 can amplify the stronger auditory TC inputs (Petrus et al., 2014), weaker lateral synapses in A1 L2/3 may serve to reduce short and long range inputs to make the most of the incoming auditory signal. This combined with a stronger feed-forward connection between A1 L4 and L2/3 after DE would increase the signal:noise ratio in A1, and is predicted to enhance the sensitivity of A1 neurons to auditory signals after the loss of sight. This together with visual deprivation-induced cross-modal facilitation of LTP at L4 to L2/3 synapses in S1BF (Jitsuki et al., 2011), suggest that cross-modal enhancement of feed-forward sensory processing in the spared senses is a general feature across different sensory cortices.

Thalamocortical synapses are not stronger or more numerous than other synapses (Gil and Amitai, 1996; Gil et al., 1999), so their ability to drive cortical activity may be mediated by strong recurrent connections within L4 (Douglas et al., 1995; Liu et al., 2007; Li et al., 2013). Similarly, feed-forward (FF) connections within cortex from L4 to L2/3 (Mitani et al., 1985) represent a strong but minority of inputs to L2/3, with more numerous lateral connections between L2/3 neurons at least in V1 (Binzegger et al., 2004). A1 L2/3 neurons may play a role in further processing auditory signals as they arrive from thalamorecipient layers (Winkowski and Kanold, 2013). Long-range lateral projections in cat A1 L2/3 show segregation due to characteristic frequency selectivity and bandwidth (Matsubara and Phillips, 1988; Read et al., 2001), and can even innervate secondary auditory fields (Wallace et al., 1991). Intra-cortical connections in rodent A1 have been implicated in sharpening characteristic frequency (CF) receptive fields via superficial L2, and upper L3, while TC inputs to deep L3 and L4 mediate only initial CF tuning (Kaur et al., 2004; Happel et al., 2010). In sum, the stronger FF projections to A1-

L2/3 may enhance the initial tuning to CF at the expense of lateral inputs' sharpening of these inputs. Although reducing tuning precision may not be considered beneficial, lowering the detection threshold may be deemed more relevant to the blind organism, thus sacrificing tuning to enhance signal detection may be more beneficial.

PV^+ interneurons are thought to mediate many changes in cortical function after experience (Chattopadhyaya et al., 2004) and may represent the majority of interneurons in V1 (Meskenaite, 1997). PV^+ interneurons have recently been shown to inhibit each other, while somatostatin (SOM^+) expressing neurons also provide inhibitory inputs to PV^+ networks (Pfeffer et al. 2013), indicating PV^+ to pyramidal inputs may reflect SOM^+ activity as well. Additionally, SOM^+ neurons preferentially target fast spiking inhibitory neurons in L4, but pyramidal cells in L2/3 (Xu et al., 2013). Optogenetically inhibiting SOM^+ neurons results in increased firing of L2/3 pyramidal neurons, but decreased firing in L4, which indicates SOM^+ neurons may be part of a disinhibitory network with PV neurons in L4, but may preferentially target pyramidal cells in L2/3 (Xu et al., 2013). While the ratio of PV^+ neurons to other interneurons is higher in L4, the proportion of SOM^+ and PV^+ neurons are about equal in L2/3 (Lee et al., 2010; Rudy et al., 2010). It is possible that the lack of a change in Sr^{2+}-mIPSCs from PV^+ to L2/3 principal neurons despite an increase in mIPSC frequency may be due to the larger contribution of SOM^+ neuronal inputs to mIPSCs in this layer. In addition, excitatory inputs to interneurons have recently shown to be laminar specific, with SOM^+ neurons regulated primarily by L2/3 inputs, while PV^+ inputs arrive from more widespread sources (Xu and Callaway, 2009), which would produce changes in inhibitory networks of both layers in possibly opposite directions. However, considering that the SOM^+ inputs mainly synapse distally,

we surmise that their contribution to mIPSCs would be small, especially because we only sample mIPSCs with fast rise times that would be from proximal synapses. We observe stronger PV^+ mediated inhibition onto A1 L4 neurons after DE, hence we may expect to see sharper CF tuning, which may mediate enhanced auditory perception after the loss of sight (Petrus et al., 2014). Together these changes in inhibition suggest that an increase in A1 L2/3 spontaneous inhibition may suppress sub-threshold events, while an increase in evoked inhibition in A1 L4 may sharpen tuning.

Alternatively, the increased strength of inhibition may be A1's attempt to balance the increase in excitatory drive from the thalamus (Petrus et al., 2014) and from lateral A1 L4 connections, which would agree with the model that inhibition and excitation amplitudes are equal in A1 L4 (Wehr and Zador, 2003). This model could also serve to explain why evoked inhibition to A1 L2/3 neurons did not change after DE, as FF inputs were strengthened while lateral inputs were weakened, resulting in a net zero change as inhibitory inputs may increase at some synapses but decreased at others.

The laminar specificity of inhibitory changes observed in A1 after DE may be due to the different functions of evoked vs. spontaneous inhibition. While evoked inhibition in A1 L4 may refine tuning, the increase in mIPSC frequency in A1-L2/3 may serve to tonically inhibit sub-threshold inputs, which have been implicated to respond to non-CFs (Bandyopadhyay et al., 2010). By decreasing the impact of sub-threshold stimuli, blind subjects could reduce the system's "noisy events" and focus on the FF events carrying sensory "signal". Conversely, the deprived V1 L2/3 increase in mEPSC amplitudes and stronger lateral projections could increase the impact of subthreshold events, rendering V1 ripe for recruitment for processing other modalities. Recently studies implicate the

scaling up of mEPSC amplitudes in V1 after DE as facilitating LTP induction (Guo et al., 2013), which may help strengthen previously subthreshold inputs.

The loss of one sense can trigger compensatory changes in remaining senses, which has long been observed at the systems level. The results described here elucidate the results of visual deprivation on auditory and visual cortices at the circuit level. Information processing in primary sensory cortex is lamina specific, with each level performing unique input analysis. Overall, these results demonstrate the myriad of changes in excitation and inhibition in deprived and spared sensory cortex after the loss of one sensory modality.

Chapter 6: Cross-modal and Unimodal Plasticity Require Activity Regulated Molecules

** The results presented in this section regarding BACE1 is reproduced with journal's permission from (Petrus and Lee, 2014).

Abstract

Changes in sensory experience result in circuit-wide changes in synaptic strength, which are mediated by biochemical pathways at the molecular level. Increased activity has been shown to recruit Arc mediated internalization of AMPA receptors located at the postsynaptic density, which homeostatically scales down excitatory synaptic strength. This may be important for regulating neuronal activity such that excitotoxicity does not occur in overly-stimulated systems. Interestingly, Arc has also been shown to interact with endosomes containing β-secretase (BACE1) and APP, which work together to generate amyloid beta (Aβ), the neurotoxic peptide associated with Alzheimer's Disease (AD). Although Aβ is involved in pathology, it is also implicated in maintenance of normal physiology of neurons. We found that both Aβ and Arc are important for regulating homeostasis of excitatory synapses in primary sensory cortices. Mice lacking Arc and BACE1 were unable to homeostatically scale up or down excitatory synaptic strength after visual deprivation. These results indicate that these two pathways are important for maintaining homeostasis of neural networks in primary sensory cortices.

Introduction

Experience is essential for the development and maintenance of neuronal circuits, especially those of the primary sensory cortex associated with each sense. Changes in experience can cause alterations in juvenile and adult sensory cortex, for example visual deprivation results in many changes in primary visual cortex (V1), including homeostatic scaling up of mEPSC amplitudes in the principal neurons of layer 2/3 (L2/3) (Goel and Lee, 2007) and layer 6 (Petrus et al., 2011), which is dependent on complete loss of visual inputs (He et al., 2012). Cross-modal plasticity refers to the functional changes experienced by spared sensory modalities after the loss of one sense (Bavelier and Neville, 2002). Interestingly, loss of vision scales down mEPSC amplitudes in L2/3 of rodent somatosensory cortex barrel fields (S1BF) and auditory cortex (A1) (Goel et al., 2006). In addition, LTP induction is facilitated from layer 4 (L4) to L2/3 inputs following visual deprivation, which depends on serotonin (Jitsuki et al., 2011).

Synaptic activity triggers signaling from synapse to nucleus to influence gene transcription and translation, which can transfer this activity to lasting changes in protein composition and synaptic strength. Arc (activity related cytoskeletal associated protein, also known as Arg3.1) is known to be positively regulated by neuronal activity and is targeted to dendrites (Link et al., 1995; Lyford et al., 1995) where it may be translated locally (Steward et al., 1998). Arc traffics AMPA receptors out of the postsynaptic density following periods of high activity in a homeostatic manner (Chowdhury et al., 2006; Rial Verde et al., 2006; Shepherd et al., 2006). The homeostatic scaling of mEPSC amplitudes in V1 *in vivo* has been shown to be Arc dependent, as Arc knockout (KO)

mice fail to scale up following visual deprivation or reverse with light exposure (Gao et al., 2010; McCurry et al., 2010).

Recently, Arc has been implicated in Alzheimer's Disease (AD) pathology as a regulator of the toxic neuropeptide associated with neural death, amyloid beta (Aβ). This peptide is produced by sequential cleavage of APP by β- and γ-secretases in an activity dependent manner (Kamenetz et al., 2003; Venkitaramani et al., 2007; Bero et al., 2011). Endosomes associated with Arc have recently been shown to traffic amyloid precursor

Treatment	Brain Area	Arc levels	Aβ levels
BDNF Application	Hippocampus	↑ (Korb 2013)	↑ (Ruiz-Leon & Pascual 2001)
Environmental Enrichment/ Novel Environment	Hippocampus	↑(Korb 2013, Guzowski 2000)	↑ (Jankowsky 2003) ↓ (Lazarov 2005)
Visual Deprivation	V1	↑↓ ODP timed (Tagawa 2005) No Δ (Gao 2010)	
Alzheimer's Disease	Hippocampus	↑ (Wu 2011)	↑

Table 6.1: Effects of Treatment on Arc and Aβ levels

protein (APP) and β-secretase (BACE1), leading to the production of Aβ peptides following the amyloidogenic processing pathway (Wu et al., 2011b). Indeed, APP overexpressing mice with inhibited cell surface endocytosis exhibit reduced Aβ levels (Cirrito et al., 2008). Arc KO mice, which presumably have reduced ability to traffic BACE1, have reduced Aβ levels even when crossed with a transgenic mouse model of AD, in this case the APP_{SWE};PS1 transgenic mouse (Wu et al., 2011b), which indicates that Aβ production is not only activity dependent, but also requires endosomes trafficking at least partially mediated by Arc.

Reduction of Aβ load has been the target of many therapies aimed at treating AD (Wang et al., 2012). One method explored is via deletion of BACE1, which is a key enzyme that converts amyloid precursor protein (APP) to Aβ (Cai et al., 2001). In BACE1 KOs pathogenic Aβ peptides are abolished, and initial characterization reported that the mice exhibited mostly normal behavior (Luo et al., 2001; Roberds et al., 2001; Hitt et al., 2010). However, latter detailed studies found significant problems with BACE1 KO mice. These abnormalities included neuronal hyperexcitability leading to noticeable seizures in these animal (Hu et al., 2010), hippocampal presynaptic function and plasticity deficits, and memory impairments (Laird et al., 2005; Wang et al., 2008, 2010).

Much work has been done to characterize the synaptic deficits of BACE1 KO mice in the hippocampus, but little is known about how the loss of BACE1 (and Aβ) may affect other brain regions or homeostatic forms of plasticity. A few clues arise from AD patients who experience impairments in visual processing (Katz and Rimmer, 1989; Lee and Martin, 2004), especially a subset of AD patients with Balint's syndrome, whose patients experience visual perception deficits (Hof et al., 1989, 1990). Hallmarks of AD, including Aβ plaques, are present in V1 in human patients and mouse models of the disease (Hof et al., 1989, 1990, 1997; Beker et al., 2012; Grienberger et al., 2012). In fact, Aβ loads proportionally increased with progressive loss in orientation tuning and decline in visual pattern discrimination (Grienberger et al., 2012). Interestingly the neurons located near Aβ plaques exhibit hyperactivity, similar to the phenomenon observed in BACE1 KOs (Busche et al., 2008; Hu et al., 2010), indicating an additional role for Aβ in regulating normal neuronal physiology. Ocular dominance plasticity is

also negatively impacted in AD mice, even before Aβ plaques have formed, suggesting a role for Aβ in regulating normal sensory cortex plasticity (William et al., 2012).

Given the interplay between Arc and Aβ, and the involvement of Arc in homeostatic regulation of excitatory synapses, it seems Aβ may be required for these functions, and that lack of Aβ in BACE1 KOs would lead to altered homeostatic plasticity. To test this hypothesis we studied changes in mEPSC amplitudes in visual cortex, layer 2/3 (V1 L2/3) of BACE1 KO and WT mice after dark exposure (DE) and re-exposure to light (LE), known triggers of homeostatic scaling in V1. The second aim of this study was to uncover the role of Arc in cross-modal plasticity, and if this type of plasticity requires similar mechanisms to unimodal plasticity. Arc KO mice have been shown to exhibit impaired scaling down of excitatory synapses in V1 after LE (Gao et al., 2010). We found that BACE1 KO mice also exhibit a similar phenotype, which suggests a novel role of BACE1 in homeostatic synaptic plasticity. We also report that Arc also plays a critical role in scaling down excitatory synapses in layer 2/3 (L2/3) of A1 after cross-modal deprivation of vision (DE). This result suggests a universal role of Arc in experience-dependent scaling down of excitatory synapses in primary sensory cortices.

Results

BACE1 is required for scaling of mEPSC amplitudes in V1 after DE

To examine the role of BACE1 in V1 synaptic function and plasticity, we recorded mEPSCs in L2/3 pyramidal neurons of V1 in BACE1 WT and KO mice. To alter visual experience, mice were dark exposed (DE) between postnatal day 22-24 (P22-

24) for 2 days and a subset of them was returned to a lighted environment for 2 hours (light exposed, LE). Age matched control mice (normal reared, NR) were kept in a normal light/dark cycle. As reported previously, in WTs 2 days of DE scaled up the amplitude of mEPSCs, which then returned to NR values after 2 hours of LE (**Fig. 6.1A**) We found that BACE1 KO mice have significantly larger mEPSCs compared to BACE1 WTs under normal conditions (**Fig. 6.1B**). This is consistent with a potential deficit in developmental downscaling mechanisms in BACE1 KOs, which would result in larger basal mEPSCs. Furthermore, BACE1 KOs failed to significantly increase or decrease mEPSC amplitude with DE or LE respectively (one-factor ANOVA: $p = 0.4$; **Fig. 6.1C**), which suggests a lack of experience-dependent homeostatic synaptic plasticity. There was no statistically significant difference in mEPSC frequency or kinetics across genotype or experimental conditions (**Fig. 6.2,** appendix Table 6.2).

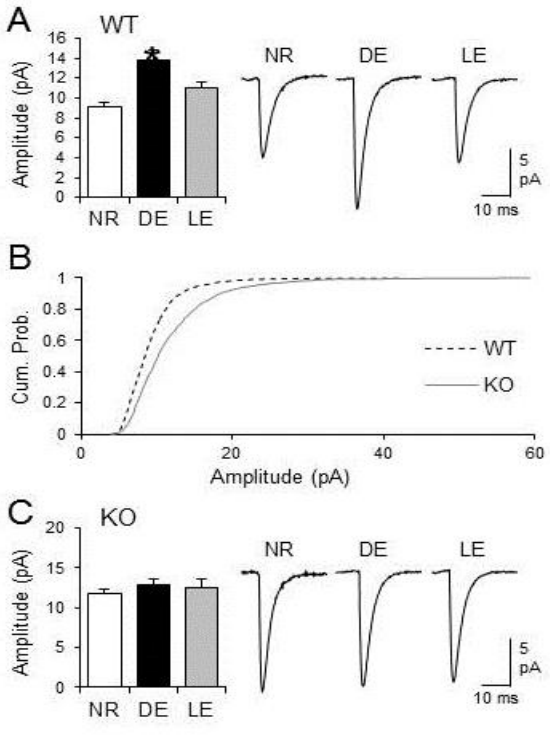

Figure 6.1: BACE1 KO mice exhibit stronger basal excitatory synaptic transmission and lack experience-dependent homeostatic regulation in superficial layers of V1. **A.** In WT mice, 2 days of DE significantly increased the average amplitude of mEPSCs, which reversed to NR levels with 2 hours of LE (one-factor ANOVA: $p < 0.001$, Newman-Keuls *post hoc* test: $p < 0.01$). Left: Comparison of average mEPSC amplitude. Right: Average mEPSC traces from each group. **B.** Cumulative probability graph comparing the mEPSC amplitude distribution of normal-reared WT (black dotted line) and KO (gray solid line). There was a statistically significant difference between WT and KO (Kolmogorov-Smirnov test: $p < 0.0001$). **C.** In KO mice, there was no significant difference in the average mEPSC amplitude across groups (one-factor ANOVA: $p > 0.39$). Left: Comparison of average mEPSC amplitude. Right: Average mEPSC traces from each group.

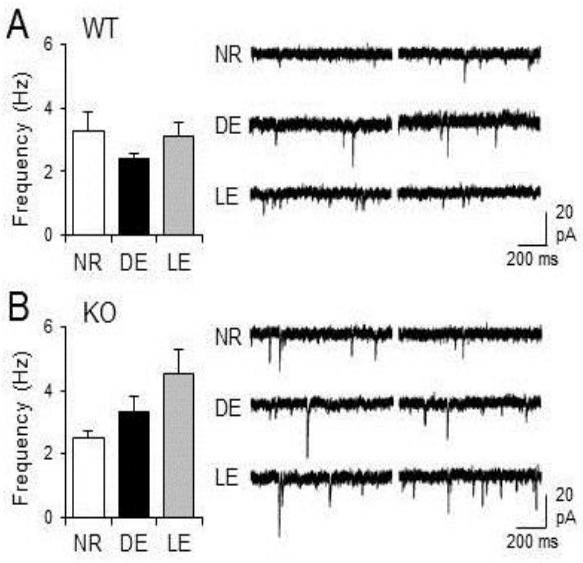

Figure 6.2: Changes in visual experience does not alter mEPSC frequency in both WT and KOs. Left: Comparison of average mEPSC frequency of WT mice **A** and BACE1 KO **B**. There was no significant difference across groups (one-factor ANOVA: $p > 0.2$). Right: Example raw mEPSC traces from each group.

BACE1 KO mice have normal intrinsic excitability

Previous studies showed that BACE1 KOs display heightened spontaneous seizure-like activity and display alterations in voltage-gated Na^+ channel density (Kim et al., 2009; Hitt et al., 2010; Hu et al., 2010). Therefore, the increase in basal mEPSCs of BACE1 KOs could have been due to increased spontaneous activity. However, we did not find a significant difference in the intrinsic excitability of L2/3 neurons in V1 of BACE1 KOs compared to BACE1 WTs (**Fig. 6.3A**). Furthermore, there was no difference in the Rheo base (**Fig. 6.3B**), resting membrane potential (**Fig. 6.3C**), action potential threshold (**Fig. 6.3D**) or input resistance (**Fig. 6.3E)** measured in current clamp from neurons of BACE1 WT and KO.

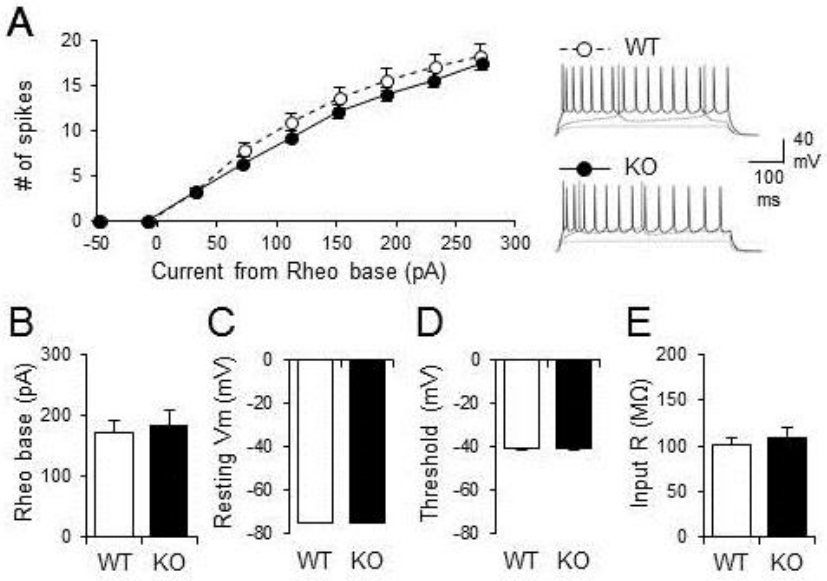

Figure 6.3: BACE1 KOs exhibit normal intrinsic excitability in L2/3 of V1. **A.** Left: Comparison of average action potential number with increase in current injection normalized to Rheo base. N = 10 cells each group, 2 WT and 3 KO mice per group, 1-2 cells per slice, 2-3 slices per mouse. Right: Example overlayed voltage traces taken at -40 pA (light gray), +40 pA (dark gray), and +120 pA (black) from Rheo base. **B-E.** Comparison of average Rheo base **B**, resting membrane potential **C**, action potential threshold **D**, and input resistance **E** measured in current clamp.

Arc/Arg3.1 levels are cross-modally regulated by visual experience

To examine the role of Arc in cross-modal plasticity, we first studied the levels of Arc protein in visual, auditory and somatosensory cortices. Initially, we confirmed that Arc protein was completely absent in Arc KO mice compared to WT (**Fig. 6.4A, 6D top panels**). We also confirmed that Arc immunohistochemical staining can detect increase in Arc protein levels in response to periods of high activity. To do this WT mice were dark exposed (DE) for 2 days and then re-exposed to light (LE) for two hours, which dramatically increased the Arc expression in V1 L2/3 neurons (**Fig. 6.4B**) as described previously (Gao et al., 2010). Because we observed that Arc is specifically necessary for down scaling excitatory synapses in V1 (Gao et al., 2010), we determined whether cross-

modal scaling down of synapses in L2/3 of A1 or S1 is associated with similar increases in Arc. To examine this, we immunostained for Arc protein in A1 and S1 after 7 days of DE, which we have previously shown to down scale mEPSCs in L2/3 of A1 (Goel et al., 2006; Petrus et al., 2014) and S1 (Goel et al., 2006; He et al., 2012). We found that Arc protein expression significantly increased in the neuropils of L2/3 in both A1 and S1 (**Fig. 6.4C,D**, appendix Table 6.3), while no increases in Arc levels were observed in V1 L2/3 after 2d-DE or 7d-DE (**Fig. 6.4C, D,** appendix Table 6.3).

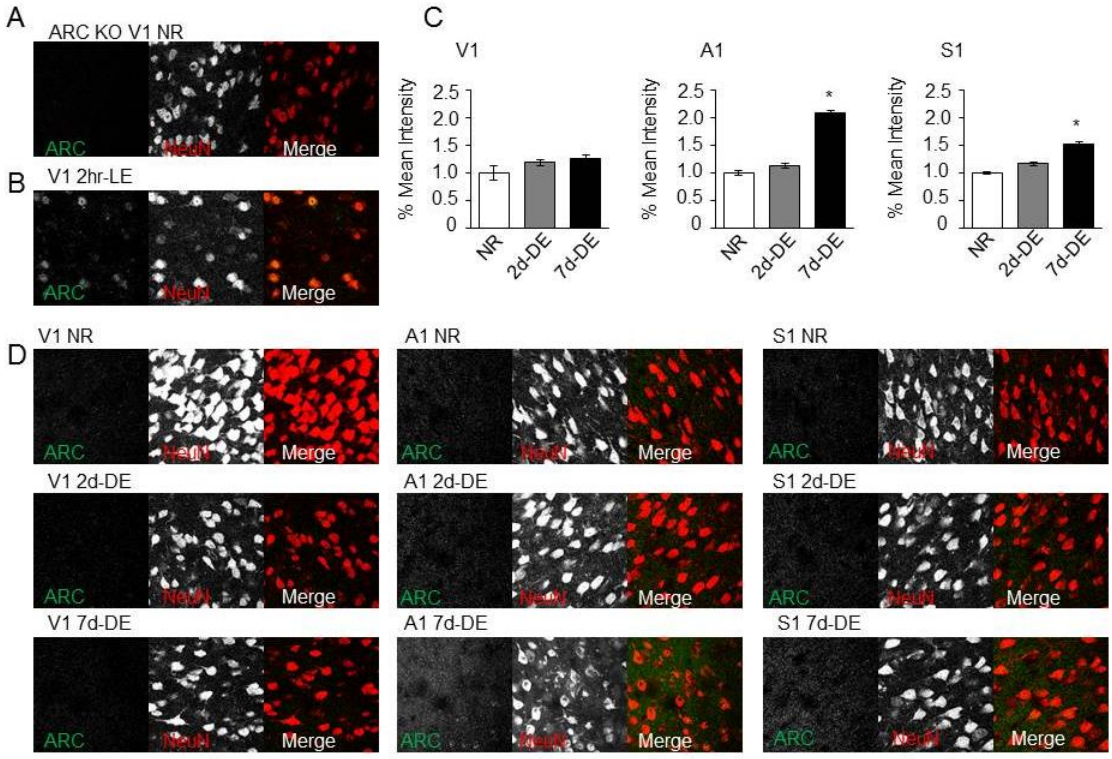

Figure 6.4: Cross-modal plasticity recruits increased Arc levels. **A.** KO mice express no Arc protein. **B.** 2 hours light exposure (LE) induces rapid increases in Arc expression in V1 L2/3. **C.** Arc expression increases in A1 and S1 after 7 days but not 2 days of dark exposure, no change was observed in V1. **D.** Representative confocal images displaying increased Arc intensity recruited cross-modally. Green is Arc protein, red is NeuN neurons. There was no significant difference in neuronal density across the groups (NR: 15.10 ± 0.30 cells/10,000 μm^2, n = 30 sections from 3 mice; DR2d: 15.05 ± .67 cells/10,000 μm^2, n = 30 sections from 3 mice; DR7d: 314.85 ± 0.32 cell/10,000 μm^2, n = 30 sections from 3 mice; one-way ANOVA: $F(2,87) = 0.322$, $p = 0.73$; see Table 6.3).

These results indicate that down-scaling in V1 after LE and in S1/A1 after DE both accompany an increase in Arc expression. However, the increase in Arc was restricted to neuropils, which is different from the increase in soma as observed in V1 following 2 hours of LE (**Fig. 6.2B**). However this pattern of Arc increase is similar to what we observed in V1 after 1 day of LE, which is the condition that scales down V1 mEPSCs (Gao et al., 2010).

Arc is required for cross-modal scaling of mEPSC amplitudes in A1 after DE

Next we examined whether Arc is necessary for cross-modal down scaling of mEPSC amplitudes in A1 L2/3. To do this, we compared the mEPSC amplitudes in A1 L2/3 pyramidal neurons of Arc KOs to Arc WT mice following 7 days dark exposure (7d-DE). In WT mice, A1 L2/3 mEPSC amplitudes after DE was decreased, which reversed after 7 days light exposure (7d-LE) (**Fig. 6.5A**). However, KO mice failed to scale down after 7d-DE or up after 7d-LE in A1-L2/3 (**Fig. 6.5B**). There was no significant change in mEPSC frequency in WT or KO mice after changes in visual experience (**Fig. 6.5A & B**), and no significant difference between mEPSC kinetics in WT vs. KO mice (appendix Table 6.4). In WTs, DE-induced scaling down of mEPSCs and LE-induced scaling up of mEPSCs did not occur via multiplicative mechanisms (Kolomogorov-Smirnoff test $p > 0.05$ both groups - **Fig 6.5C,D**), which suggest that the changes are not global across all synapses.

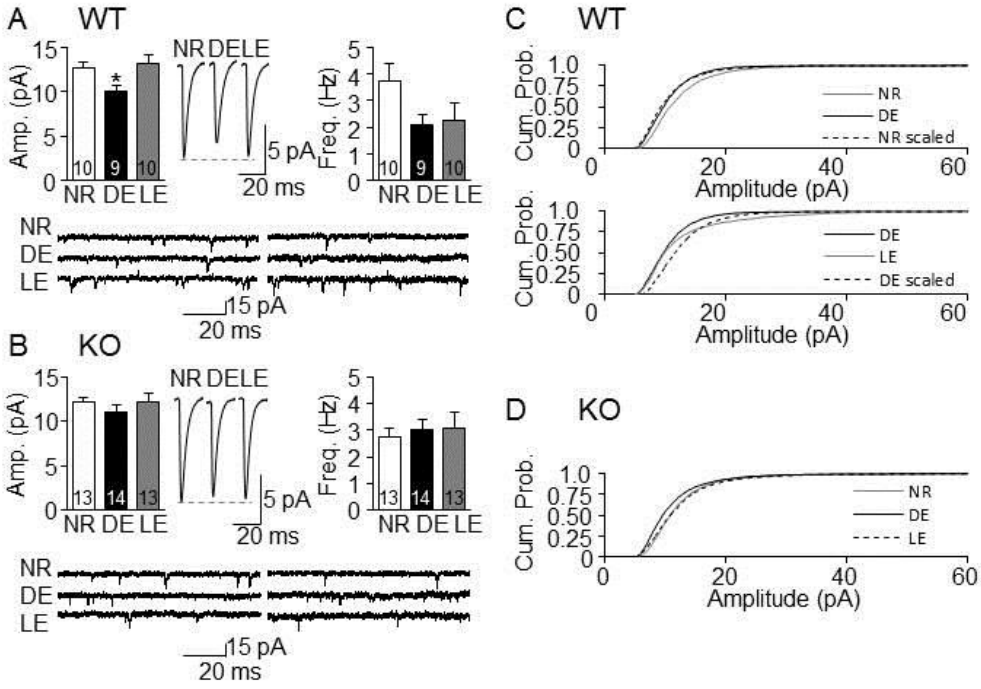

Figure 6.5: Arc KO mice do not scale in response to cross-modal sensory deprivation. **A.** Arc WT littermates experience scaling down in A1 L2/3 after 7 days dark exposure (DE), which reverses with 7 days light exposure (LE). **B.** Arc KO mEPSC amplitudes do not scale in response to cross-modal sensory deprivation. Neither WT or KO mice experience changes in mEPSC frequency. **C & D.** Scaling in Arc WT after DE or LE does not occur via a multiplicative mechanism. Arc KO mice do not scale mEPSC amplitudes after DE or LE.

Discussion

Here I have described the effects of visual deprivation on V1 L2/3 neurons in BACE1 WT vs. KO mice. I found that 2 days of DE and 2 hours of LE were sufficient to homeostatically scale mEPSC amplitudes up and down respectively, but BACE1 KO mice were unable to scale in either direction under the same circumstances. This points to a physiological role for BACE1 and the activity dependent production of Aβ in normal synaptic function in V1. I also found that the activity regulated protein Arc is upregulated in spared sensory cortices (S1 and A1) after DE, which indicates an increase in activity in spared cortex, which may enhance processing of spared sensory modalities.

These increases in Arc correlated with a down-scaling of mEPSC amplitude in spared A1, which was abolished in Arc KO mice. These results indicate a requirement for activity dependent production of proteins, which may mediate homeostatic responses to sensory deprivation.

Homeostatic plasticity requires multiple mechanisms

Visual deprivation induces homeostatic scaling up of mEPSC amplitudes in V1 L2/3 neurons which occurs independently of development (Desai et al., 2002; Goel and Lee, 2007). These changes are inverse to those found in L2/3 of spared sensory cortices such as S1 and A1, where mEPSC amplitudes scale down (Goel et al., 2006; He et al., 2012). Bidirectional homeostatic synaptic plasticity induced by changes in visual experience recruit distinct molecular signaling, which are not exactly the inverse of each other. For example, up-scaling of V1 mEPSCs induced by losing vision requires phosphorylation of AMPA receptors and synaptic expression of Ca^{2+}-permeable AMPA receptors (Goel et al., 2011), while down-scaling by visual experience depends on Arc (Gao et al., 2010) and a reduction in the number of AMPA receptors (He et al., 2012). Arc is also required for activity dependent Aβ production, as it associates with BACE1, APP, and PS1 (Wu et al., 2011b). Post-mortem studies of patients with AD have high levels of Arc and Aβ (Khachaturian, 1985; Wu et al., 2011b), and high levels of BACE1 activity (Fukumoto et al., 2002; Holsinger et al., 2002; Yang et al., 2003) (**See Table 6.1**). This indicates that the increase in Aβ may be triggered by hyperexcitability of neural networks in AD brain. Interestingly, models of AD depict a complex story regarding Aβ's influence on neuronal networks. There are reports of higher numbers of

"silent" or failed synapses in AD patients (Silverman et al., 2001; Prvulovic et al., 2005), leading to a larger proportion of quiet neurons in the network, but it has recently been observed that neurons near Aβ plaques exhibit hyperexcitability, even in young pre-AD symptomatic animals (Busche et al., 2008, 2012). On the other hand, BACE1 KO mice also experience hyperexcitability (Hu et al., 2010), thus eliminating the production of Aβ may have similar consequences. In any case, both Arc and Aβ has been shown to cause a reduction in the strength of excitatory synapses (Kamenetz et al., 2003; Chowdhury et al., 2006; Hsieh et al., 2006; Shepherd et al., 2006), hence the increase in Arc and Aβ in AD brains is likely to cause a reduction in excitatory synaptic transmission. The results in this chapter show a lack of activity-dependent down scaling of mEPSCs in BACE1 KO and Arc KO is consistent with this idea.

Arc is required for cross-modal plasticity

Arc is implicated in being essential for AMPAR internalization after periods of high neuronal activity (Chowdhury et al., 2006; Rial Verde et al., 2006; Shepherd et al., 2006), which may play a role in homeostatic scaling down and/or sliding the LTP induction threshold to favor LTD (Shepherd and Bear, 2011). The experiments performed in this study looked at the role of Arc in cross-modal regulation of synaptic strength by loss of visual experience. Much work has been devoted to elucidating Arc's role in AMPA receptor internalization *in vitro* (Chowdhury et al., 2006; Rial Verde et al., 2006; Shepherd et al., 2006) and in unimodal sensory deprivation paradigms *in vivo* (Gao et al., 2010). Here we report that Arc is also required for cross-modal regulation of global synaptic scaling, as Arc KO mice are unable to scale down synaptic strength in A1 L2/3 after DE (**Fig. 6.5**). These results indicate cross-modal scaling down of synaptic strength

shares similar molecular mechanisms to others studied thus far. A global scaling down of synaptic strength may require Arc regardless of the triggering stimulus or sensory requirement.

Here we add that Arc plays a universal role at downscaling excitatory synapses by demonstrating that it is also recruited for cross-modal synaptic scaling. A1 compensates for the loss of vision by potentiating feed-forward synaptic strength and strengthening L4 lateral connections (**Chapters 4, 5**). This potentiation likely increases the activity in A1, which would cause the increase in Arc levels seen here (**Fig. 6.4**). Additionally, the scaling down of mEPSC amplitude in A1 and S1 L2/3 neurons is thought to be in response to an increase in global activity of spared sensory cortex (Goel et al., 2006; He et al., 2012). However, scaling down of mEPSCs in L2/3 of spared cortex is not accompanied by an increase in bottom-up sensory inputs (He et al., 2012), which suggests this increased activity is likely mediated by an internal or intrinsic mechanism within the cortical or thalamocortical circuitry. We surmise that potentiation of the feedforward excitatory synapses as shown here may be responsible for triggering Arc-dependent downscaling. Cross-modally induced synaptic changes mediate enhanced sensory processing in the form of lowering the response threshold to softer sounds, and sharpening the tuning shoulder at least in A1 neurons after loss of vision (Petrus et al., 2014). These results indicate that a lack of plasticity in spared sensory cortices may render Arc KO mice unable to compensate for the loss of vision in addition to lacking other forms of synaptic plasticity and memory consolidation.

Although most studies use Arc to report increases in activity with a subsequent scaling down of AMPA receptor mediated responses, previous reports also demonstrated

scaling up in V1 L2/3 after DE is also impaired in Arc KO mice (Gao et al., 2010; McCurry et al., 2010). Basal mEPSC amplitudes are larger in V1 of Arc KO mice (Gao et al., 2010), indicating that the lack of up scaling may be due to occlusion. Arc is also necessary for normal LTP function as KO mice display enhanced early LTP but lack late phase LTP (Plath et al., 2006). LTP is a cellular correlate of memory, and so without Arc and normal LTP, Arc KO mice are unable to consolidate memory on behavioral tasks (Guzowski et al., 2000; Miyashita et al., 2008; Ploski et al., 2008). These results all point to abnormal plasticity and memory function in systems lacking Arc, thus demonstrating its important role in synaptic plasticity.

BACE1 is required for regulating neuronal activity

Recently manipulations that prevent Aβ production have revealed a crucial role of Aβ in normal synaptic function (Wang et al., 2012), particularly homeostatic processes that provide stability to neuronal activity (Kamenetz et al., 2003; Hsieh et al., 2006; Venkitaramani et al., 2007). In hippocampal neurons, overproduction or exogenous application of Aβ can induce endocytosis of AMPA receptors to reduce synaptic drive (Kamenetz et al., 2003; Almeida et al., 2005; Hsieh et al., 2006). Furthermore, Aβ production is activity-dependent (Bero et al., 2011), which lead to the hypothesis that it may act as a homeostatic regulator of excitatory synaptic strength (Kamenetz et al., 2003). A recent study showed that Arc plays a critical role in activity-dependent production of Aβ (Wu et al., 2011b). It is suggested that Arc acts as an activity "sensor" and interacts with presenilin 1 (PS1), which is the catalytic component of the γ-secretase complex. This provides a means for BACE1 to interact with Arc signaling for regulating Aβ production. Therefore, it is not a surprise that the larger basal excitatory synaptic

transmission and lack of activity-dependent down scaling seen in V1 L2/3 neurons of BACE1 KOs mirrors the phenotype seen in Arc KOs (Gao et al., 2010).

The loss of BACE1 and Arc has similar consequences

Arc, which is produced upon increase in neural activity, interacts with presenilin-1, and hence promotes Aβ production downstream of BACE1 (De Strooper, 2003; Wu et al., 2011b) (**Fig. 6.6**). The higher basal amplitude of mEPSCs in BACE1 KO mice further support the idea that Aβ may be important for the maintenance of homeostasis in the cortical network.

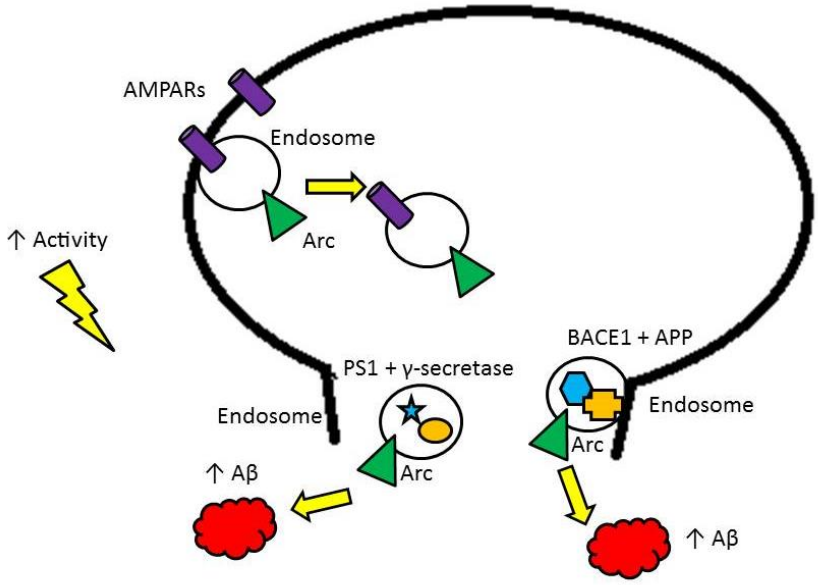

Figure 6.6: Increased activity induces Arc mediated AMPA receptor internalization and Aβ production. Arc brings PS1 + γ-secretase and BACE1 + APP together in endosomes to increase Aβ production in an activity dependent manner.

Furthermore, Aβ levels may help regulate mEPSC amplitudes during development and into adulthood, as younger animals have larger mEPSC amplitudes than adults (Turrigiano and Nelson, 2004; Goel and Lee, 2007). The increasing levels of Aβ as the organism ages may regulate this reduction of amplitude. Previously we reported Arc KO mice exhibit higher basal AMPA mediated mEPSC amplitudes in V1 L2/3 (Gao et al.,

2010), however the Arc KO mEPSC amplitudes were not significantly larger in A1 L2/3 neurons. This may be due to a difference in cortical area (A1 vs. V1), or age of the animals. In the study performed by Gao et al. mice were P23, however the Arc KO mice used here were between P28 and P35, and others using slightly older mice also observed normal amplitude visually evoked responses in Arc KO (McCurry et al., 2010). It is possible that age plays a role in how AMPA receptors are basally trafficked into and out of synapses, with younger ages being more sensitive to the lack of BACE1 or Arc. Alternatively, AMPA receptor trafficking deficits in younger BACE or Arc KO mice may be overcome as the animals age.

Both Arc KO and BACE1 KO are not able to scale up or down in response to sensory deprivation. Homeostatic plasticity is mediated by AMPA receptor trafficking (Chowdhury et al., 2006; Shepherd et al., 2006), so without Arc, spared sensory cortices cannot scale in response to sensory deprivation (Goel et al., 2006). Because Arc is involved in Aβ production, it is unsurprising to find Arc KOs and BACE1 KO mice share similar phenotypes. Arc regulates Aβ formation by its association with endosomes which contain BACE1 and APP (Wu et al., 2011b). Because higher activity induces increased Arc expression, this also induces increased Aβ production (Wu et al., 2011b). Lacking Arc and Aβ disables synapses from removing AMPA receptors from synapses after high levels of activity, hence the synapses in Arc KO and BACE1 KO mice may be already maximally scaled up and are unable to scale up any further.

AMPA receptor endocytosis is an Arc mediated response to increased levels of neuronal activity. Lacking Arc and BACE1 (and thus downstream Aβ) both result in higher basal mEPSC amplitudes (**Fig 6.1**, Gao et al., 2010). These results indicate that

Arc and Aβ are both important in maintaining network homeostasis, especially for scaling down synaptic strength during periods of high activity. In normal networks activity levels may fluctuate depending on sensory experience, and even sleep is implicated in scaling down synaptic strength after a long day of heightened neuronal experience (Tononi and Cirelli, 2003, 2006). Patients suffering from Alzheimer's disease experience heightened default network activity [for review: (Mevel et al., 2011)], which is implicated in daydreaming or periods of quiet wakefulness (Gusnard and Raichle, 2001). Because Alzheimer's disease patients also express high levels of Arc (Wu et al., 2011b), this heightened activity may be the pathology's trigger leading to global reduction in excitatory synaptic strength and eventual synaptic loss.

Chapter 7: Discussion

Sensory experience influences how cortical circuits are initially wired, but also their maintenance throughout life. The goal of this project was to study the role of homeostatic and Hebbian plasticity mechanisms which respond to changes in experience beyond the critical period. A sensory neuronal network must efficiently process incoming information based on the needs of the organism, and the ability to adapt after the loss of one sense has profound effects on synaptic weights in deprived and spared sensory cortex. Here I have described the effects of sensory deprivation on excitatory and inhibitory cortical circuits in adult mice. The changes observed are experience dependent, lamina specific and in some cases readily reversible. My results indicate that the neurons in cortex are set up for precise sensory processing, and remain plastic well beyond the critical period for visual or auditory plasticity when sensory deprivation occurs cross-modally. Moreover, the molecular mechanisms underlying plastic changes appear to be shared between uni- and cross-modal plasticity.

1. Homeostatic adaptations vary with age in a laminar-specific manner

Homeostatic plasticity was first described *in vitro* among cultured cortical neurons, where a global blockade of activity by TTX application increased the amplitude of mEPSCs multiplicatively, while a blockade of inhibition (resulting in increased network activity) induced opposite changes (Turrigiano et al., 1998). These results were recapitulated in mouse visual cortex slices contralateral to a TTX-injected eye, where L2/3 and L4 neurons multiplicatively increased mEPSC amplitudes (Desai et al., 2002).

Interestingly, L4 neurons do not undergo these changes after postnatal day 23 (P23), while L2/3 neurons do not start this process until after at least P16 (Desai et al., 2002), but probably between P21-P23 (Goel et al., 2006; Gao et al., 2010). L2/3 neurons also retain the ability to scale up synaptic strength after visual deprivation until at least P90 (Goel and Lee, 2007), which is mediated by synaptic AMPA receptor trafficking (Goel et al., 2011). In addition, L5 neurons in the contralateral hemisphere to brief (2 day) monocular lid suture increase their intrinsic excitability between p18-p21 (Nataraj et al., 2010). Adding to this complexity, I found that excitatory synapses on layer 6 (L6) pyramidal neurons of visual cortex undergo homeostatic strengthening after visual deprivation in young mice (**Chapter 3**). Interestingly, the response of L6 neurons to visual deprivation reverses in older mice, such that instead of scaling up mEPSC amplitudes as seen in young mice, older mice reduce mEPSC amplitude in a non-multiplicative manner (**Chapter 3, Fig 3.3**). I found that some synapses were strengthened while others were weakened, which indicates synapse specific modification instead of a global response to lack of visual input to V1 L6. This synapse specificity is more indicative of Hebbian LTP and LTD type mechanisms, which may be more useful for a mature animal, or a subset of neurons which receives a wide variety of synaptic inputs. These findings suggest that V1 L6 neurons do adjust homeostatically to changes in visual experience, but the age of the animal and duration of visual deprivation both influence the type of mechanism used (i.e. multiplicative homeostatic vs. Hebbian LTP/LTD). Furthermore these data suggest that even though L6 neurons receive thalamocortical inputs similar to L4, they remain malleable beyond the critical period of neurons located in L4.

L6 integrates intracortical inputs and plays an integral role in the thalamo-cortico-thalamic feed-back loops. At p16 brief dark exposure (DE) scales up mEPSC amplitudes in L6 (**Chapter 3**), like the changes observed in L4 (Desai et al., 2002). Interestingly, at P21 a longer duration (7 days) produced a reversible reduction in mEPSC amplitudes in L6 neurons. The change in polarity of synaptic changes with age suggests that L6 initially adapts homeostatically to loss of vision, but later responds via Hebbian mechanism to reduce synaptic gain with decreased visual input perhaps via an LTD-like mechanism. The age at which L6 switched its response to visual deprivation is past the proposed critical period of L4 (Jiang et al., 2007), but within the range of plasticity in superficial cortical layers (Goel and Lee, 2007). One interesting observation of homeostatic synaptic changes in L6 is that it is not multiplicative in nature (**Chapter 3, Fig. 3.3E&F)**. Global multiplicative scaling occurs in cultures and young mice (Turrigiano et al., 1998; Desai et al., 2002; Goel and Lee, 2007), but in adults it is not observed in L2/3, which could indicate adults use different homeostatic mechanisms or that only a subset of inputs undergo homeostatic synaptic scaling (Goel and Lee, 2007). L6 neurons receive a variety of inputs, a small number originating from the thalamus (Ribak and Peters, 1975; Levay and Gilbert, 1976; da Costa and Martin, 2009), and many more from almost every layer within V1 (Zarrinpar and Callaway, 2006). This variety of inputs could be one reason L6 does not undergo multiplicative scaling, as changes in visual experience may only affect a subset of inputs to L6 neurons. In addition to receiving a variety of inputs, L6 neurons also project to diverse targets. They provide critical feedback to the thalamus to modulate its activity, but also to multiple layers of cortex, including L4 and L5. Hence L6 shares a feature with L4 in that it receives TC inputs, but it is likely more varied in

functionality and this may explain its complex plasticity compared to L4. Furthermore, the fact that L6 neurons respond to vision loss depending on the different developmental age indicates that their functional plasticity is likely determined by developmental changes in the required functionality of the L6 circuit. In sum, it is apparent that the layer and variety of inputs to the neurons may be more influential in determining what type of mechanism the visual cortical neurons employ to adapt to novel sensory experience.

2. Regulation of specific excitatory synapses in spared and deprived cortices

Homeostatic plasticity is useful for the maintenance of overall neural activity in a cortical circuit, but Hebbian plasticity is critical for potentiating or depressing specific synapses in response to changes in sensory experience.

The first description of cross-modal plasticity at the synaptic level was homeostatic changes in L2/3 of auditory (A1) and somatosensory cortex (S1) after a week of dark exposure (Goel et al., 2006) in young (P21-28) animals. In contrast to the homeostatic scaling up of mEPSC amplitudes observed in V1 L2/3 (Desai et al., 2002; Goel and Lee, 2007), mEPSCs scaled down in A1 and S1 (Goel et al., 2006). The overall decrease in V1 activity may cause neurons to scale up synaptic strength, while the scaling down observed in spared cortices may be in response to increased activity as the spared cortex increases its processing to compensate for the lost sense (reviewed in Whitt et al., 2013). A subsequent study showed that the cross-modal synaptic plasticity in S1 barrel cortex (S1BF) is dependent on whisker inputs (He et al., 2012), and that synaptic AMPA receptor content is increased between L4 to L2/3 synapses (Jitsuki et al., 2011). Here I

discovered that after DE, feed-forward (FF) synapses in A1 are strengthened while FF synapses in V1 remain unchanged (**Chapter 4, Fig. 4.1**). These findings suggest that the inputs arriving at L2/3 of A1 or S1 are indeed increased when losing vision, hence this increase in feedforward sensory drive could in principle trigger the global scaling down of L2/3 synapses. One functional consequence of the stronger FF processing combined with a weaker lateral input to the superficial layer neurons of A1 may be to enhance the signal to noise ratio, thus enhancing processing of auditory stimuli after loss of vision. In A1, L2/3 neurons have recently been shown to integrate suprathreshold spiking inputs with subthreshold depolarizations when responding to sound stimuli (Chen et al., 2011). These subthreshold inputs may originate in other sensory modalities (Lakatos et al., 2007) or higher order information from prefrontal cortex (Fritz et al., 2003, 2007). There is evidence that superficial lateral inputs in A1 L2/3 may be involved in frequency tuning (Atzori et al., 2001; Read et al., 2001), while feed-forward inputs are important for intensity (Kaur et al., 2004, 2005; Happel et al., 2010). If this is the case, there may be enhanced signal detection at the expense of losing frequency tuning in A1 L2/3, which may benefit the visually deprived animal by allowing them to respond to softer sounds in the environment.

L2/3 neurons display a long window of plasticity after sensory deprivation in V1 (Desai et al., 2002; Goel and Lee, 2007), hence it is not surprising that A1 L2/3 neurons respond to cross-modal sensory deprivation even at P90 (**Chapter 5**, **Fig 7.1**). The lack of synaptic plasticity in adult V1 L4 with DE (**Chapter 4 & Fig. 7.1**) was also expected, and is consistent with a narrow plastic window in L4 as described previously (Desai et al., 2002; Jiang et al., 2007). However, the observed potentiation of TC inputs to A1 in

adult mice deprived of vision was unexpected (**Chapter 4 & Fig. 7.1**) and suggests that cross-modal sensory deprivation can restore plasticity of TC inputs. TC synapses are thought to be generally aplastic after an early critical period in A1 (P12-15 in mice) (de Villers-Sidani et al., 2007; Insanally et al., 2009; Sanes and Bao, 2009; Barkat et al., 2011) and in other sensory cortices [reviewed in (Hensch, 2005)], but recently this dogma has been challenged by numerous groups using a variety of sensory deprivation mechanisms across multiple sensory systems (Montey and Quinlan, 2011; Oberlaender et al., 2012; Yu et al., 2012).

My results demonstrate that plasticity of TC synapses are more readily recruited by cross-modal sensory deprivation than unimodal paradigms in adults (**Chapter 4**). This seems to be a general phenomenon as it occurs in A1 after loss of sight, and in V1 after loss of hearing (**Chapter 4**). I also found that cross-modal potentiation of L4 synaptic strength is not only mediated by stronger thalamocortical (TC) inputs from the auditory thalamus, but also by potentiation of lateral inputs within A1 L4 after DE (**Chapter 4 & Fig 7.1**). The stronger feed-forward (FF) inputs from thalamus may serve to enhance the auditory signal arriving which mediates better sound processing in A1 L4 neurons *in vivo* (Petrus et al., 2014), while lateral inputs in A1 L4 may further amplify the signal as it is passed onward through the cortical circuit (Wu et al., 2011a; Li et al., 2013) (**Chapter 5 & Fig 7.1**).

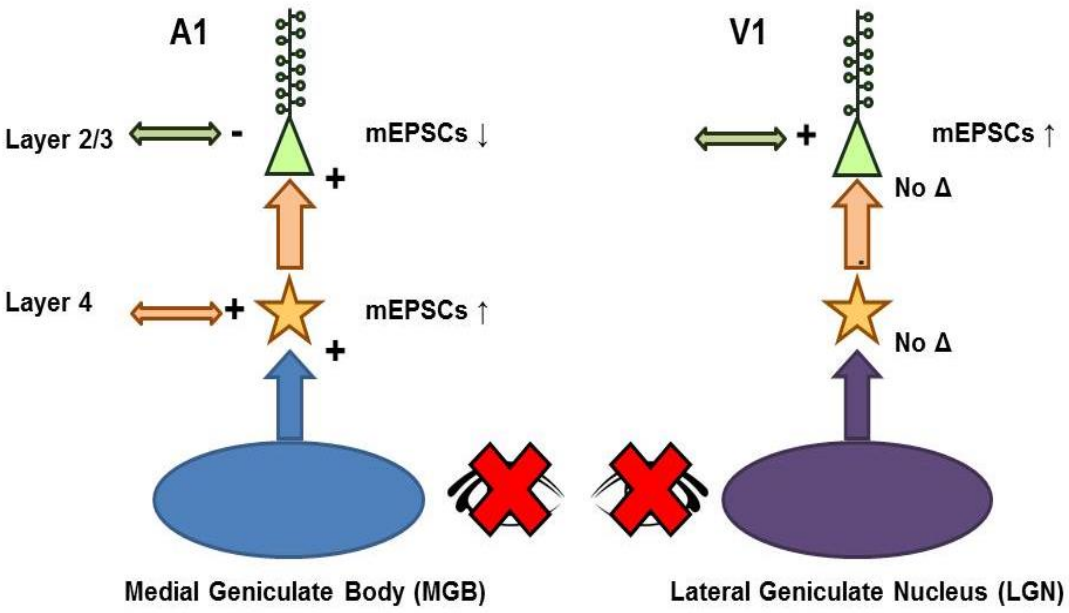

Figure 7.1: Changes in excitatory synaptic strength in A1 and V1 after visual deprivation

The changes observed in A1 may mediate enhanced processing of auditory signals, but the changes in V1 are also important to consider. V1 L4 lacks experience-dependent plasticity after an early critical period, consistent with earlier reports (Desai et al., 2002; Jiang et al., 2007; Petrus et al., 2014), as neither FF inputs from LGN to L4 or inputs from L4 to L2/3 changes after DE (**Chapters 4, 5 & Fig. 7.1)**. However, mEPSC amplitudes in L2/3 scaled up consistent with previous findings (Desai et al., 2002; Goel et al., 2006; Goel and Lee, 2007; Gao et al., 2010), which I found is mainly due to stronger lateral inputs (**Chapter 5 & Fig. 7.1)**. Lateral inputs to V1 L2/3 neurons play an important role in integrating micro-circuit visual processing, such as understanding to what nearby groups of cells are responding, which is especially true in the well-organized

V1 of cat (Douglas and Martin, 2004). In primate they may also be involved in integrating long range lateral inputs from other cortical areas (Lakatos et al., 2007; Kayser et al., 2009). Therefore, potentiation of lateral inputs to L2/3 may serve as a potential mechanism for the primary sensory cortex to be recruited for processing other sensory modalities after losing its primary sense. Potentiation of the lateral connections into L2/3 may allow subthreshold lateral inputs carrying multimodal signals in deprived cortex to reach action potential threshold, which may allow the deprived cortical circuit to process information arising from other modalities.

3. Regulation of inhibitory synapses in spared cortex

Inhibition is integral in maintaining the excitatory/inhibitory balance in cortex, but also is important for sharpening tuning in sensory systems. I found lamina specific changes associated with evoked and spontaneous inhibition in auditory cortex after dark exposure. These changes may work together with excitation to enhance auditory processing after the loss of vision.

A balance of excitation and inhibition is thought to lend stability to a neuronal network, prevent both runaway excitation and inhibition and either broaden or sharpen tuning to stimuli (Troyer et al., 1998; Wehr and Zador, 2003; Issacson and Scanziani, 2012). This balance may be altered by variations in experience, and may be mediated by specific neuronal subtypes. Parvalbumin (PV^+) interneurons preferentially target the soma of excitatory neurons and are regulated by activity (Kawaguchi and Kubota, 1997; Huang et al., 1999; Morales et al., 2002). Because PV^+ neurons target the soma they represent the major source of mIPSCs recorded in pyramidal neurons. Employing a rise

time cutoff to exclude events occurring from distal dendrites further ensures that this activity is from somatically targeted PV^+ synapses (Rall, 1969; Williams and Mitchell, 2008). Although PV^+ neurons may mediate the changes observed in both evoked IPSCs and mIPSCs, these two types of inhibitory synaptic transmission may not be co-regulated (Fredj and Burrone, 2009; Gao et al., 2011; Melom et al., 2013). The lamina specificity of inhibitory changes induced by cross-modal sensory deprivation indicates that spontaneous and evoked inhibition may mediate different effects for sensory processing.

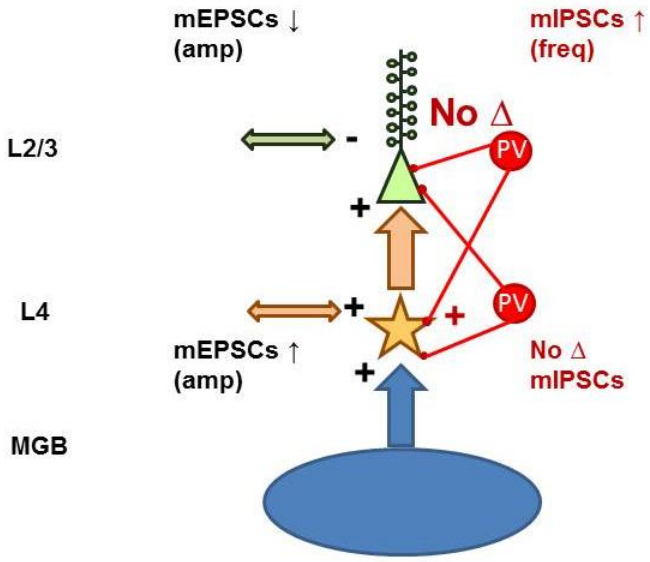

Figure 7.2: Changes in excitatory & inhibitory synaptic strength in A1 after visual deprivation

Visual deprivation via DE induced lamina specific changes in mIPSCs, such that frequency was increased in A1 L2/3, but did not change in L4. Conversely, evoked inhibition was stronger in A1 L4, but not significantly different in A1 L2/3 (**Chapter 5 & Fig. 7.2**). The increased frequency of mIPSCs in A1 L2/3 may increase the tonic level of

inhibition in L2/3, thereby suppressing non-characteristic frequency subthreshold inputs (Bandyopadhyay et al., 2010). Combined with a reduction in mEPSC amplitudes these spontaneous events could shift the system to a less excitable, more inhibited network, which would further narrow the window of evoked inputs resulting in action potentials for recipient neurons. This would ensure that only supra-threshold, "salient" auditory feed-forward signals to result in neuronal spiking.

The lack of change in evoked, PV^+ mediated inhibitory strength in A1 L2/3 could be due to a multitude of factors. If the system is balancing excitation and inhibition, evoked excitation arriving to A1 L2/3 is increasing from L4, but decreasing from lateral inputs. This may result in zero net change in evoked inhibition as synapses tailor to specific neurons receiving both stronger and weaker inputs from different sources. It is also possible that evoked inhibition to L2/3 neurons may be mediated by other subtypes of interneurons. In many cortical areas PV^+ neuronal are the majority of inhibitory neurons, in L2/3 PV^+ neurons represent a smaller majority (Desgent et al., 2005; Rudy et al., 2010; Pfeffer et al., 2013). Therefore, it is possible that the changes in mIPSCs in L2/3 are not from PV^+ neurons but from the second most abundant cell type, somatostatin-positive (SOM^+) interneurons.

Alternatively, vasoactive intestinal peptide (VIP^+) expressing interneurons are located primarily in L2/3 of V1 (Pfeffer et al., 2013). Neuromodulators have been shown to be involved in focusing attention (Noudoost and Moore, 2011), influencing synaptic plasticity (Hu et al., 2007; Seol et al., 2007) and mediating cross-modal plasticity (Jitsuki et al., 2011; Zheng et al., 2014). VIP^+ neurons in rat motor cortex are selectively activated by nicotinic acetylcholine receptor agonists (Porter et al., 1999), and VIP has

been shown to co-localize with acetylcholine in various brain areas (Halbach and Dermietzel, 2006). It may be that neuromodulation of inhibition, which plays a large role in gating multiple types of cortical plasticity, also occurs during cross-modal plasticity.

VIP^+ neurons in V1 preferentially inhibit SOM^+ neurons, which then target other interneuron subtypes, including PV^+ neurons, resulting in multi-synaptic inhibition/disinhibition (Pfeffer et al., 2013; Xu et al., 2013). However, VIP^+ interneurons have been shown to innervate PV^+ neurons directly in S1 (Dávid et al., 2007), or both calbindin expressing and pyramidal neurons in hippocampus (Acsady et al., 1996). Though there is a variety of morphological connections apparent between VIP^+ interneurons and other cell types, their function in vivo has recently been demonstrated. Optogenetic activation of VIP^+ interneurons disinhibits principle neurons in A1, which further demonstrates their role as regulators of inhibitory circuits (Pi et al., 2013). By increasing VIP^+ interneuron activity with neuromodulators, this net domino effect could result in more PV^+ mediated inhibition of pyramidal neurons, which could explain the increase in mIPSC frequency observed in L2/3 of A1 after DE.

In contrast to A1 L2/3, we observed stronger evoked IPSCs from PV^+ neurons in A1 L4 after DE, but no changes in mIPSC amplitude or frequency (**Chapter 5 & Fig, 7.2**). The stronger evoked inhibition from PV^+ neurons may help sharpen characteristic frequency tuning in the thalamorecipient layer (Wu et al., 2008), and PV^+ neurons would be well situated to mediate these changes. They are most prevalent in cortical layers 4, 5 and 6 (Desgent et al., 2005), and provide the strongest inhibition to pyramidal neurons in visual cortex (Pfeffer et al., 2013). While overall increases in mIPSC frequency would serve to dampen the network activity, an increase in evoked IPSC amplitude would

sharpen the temporal window of neural firing. PV^+ inputs to L4 principle neurons can sharpen their tuning and enhance temporal fidelity to incoming auditory signal (Zhang et al., 2011). PV^+ neurons in L4 receive excitatory TC and local L4 inputs and are co-tuned to excitatory inputs form the thalamus (Wehr and Zador, 2003; Zhang et al., 2003; Wu et al., 2006). Hence, the increased strength of eIPSCs onto A1 L4 neurons would serve to sharpen processing of audition to compensate for the loss of vision. Alternatively, the stronger evoked inhibition from PV^+ neurons may be increasing merely to match the increased evoked excitation arriving to A1 L4. Because feed-forward inputs from the thalamus and lateral inputs among L4 neurons are both stronger in A1 after DE, stronger inhibition may be required to balance the system. Regardless of how these changes come about, the loss of vision enhances sound sensitivity and sharpens tuning in A1 L4 neurons (Petrus et al., 2014), and evoked inhibition may contribute to these changes (Wu et al., 2008; Zhang et al., 2011). Spontaneous inhibitory events in A1 L4, on the other hand, did not change in amplitude or frequency (**Chapter 5 & Fig. 7.2**). It may be that spontaneous events play a different role depending on the lamina, and the system's requirements for regulation of spontaneous inhibition may be independent from evoked inhibition or spontaneous excitation. Thus A1 L2/3 may have a larger need for mIPSC regulation, while L4 depends more on evoked inhibition to mediate changes in cortical response and excitation/inhibition balance.

4. Potential molecules involved in uni- and cross-modal plasticity

Activity levels dictate synaptic strength, but first it regulates a host of biochemical pathways that mediate these changes. Many proteins and molecules are implicated in

regulating homeostatic plasticity, but Arc has received specific attention as a "master regulator" (Shepherd and Bear, 2011). Here we have shown that Arc is required for cross-modal plasticity, and an enzyme with which it associates, β-secretase (BACE1), is required for uni-modal plasticity.

Experience dictates both the development and maintenance of synaptic strength in neuronal circuits. As experience changes it is necessary to alter synaptic strengths via Hebbian and/or homeostatic mechanisms for optimal performance and homeostasis maintenance (Turrigiano, 2008; Whitt et al., 2013). One way these synaptic strengths are regulated is by altering AMPA receptor number, subunit composition and dynamics at postsynaptic densities. AMPA receptor recycling is regulated by endocytosis, which is mediated by Arc, a protein positively regulated by activity (Chowdhury et al., 2006; Rial Verde et al., 2006; Shepherd et al., 2006). Visual deprivation does not homeostatically scale up V1 L2/3 mEPSC amplitudes in Arc KO mice (Gao et al., 2010). Interestingly, the inability of Arc KO mice to internalize AMPA receptors efficiently led to a basally larger mEPSC amplitude (Gao et al., 2010), which was also observed in β-secretase (BACE1) KO mice (**Chapter 6**). Recently it was shown that amyloid beta (Aβ) production is positively regulated with neuronal activity (Kamenetz et al., 2003; Cirrito et al., 2005). Production of Aβ occurs by sequential cleavage of amyloid precursor protein (APP) by β- and γ-secretases, both of which have been targets of therapies aimed at reducing Aβ load in Alzheimer's disease patients and mouse models (Wang et al., 2012). Although the genetic deletion of BACE1 does reduce Aβ levels, it can lead to a host of other issues, including synaptic plasticity deficits (Wang et al., 2008, 2010), which indicates Aβ or other products of BACE1 may play a role in normal physiological

functions. I found that BACE1 KO mice are unable to homeostatically regulate V1 L2/3 spontaneous excitatory transmission with alterations in visual experience (**Chapter 6)**. These results suggest that BACE1 activity and its downstream product, such as Aβ, are important regulators of homeostasis independent of brain region.

Wu et al. (2011b) demonstrated an interaction between Arc and endosomes containing APP and BACE1, establishing a link between Arc and Aβ. Arc also associates with presenilin-1 (PS1), which is the catalytic core of the γ-secretase. This study also found low levels of Aβ in Arc KO mice, and high levels of Arc in Alzheimer's disease patients. Recently it has been shown that Arc levels are elevated in Alzheimer's disease patients (Wu et al., 2011b). Arc has long been used as an activity readout, with high levels of Arc correlating with heightened neuronal network activity (Shepherd and Bear, 2011). Part of the pathology of AD includes high levels of Aβ plaques deposition, but recent studies are now uncovering other problems, including hyperexcitability of neurons near plaques (Busche et al., 2008), and elevated neural activity in the default network of AD patients (Mevel et al., 2011). These facts indicate the AD brain may experience heightened network activity, which would induce Arc production in an attempt to scale down synaptic strength. It may be that Arc is transcribed in AD patients in an attempt to scale down synapses, but as a result also enhance Aβ production by targeting PS1 and BACE1 to endosomal compartments. Because Aβ also reduces excitatory synaptic transmission (Kamenetz et al., 2003; Hsieh et al., 2006), this may further depress excitatory synapses and eventually lead to loss of synapses (Hsieh et al., 2006).

Cross-modal plasticity was first observed at the synaptic level as the down scaling of spared sensory cortex mEPSC amplitudes after the loss of another sense (Goel et al., 2006). This scaling down was a global phenomenon and is thought to be a response to higher levels of activity in spared sensory cortex, which may mediate the compensation of the remaining senses (Bavelier and Neville, 2002). The presence of Arc is often used to assess levels of heightened neuronal activity (**see Table 6.1)** *in vivo* (Tagawa et al., 2005; Gao et al., 2010), so an increase in Arc levels in A1 after the loss of vision was a confirmation of this theory (**Chapter 6**). We observed a potentiation of A1 feed-forward circuitry after DE. This may result in heightened activity in A1 L2/3 neurons inducing Arc expression, which then scales down AMPA receptor mediated mEPSC amplitudes. As a consequence, the lateral inputs to A1 L2/3 neurons are weakened in proportion to the feedforward inputs from L4.

Increases in neural activity induce Arc mediated AMPA receptor internalization (Chowdhury et al., 2006; Shepherd et al., 2006). Arc KO mice show elevated basal mEPSC amplitudes in V1 L2/3 (Gao et al., 2010), which we also observed in BACE1 KO mice (**Chapter 6,** Petrus and Lee, 2014). These results indicate that both Aβ and Arc are important for maintaining homeostasis in networks with elevated neural activity. Since cross-modal sensory deprivation induces increased Arc levels in spared cortex, which mediates a homeostatic scaling down of mEPSC amplitudes (Goel et al., 2006), it stands to reason that the loss of BACE1 may alter this machinery as well. If cross-modal plasticity requires the same mechanism as uni-modal sensory deprivation, BACE1 KO mice would potentially be unable to down-scale their synaptic strengths in a way similar to Arc KO mice. AD patients exhibit heightened activity in default networks, and mouse

models of AD exhibit neural hyperexcitability, especially in the vicinity of plaques (Busche et al., 2008, 2012). These results would indicate that activity-induced increased Aβ production, which may be a normal homeostatic adaptation dependent on Arc, may also be responsible for the pathophysiology of AD.

General Conclusions

Sensory experience drives the development and maintenance of cortical circuits. As we experience changes in our environment the brain's amazing ability to adapt has been well demonstrated. Hebbian plasticity allows for specific strengthening and weakening of synapses, while homeostatic plasticity responds by balancing this inherently unstable mechanism. Here I have described in detail the circuit level changes in deprived and spared sensory cortices after manipulations in sensory experience. The alterations in synaptic weights may underlie enhanced processing of spared sensory modalities after the loss of one sense, and possibly the recruitment of the deprived cortex for alternative tasks. A delicate dance between excitation and inhibition in spared sensory cortex works to ensure spared sensory modalities remain in balance but improve sensory processing. Activity regulated molecular mechanisms are also required for uni- and cross-modal homeostatic responses. A key finding of my study is that sensory experience results in laminar and cell type specific changes in cortical circuitry that can be recruited beyond the critical period.

Bibliography

Abramson BP, Chalupa LM (1985) The laminar distribution of cortical connections with the tecto- and cortico-recipient zones in the cat's lateral posterior nucleus. Neuroscience 15:81–95.

Acsady L, Gorcs TJ, Freund TF (1996) Different populations of vasoactive intestinal polypeptide-immunoreactive interneurons are specialized to control pyramidal cells or interneurons in the hippocampus. Neuroscience 73:317–334.

Adams BAD, Forrester JM (1968) The Projection of the Rat's Visual Field on the Cerebral Cortex. J Exp Physiol 53:327–336.

Adesnik H, Scanziani M (2010) Lateral competition for cortical space by layer-specific horizontal circuits. Nature 464:1155–1160.

Ahmed B, Anderson JC, Douglas RJ, Martin K a, Nelson JC (1994) Polyneuronal innervation of spiny stellate neurons in cat visual cortex. J Comp Neurol 341:39–49.

Alary F, Duquette M, Goldstein R, Elaine Chapman C, Voss P, La Buissonnière-Ariza V, Lepore F (2009) Tactile acuity in the blind: a closer look reveals superiority over the sighted in some but not all cutaneous tasks. Neuropsychologia 47:2037–2043.

Alary F, Goldstein R, Duquette M, Chapman CE, Voss P, Lepore F (2008) Tactile acuity in the blind: a psychophysical study using a two-dimensional angle discrimination task. Exp brain Res 187:587–594.

Almeida CG, Tampellini D, Takahashi RH, Greengard P, Lin MT, Snyder EM, Gouras GK (2005) Beta-amyloid accumulation in APP mutant neurons reduces PSD-95 and GluR1 in synapses. Neurobiol Dis 20:187–198.

Amedi A, Raz N, Pianka P, Malach R, Zohary E (2003) Early "visual" cortex activation correlates with superior verbal memory performance in the blind. Nat Neurosci 6:758–766.

Angelucci A, Clasca F, Sur M (1998) Brainstem Inputs to the Ferret Medial Geniculate Nucleus and the Effect of Early Deafferentation on Novel Retinal Projections to the Auditory Thalamus. J Comp Neurol 439:417–439.

Arendt A, Sarti F, Chen L (2013) Chronic inactivation of a neural circuit enhances LTP by inducing silent synapse formation. J Neurosci 33:2087–2096.

Arnold P, Murray C (1998) Memory for faces and objects by deaf and hearing signers and hearing nonsigners. J Psycholinguist Res 27:481–497.

Atasoy D, Ertunc M, Moulder KL, Blackwell J, Chung C, Su J, Kavalali ET (2008) Spontaneous and evoked glutamate release activate two populations of NMDA receptors with limited overlap. J Neurosci 28:10151–10166.

Aton SJ, Seibt J, Dumoulin M, Jha SK, Steinmetz N, Coleman T, Naidoo N, Frank MG (2009) Mechanisms of sleep-dependent consolidation of cortical plasticity. Neuron 61:454–466.

Atzori M, Lei S, Evans DI, Kanold PO, Phillips-Tansey E, McIntyre O, McBain CJ (2001) Differential synaptic processing separates stationary from transient inputs to the auditory cortex. Nat Neurosci 4:1230–1237.

Auer ET, Bernstein LE, Sungkarat W, Singh M (2007) Vibrotactile Activation of the Auditory Cortices in Deaf versus Hearing Adults. Neuroreport 18:645–648.

Bandyopadhyay S, Shamma SA, Kanold PO (2010) Dichotomy of functional organization in the mouse auditory cortex. Nat Neurosci 13:361–368.

Barbour DL, Callaway EM (2008) Excitatory local connections of superficial neurons in rat auditory cortex. J Neurosci 28:11174–11185.

Barkat TR, Polley DB, Hensch TK (2011) A critical period for auditory thalamocortical connectivity. Nat Neurosci 14:1189–1194.

Bavelier D, Neville HJ (2002) Cross-modal plasticity: where and how? Nat Rev Neurosci 3:443–452.

Bavelier D, Tomann A, Hutton C, Mitchell T, Corina D, Liu G, Neville H (2000) Visual attention to the periphery is enhanced in congenitally deaf individuals. J Neurosci 20:RC93.

Bear MF (1995) Mechanism for a sliding synaptic modification threshold. Neuron 15:1–4.

Bear MF, Cooper LN, Ebner FF (1987) A Physiological Basis for a Theory of Synaptic. Science (80-) 237:42–48.

Béïque J, Na Y, Kuhl D, Worley PF, Huganir RL (2011) Arc-dependent synapse-specific homeostatic plasticity. PNAS 108:816–821.

Beker S, Kellner V, Kerti L, Stern E a (2012) Interaction between amyloid-β pathology and cortical functional columnar organization. J Neurosci 32:11241–11249.

Bender DB (1983) Visual activation of neurons in the primate pulvinar depends on cortex but not colliculus. Brain Res 279:258–261.

Benevento L a, Bakkum BW, Cohen RS (1995) gamma-Aminobutyric acid and somatostatin immunoreactivity in the visual cortex of normal and dark-reared rats. Brain Res 689:172–182.

Bero AW, Yan P, Roh JH, Cirrito JR, Stewart FR, Raichle ME, Lee J-M, Holtzman DM (2011) Neuronal activity regulates the regional vulnerability to amyloid-beta deposition. Nat Neurosci 14:750–756.

Bienenstock EL, Cooper LN, Munro PW (1982) Theory for the development of neuron selectivity: orientation specificity and binocular interaction in visual cortex. J Neurosci 2:32–48.

Binzegger T, Douglas RJ, Martin K a C (2004) A quantitative map of the circuit of cat primary visual cortex. J Neurosci 24:8441–8453.

Blais BS, Frenkel MY, Kuindersma SR, Muhammad R, Shouval HZ, Cooper LN, Bear MF (2008) Recovery from monocular deprivation using binocular deprivation. J Neurophysiol 100:2217–2224.

Bochet P, Audinat E, Lambolez B, Crepe F, Rossier J (1994) Subunit Composition at the Singl & ell Level Explains Functional Properties of a GlutamateCated Channel. Neuron 12:383–388.

Bourassa J, Deschenes M (1995) CORTICOTHALAMIC PROJECTIONS FROM THE PRIMARY VISUAL CORTEX IN RATS : A SINGLE FIBER STUDY USING BIOCYTIN AS AN ANTEROGRADE TRACER. Neuroscience 66:253–263.

Briggs F (2010) Organizing principles of cortical layer 6. Front Neural Circuits 4:3.

Briggs F, Usrey WM (2009) Parallel processing in the corticogeniculate pathway of the macaque monkey. Neuron 62:135–146.

Büchel C (1998) Functional neuroimaging studies of Braille reading: cross-modal reorganization and its implications. Brain 121 (Pt 7:1193–1194.

Burkhalter a (1989) Intrinsic connections of rat primary visual cortex: laminar organization of axonal projections. J Comp Neurol 279:171–186.

Burkhalter A, Charles V (1990) Organization of local axon collaterals of efferent projection neurons in rat visual cortex. J Comp Neurol 302:920–934.

Burnashev N, Monyer H, Seeburg PH, Sakmann B (1992) Divalent ion permeability of AMPA receptor channels is dominated by the edited form of a single subunit. Neuron 8:189–198.

Burton H, Snyder AZ, Conturo TE, Akbudak E, Ollinger JM, Raichle ME (2002) Adaptive Changes in Early and Late Blind: A fMRI Study of Braille Reading. J Neurophysiol 87:589–607.

Busche MA, Chen X, Henning H a, Reichwald J, Staufenbiel M, Sakmann B, Konnerth A (2012) Critical role of soluble amyloid-β for early hippocampal hyperactivity in a mouse model of Alzheimer's disease. Proc Natl Acad Sci U S A 109:8740–8745 Available at: http://www.pubmedcentral.nih.gov/articlerender.fcgi?artid=3365221&tool=pmcentrez&rendertype=abstract [Accessed April 30, 2014].

Busche MA, Eichhoff G, Adelsberger H, Abramowski D, Wiederhold K, Haass C, Staufenbiel M, Konnerth A, Garaschuk O (2008) Clusters of Hyperactive Neurons Near Amyloid Plaques in a Mouse Model of Alzheimer ' s Disease. Science (80-) 321:1686–1689.

Buzsaki G (1984) Feed-Forward Inhibition in the Hippocampal Formation. Prog Neurobiol 22:131–153.

Cai H, Wang Y, McCarthy D, Wen H, Borchelt DR, Price DL, Wong PC (2001) BACE1 is the major beta-secretase for generation of Abeta peptides by neurons. Nat Neurosci 4:233–234.

Callaway EM (1998) LOCAL CIRCUITS IN PRIMARY VISUAL CORTEX OF THE MACAQUE MONKEY. Annu Rev Neurosci 21:47–74.

Callaway EM (2003) Cell type specificity of local cortical connections. J Neurocytol 31:231–237.

Callaway EM (2004) Feedforward, feedback and inhibitory connections in primate visual cortex. Neural Netw 17:625–632.

Cardin JA, Palmer LA, Contreras D (2007) Stimulus Feature Selectivity in Excitatory and Inhibitory Neurons in Primary Visual Cortex. J Neurosci 27:10333–10344.

Carr CE (1993) PROCESSING OF TEMPORAL INFORMATION IN THE BRAIN. Annu Rev Neurosci 16:223–243.

Casagrande VA, Kaas JH (1994) The Afferent , Intrinsic , and Efferent Connections of Primary Visual Cortex in Primates. Cereb cortex 10:201–259.

Castro JB, Kandler K (2010) Changing tune in auditory cortex. Nat Neurosci 13:271–273.

Chang MC, Park JM, Pelkey KA, Grabenstatter HL, Xu D, Linden DJ, Sutula TP, McBain CJ, Worley PF (2010) Narp regulates homeostatic scaling of excitatory synapses on Parvalbumin interneurons. Nat Neurosci 13:1090–1097.

Chao SZ, Lu W, Lee H-K, Huganir RL, Wolf ME (2002) D(1) dopamine receptor stimulation increases GluR1 phosphorylation in postnatal nucleus accumbens cultures. J Neurochem 81:984–992.

Chattopadhyaya B, Di Cristo G, Higashiyama H, Knott GW, Kuhlman SJ, Welker E, Huang ZJ (2004) Experience and activity-dependent maturation of perisomatic GABAergic innervation in primary visual cortex during a postnatal critical period. J Neurosci 24:9598–9611.

Chen X, Leischner U, Rochefort NL, Nelken I, Konnerth A (2011) Functional mapping of single spines in cortical neurons in vivo. Nature 475:501–505.

Chittajallu R, Issac JTR (2010) Emergence of cortical inhibition by coordinated sensory-drive plasticity at distinct synaptic loci. Nat Neurosci 13:1240–1248.

Chowdhury S, Shepherd JD, Okuno H, Lyford G, Petralia RS, Plath N, Kuhl D, Huganir RL, Worley PF (2006) Arc Interacts with the Endocytic Machinery to Regulate AMPA Receptor Trafficking. Neuron 52:445–459.

Cirrito JR, Kang J-E, Lee J, Stewart FR, Verges DK, Silverio LM, Bu G, Mennerick S, Holtzman DM (2008) Endocytosis is required for synaptic activity-dependent release of amyloid-beta in vivo. Neuron 58:42–51.

Cirrito JR, Yamada K a, Finn MB, Sloviter RS, Bales KR, May PC, Schoepp DD, Paul SM, Mennerick S, Holtzman DM (2005) Synaptic activity regulates interstitial fluid amyloid-beta levels in vivo. Neuron 48:913–922 Available at: http://www.ncbi.nlm.nih.gov/pubmed/16364896 [Accessed March 22, 2014].

Clem RL, Barth A (2006) Pathway-specific trafficking of native AMPARs by in vivo experience. Neuron 49:663–670.

Cohen LG, Celnik P, Pascual-Leone A, Corwell B, Falz L, Dambrosia J, Honda M, Sadato N, Gerloff C, Catalá MD, Hallett M (1997) Functional relevance of cross-modal plasticity in blind humans. Nature 389:180–183.

Cooke SF, Bear MF (2010) Visual experience induces long-term potentiation in the primary visual cortex. J Neurosci 30:16304–16313.

Crair MC, Malenka RC (1995) A critical period for long-term potentiation at thalamocortical synapses. Lett to Nat 375:325–328.

Creutzfeldt OD (1977) Generality of the functional structure of the neocortex. Naturwissenschaften 64:507–517.

Crook JM, Eysel UT (1992) GABA-induced inactivation of functionally characterized sites in cat visual cortex (area 18): effects on orientation tuning. J Neurosci 12:1816–1825.

Crook JM, Kisvárday ZF, Eysel UT (1998) Evidence for a contribution of lateral inhibition to orientation tuning and direction selectivity in cat visual cortex: reversible inactivation of functionally characterized sites combined with neuroanatomical tracing techniques. Eur J Neurosci 10:2056–2075.

Cruikshank SJ, Rose HJ, Metherate R (2002) Auditory thalamocortical synaptic transmission in vitro. J Neurophysiol 87:361–384.

Da Costa NM, Martin K a C (2009) Selective targeting of the dendrites of corticothalamic cells by thalamic afferents in area 17 of the cat. J Neurosci 29:13919–13928.

Dávid C, Schleicher A, Zuschratter W, Staiger JF (2007) The innervation of parvalbumin-containing interneurons by VIP-immunopositive interneurons in the primary somatosensory cortex of the adult rat. Eur J Neurosci 25:2329–2340 Available at: http://www.ncbi.nlm.nih.gov/pubmed/17445231 [Accessed March 25, 2014].

De Labra C, Rivadulla C, Grieve K, Mariño J, Espinosa N, Cudeiro J (2007) Changes in visual responses in the feline dLGN: selective thalamic suppression induced by transcranial magnetic stimulation of V1. Cereb Cortex 17:1376–1385.

De Strooper B (2003) Aph-1, Pen-2 and Nicastrin with Presenilin Generate an Active gamma-secretase Complex. Neuron 38:9–12.

De Villers-Sidani E, Chang EF, Bao S, Merzenich MM (2007) Critical period window for spectral tuning defined in the primary auditory cortex (A1) in the rat. J Neurosci 27:180–189.

Deeg KE, Aizenman CD (2011) Sensory modality-specific homeostatic plasticity in the developing optic tectum. Nat Neurosci 14:548–550.

Desai NS, Cudmore RH, Nelson SB, Turrigiano GG (2002) Critical periods for experience-dependent synaptic scaling in visual cortex. Nat Neurosci 5:783–789.

Desgent S, Boire D, Ptito M (2005) Distribution of calcium binding proteins in visual and auditory cortices of hamsters. Exp brain Res 163:159–172.

Desgent S, Boire D, Ptito M (2010) Altered expression of parvalbumin and calbindin in interneurons within the primary visual cortex of neonatal enucleated hamsters. Neuroscience 171:1326–1340.

Desgent, S., Ptito M (2012) Cortical Gabaergic Interneurons in Cross-Modal Plasticity following Early Blindness. Neural Plast 2012:1–20.

Diamond ME, Armstrong-James M, Ebner FF (1992) Somatic sensory responses in the rostral sector of the posterior group (POm) and in the ventral posterior medial nucleus (VPM) of the rat thalamus. J Comp Neurol 318:462–476.

Douglas RJ, Koch C, Mahowald M, Martin K a, Suarez HH (1995) Recurrent excitation in neocortical circuits. Science 269:981–985.

Douglas RJ, Martin KAC (2004) Neuronal circuits of the neocortex. Annu Rev Neurosci 27:419–451.

Douglas RJ, Martin KAC, Whitteridge D (1989) A Canonical Microcircuit for Neocortex. Neural Comput 1:480–488.

Dye MWG, Hauser PC, Bavelier D (2009) Is visual selective attention in deaf individuals enhanced or deficient? The case of the useful field of view. PLoS One 4:e5640.

Economo C von. (1927) Zellaufbau der Grosshirnrinde des Menschen. Berlin: J. Springer.

Ehret G (1997) The auditory cortex. J Comp Physiol A 181:547–557.

Esteban J a, Shi S-H, Wilson C, Nuriya M, Huganir RL, Malinow R (2003) PKA phosphorylation of AMPA receptor subunits controls synaptic trafficking underlying plasticity. Nat Neurosci 6:136–143.

Feldman DE, Brecht M (2005) Map Plasticity in Somatosensory Cortex. Science (80-) 310:810–815.

Feller MB, Scanziani M (2005) A precritical period for plasticity in visual cortex. Curr Opin Neurobiol 15:94–100.

Ferrer I, Fabregues I, Condom E (1986) A Golgi study of the sixth layer of the cerebral cortex. I. The lissencephalic brain of Rodentia, Lagomorpha, Insectivora and Chiroptera. J Anat 145:217–234.

Ferster D, Chung S, Wheat H (1996) Orientation selectivity of thalamic input to simple cells of cat visual cortex. Nature 380:249–252.

Ferster D, Jagadeesh B (1992) EPSP-IPSP interactions in cat visual cortex studied with in vivo whole-cell patch recording. J Neurosci 12:1262–1274.

Finnerty GT, Connors BW (2000) Sensory deprivation without competition yields modest alterations of short-term synaptic dynamics. Proc Natl Acad Sci U S A 97:12864–12868.

Fitzpatrick D (2000) Seeing beyond the receptive field in primary visual cortex. Curr Opin Neurobiol 10:438–443.

Formisano E, Kim DS, Di Salle F, van de Moortele PF, Ugurbil K, Goebel R (2003) Mirror-symmetric tonotopic maps in human primary auditory cortex. Neuron 40:859–869.

Fox K (2002) ANATOMICAL PATHWAYS AND MOLECULAR MECHANISMS FOR. Neuroscience 111:799–814.

Fredj N Ben, Burrone J (2009) A resting pool of vesicles is responsible for spontaneous vesicle fusion at the synapse. Nat Neurosci 12:751–758.

Frenkel MY, Bear MF (2004) How Monocular Deprivation Shifts Ocular Dominance in Visual Cortex of Young Mice. Neuron 44:917–923.

Fritz J, Shamma S, Elhilali M, Klein D (2003) Rapid task-related plasticity of spectrotemporal receptive fields in primary auditory cortex. Nat Neurosci 6:1216–1223.

Fritz JB, Elhilali M, Shamma SA (2007) Adaptive Changes in Cortical Receptive Fields Induced by Attention to Complex Sounds. J Neurophysiol 98:2337–2346.

Fukumoto H, Cheung BS, Hyman BT, Irizarry MC (2002) Beta-secretase protein and activity are increased in the neocortex in Alzheimer disease. Arch Neurol 59:1381–1389 Available at: http://www.ncbi.nlm.nih.gov/pubmed/12223024.

Gainey MA, Hurvitz-wolff JR, Lambo ME, Turrigiano GG (2009) Synaptic Scaling Requires the GluR2 Subunit of the AMPA Receptor. J Neurosci 29:6479–6489.

Gao M, Huang S, Jacobs C, Song L, Kirkwood A, Lee H-K (2011) Experience-dependent regulation of inhibitory synapses in the superficial layers of mouse visual cortex. Soc Neurosci Abstr.

Gao M, Sossa K, Song L, Errington L, Cummings L, Hwang H, Kuhl D, Worley P, Lee H-K (2010) A specific requirement of Arc/Arg3.1 for visual experience-induced homeostatic synaptic plasticity in mouse primary visual cortex. J Neurosci 30:7168–7178.

Gil Z, Amitai Y (1996) Properties of convergent thalamocortical and intracortical synaptic potentials in single neurons of neocortex. J Neurosci 16:6567–6578.

Gil Z, Connors BW, Amitai Y (1999) Efficacy of thalamocortical and intracortical synaptic connections: quanta, innervation, and reliability. Neuron 23:385–397.

Gilbert CD (1983) Visual cortex microcircuitry of the. Annu Rev Neurosci.

Gilbert CD, Wiesel T.N. (1979) Morphology and intracortical projections of functionally characterised neurones in the cat visual cortex. Nature 280:120–125.

Gilbert CD, Wiesel TN (1983) Clustered Intrinsic Connections in Cat Visual Cortex. J Neurosci 3:1116–1133.

Gilbert D, T.N. W (1989) Columnar Specificity of Intrinsic Horizontal Connections in Cat Visual Cortex and Corticocortical Connections in Cat Visual Cortex. J Neurosci 9:2432–2442.

Giraud a L, Price CJ, Graham JM, Truy E, Frackowiak RS (2001) Cross-modal plasticity underpins language recovery after cochlear implantation. Neuron 30:657–663.

Giraud A-L, Lee H-J (2007) Predicting cochlear implant outcome from brain organisation in the deaf. Restor Neurol Neurosci 25:381–390.

Goel A, Jiang B, Xu LW, Song L, Kirkwood A, Lee H-K (2006) Cross-modal regulation of synaptic AMPA receptors in primary sensory cortices by visual experience. Nat Neurosci 9:1001–1003.

Goel A, Lee H-K (2007) Persistence of experience-induced homeostatic synaptic plasticity through adulthood in superficial layers of mouse visual cortex. J Neurosci 27:6692–6700.

Goel A, Xu LW, Snyder KP, Song L, Goenaga-Vazquez Y, Megill A, Takamiya K, Huganir RL, Lee H-K (2011) Phosphorylation of AMPA receptors is required for sensory deprivation-induced homeostatic synaptic plasticity. PLoS One 6:e18264.

Goldreich D, Kanics IM (2003) Tactile acuity is enhanced in blindness. J Neurosci 23:3439–3445.

Gonchar Y, Burkhalter A (1997) Three distinct families of GABAergic neurons in rat visual cortex. Cereb Cortex 7:347–358.

Gordon JA, Styker MP (1996) Experience-Dependent Plasticity of Binocular Responses in the Primary Visual Cortex of the Mouse. J Neurosci 16:3274–3286.

Gougoux F, Lepore F, Lassonde M, Voss P, Zatorre RJ, Belin P (2004) Pitch discrimination in the early blind. Nature 430.

Gregory RL (2003) Seeing after blindness. Nat Neurosci 6:909–910.

Grienberger C, Rochefort NL, Adelsberger H, Henning H a, Hill DN, Reichwald J, Staufenbiel M, Konnerth A (2012) Staged decline of neuronal function in vivo in an animal model of Alzheimer's disease. Nat Commun 3:774.

Grimsley JMS, Monaghan JJM, Wenstrup JJ (2011) Development of social vocalizations in mice. PLoS One 6:e17460.

Guillery RW (1995) Anatomical evidence concerning the role of the thalamus in corticocortical communication: a brief review. J Anat 187 (Pt 3:583–592.

Guire ES, Oh MC, Soderling TR, Derkach V a (2008) Recruitment of calcium-permeable AMPA receptors during synaptic potentiation is regulated by CaM-kinase I. J Neurosci 28:6000–6009.

Guo Y, Huang S, Pasquale R d., McGehrin K, Lee H-K, Zhao K, Kirkwood A (2013) DARK EXPOSURE EXTENDS THE INTEGRATION WINDOW FOR SPIKE-TIMING DEPENDENT PLASTICITY. J Neurosci 32:15027–15035.

Gupta a. (2000) Organizing Principles for a Diversity of GABAergic Interneurons and Synapses in the Neocortex. Science (80-) 287:273–278.

Gusnard DA, Raichle ME (2001) SEARCHING FOR A BASELINE : FUNCTIONAL IMAGING AND THE RESTING HUMAN BRAIN. Nat Rev Neurosci 2:685–694.

Guzowski JF, Lyford GL, Stevenson GD, Houston FP, McGaugh JL, Worley PF, Barnes C a (2000) Inhibition of activity-dependent arc protein expression in the rat hippocampus impairs the maintenance of long-term potentiation and the consolidation of long-term memory. J Neurosci 20:3993–4001.

Halbach O, Dermietzel R (2006) Neurotransmitters and Neuromodulators.

Hallman LE, Schofield BR, Lin CS (1988) Dendritic morphology and axon collaterals of corticotectal, corticopontine, and callosal neurons in layer V of primary visual cortex of the hooded rat. J Comp Neurol 272:149–160.

Happel MFK, Jeschke M, Ohl FW (2010) Spectral integration in primary auditory cortex attributable to temporally precise convergence of thalamocortical and intracortical input. J Neurosci 30:11114–11127.

Harauzov A, Spolidoro M, DiCristo G, De Pasquale R, Cancedda L, Pizzorusso T, Viegi A, Berardi N, Maffei L (2010) Reducing intracortical inhibition in the adult visual cortex promotes ocular dominance plasticity. J Neurosci 30:361–371.

He H-Y, Hodos W, Quinlan EM (2006) Visual deprivation reactivates rapid ocular dominance plasticity in adult visual cortex. J Neurosci 26:2951–2955.

He H-Y, Ray B, Dennis K, Quinlan EM (2007) Experience-dependent recovery of vision following chronic deprivation amblyopia. Nat Neurosci 10:1134–1136.

He K, Goel A, Ciarkowski CE, Song L, Lee H-K (2011) Brain area specific regulation of synaptic AMPA receptors by phosphorylation. Commun Integr Biol 4:569–572.

He K, Petrus E, Gammon N, Lee H-K (2012) Distinct sensory requirements for unimodal and cross-modal homeostatic synaptic plasticity. J Neurosci 32:8469–8474.

He K, Song L, Cummings LW, Goldman J, Huganir RL, Lee H-K (2009) Stabilization of Ca2+-permeable AMPA receptors at perisynaptic sites by GluR1-S845 phosphorylation. Proc Natl Acad Sci U S A 106:20033–20038.

Hebb DO (1949) The Organization of Behavior: A Neuropsychological Theory.

Hefti BJ, Smith PH (2003) Distribution and kinetic properties of GABAergic inputs to layer V pyramidal cells in rat auditory cortex. J Assoc Res Otolaryngol 4:106–121.

Hensch TK (2005) Critical period plasticity in local cortical circuits. Nat Rev Neurosci 6:877–888.

Heynen a J, Bear MF (2001) Long-term potentiation of thalamocortical transmission in the adult visual cortex in vivo. J Neurosci 21:9801–9813.

Heynen AJ, Yoon B-J, Liu C-H, Chung HJ, Huganir RL, Bear MF (2003) Molecular mechanism for loss of visual cortical responsiveness following brief monocular deprivation. Nat Neurosci 6:854–862.

Hickok G, Klima E, Kritchevsky M, Bellugi U (1995) A CASE OF "SIGN BLINDNESS" FOLLOWING LEFT OCCIPITAL DAMAGE IN A DEAF SIGNER. Neuropsychologia 33:1597–1606.

Hitt BD, Jaramillo TC, Chetkovich DM, Vassar R (2010) BACE1-/- mice exhibit seizure activity that does not correlate with sodium channel level or axonal localization. Mol Neurodegener 5:31.

Hof PR, Bouras C, Constantinidis J, Morrison JH (1989) Balint ' s syndrome in Alzheimer ' s disease : specific disruption of the occipito-parietal visual pathway. Brain Res 493:368–375.

Hof PR, Bouras C, Constantinidis J, Morrison JH (1990) Selective Disconnection of Specific Visual Association Pathways in Cases of Alzheimer's Disease Presenting with Balint's Syndrome. J Neuropathol Exp Neurol 49:168–184.

Hof PR, Vogt B a, Bouras C, Morrison JH (1997) Atypical form of Alzheimer's disease with prominent posterior cortical atrophy: a review of lesion distribution and circuit disconnection in cortical visual pathways. Vision Res 37:3609–3625.

Holsinger RMD, McLean CA, Beyreuther K, Masters CL, Evin G (2002) Increased expression of the amyloid precursor B-secretase in Alzheimer's Disease. Ann Neurol 51:783–786.

Hsieh H, Boehm J, Sato C, Iwatsubo T, Tomita T, Sisodia S, Malinow R (2006) AMPAR removal underlies Abeta-induced synaptic depression and dendritic spine loss. Neuron 52:831–843.

Hu H, Real E, Takamiya K, Kang M-G, Ledoux J, Huganir RL, Malinow R (2007) Emotion enhances learning via norepinephrine regulation of AMPA-receptor trafficking. Cell 131:160–173.

Hu X, Zhou X, He W, Yang J, Xiong W, Wong P, Wilson CG, Yan R (2010) BACE1 deiciency causes altered neuronal activity and neurodegeneration. J Neurosci 30:8819–8829.

Huang CL, Winer J a (2000) Auditory thalamocortical projections in the cat: laminar and areal patterns of input. J Comp Neurol 427:302–331.

Huang S, Treviño M, He K, Ardiles A, Pasquale R De, Guo Y, Palacios A, Huganir R, Kirkwood A (2012) Pull-push neuromodulation of LTP and LTD enables bidirectional experience-induced synaptic scaling in visual cortex. Neuron 73:497–510.

Huang ZJ, Kirkwood A, Pizzorusso T, Porciatti V, Morales B, Bear MF, Maffei L, Tonegawa S (1999) BDNF regulates the maturation of inhibition and the critical period of plasticity in mouse visual cortex. Cell 98:739–755.

Hubel DH (1963) Visual Cortex of the Brain. Sci Am 209:54–63.

Hubel DH, Wiesel T. (1970) The Period of Susceptibility to the Physiological Effects of Unilateral Eye Closure in Kittens. J Physiol 206:419–436.

Huse JT, Pijak DS, Leslie G., V.M-Y. L, Doms R (2000) Maturation and endosomal targeting of beta-site amyloid precursor protein-cleaving enzyme. The Alzheimer's disease beta-secretase. J Biol Chem 275:33729–33737.

Imig TJ, Morel A (1985) Tonotopic organization in ventral nucleus of medial geniculate body in the cat. J Neurophysiol 53:309–340.

Insanally MN, Köver H, Kim H, Bao S (2009) Feature-dependent sensitive periods in the development of complex sound representation. J Neurosci 29:5456–5462.

Isa T, Itazawa S, Iino M, Tsuzuki K, Ozawa S (1996) Distribution of neurones expressing inwardly rectifying and Ca(2+)-permeable AMPA receptors in rat hippocampal slices. J Physiol 491 (Pt 3:719–733.

Isaac JTR, Ashby MC, McBain CJ (2007) The role of the GluR2 subunit in AMPA receptor function and synaptic plasticity. Neuron 54:859–871.

Issacson JS, Scanziani M (2012) How Inhibition Shapes Cortical Activity. Neuron 72:231–243.

Ito M, Sanides D, Creutzfeldt OD (1977) Brain A Study of Binocular Convergence in Cat Visual Cortex Neurons. Exp Brain Res 28:21–35.

Jiang B, Huang S, Pasquale R De, Millman D, Song L, Lee H, Tsumoto T, Kirkwood A (2010) The maturation of GABAergic transmission in visual cortex requires endocannabinoid-mediated LTD of inhibitory inputs during a critical period. Neuron 66:248–259.

Jiang B, Treviño M, Kirkwood A (2007) Sequential development of long-term potentiation and depression in different layers of the mouse visual cortex. J Neurosci 27:9648–9652.

Jitsuki S, Takemoto K, Kawasaki T, Tada H, Takahashi A, Becamel C, Sano A, Yuzaki M, Zukin RS, Ziff EB, Kessels HW, Takahashi T (2011) Serotonin mediates cross-modal reorganization of cortical circuits. Neuron 69:780–792.

Kaas JH (1997) Topographic maps are fundamental to sensory processing. Brain Res Bull 44:107–112.

Kaas JH, Guillery RW, Allman JM (1972) Some principles of organization in the dorsal lateral geniculate nucleus. Brain Behav Evol 6:253–299.

Kaas JH, Hackett T a (2000) Subdivisions of auditory cortex and processing streams in primates. Proc Natl Acad Sci U S A 97:11793–11799.

Kamenetz F, Tomita T, Hsieh H, Seabrook G, Borchelt D, Iwatsubo T, Sisodia S, Malinow R, Point W (2003) APP Processing and Synaptic Function. Neuron 37:925–937.

Kameyama K, Sohya K, Ebina T, Fukuda A, Yanagawa Y, Tsumoto T (2010) Difference in binocularity and ocular dominance plasticity between GABAergic and excitatory cortical neurons. J Neurosci 30:1551–1559.

Kaneko M, Stellwagen D, Malenka RC, Stryker MP (2008) Tumor necrosis factor-alpha mediates one component of competitive, experience-dependent plasticity in developing visual cortex. Neuron 58:673–680.

Karmarkar UR, Buonomano D V (2007) Timing in the absence of clocks: encoding time in neural network states. Neuron 53:427–438.

Katz B, Rimmer S (1989) Ophthalmologic Manifestations of Alzheimer ' s Disease. Surv Opthalmology 34:31– 43.

Katz LC (1987) Local circuitry of identified projection neurons in cat visual cortex brain slices. J Neurosci 7:1223–1249.

Katz LC, Crowley JC (2002) Development of cortical circuits: lessons from ocular dominance columns. Nat Rev Neurosci 3:34–42.

Kaur S, Lazar R, Metherate R (2004) Intracortical pathways determine breadth of subthreshold frequency receptive fields in primary auditory cortex. J Neurophysiol 91:2551–2567.

Kaur S, Rose HJ, Lazar R, Liang K, Metherate R (2005) Spectral integration in primary auditory cortex: laminar processing of afferent input, in vivo and in vitro. Neuroscience 134:1033–1045.

Kawaguchi Y, Kubota Y (1997) GABAergic cell subtypes and their synaptic connections in rat frontal cortex. Cereb Cortex 7:476–486.

Kayser C, Petkov CI, Logothetis NK (2009) Multisensory interactions in primate auditory cortex: fMRI and electrophysiology. Hear Res 258:80–88.

Kerr JND, de Kock CPJ, Greenberg DS, Bruno RM, Sakmann B, Helmchen F (2007) Spatial organization of neuronal population responses in layer 2/3 of rat barrel cortex. J Neurosci 27:13316–13328.

Khachaturian ZS (1985) Diagnosis of Alzheimer's Disease. Arch Neurol 42:1097–1105.

Kilman V, van Rossum MCW, Turrigiano GG (2002) Activity deprivation reduces miniature IPSC amplitude by decreasing the number of postsynaptic GABA(A) receptors clustered at neocortical synapses. J Neurosci 22:1328–1337.

Kim DY, Carey BW, Wang H, Ingano LAM, Alexander M, Wertz MH, Pettingell WH, He P, Lee VM, Clifford J, Kovacs DM (2009) BACE1 regulates voltage-gated sodium channels and neuronal activity. Nat Cell Biol 9:755–764.

Kim J, Tsien RW (2008) Synapse-specific adaptations to inactivity in hippocampal circuits achieve homeostatic gain control while dampening network reverberation. Neuron 58:925–937.

Kimura a, Donishi T, Sakoda T, Hazama M, Tamai Y (2003) Auditory thalamic nuclei projections to the temporal cortex in the rat. Neuroscience 117:1003–1016.

Komura Y, Tamura R, Uwano T, Nishijo H, Kaga K, Ono T (2001) Retrospective and prospective coding for predicted reward in the sensory thalamus. Nature 412:546–549.

Kotak VC, Fujisawa S, Lee FA, Karthikeyan O, Aoki C, Sanes DH (2005) Hearing loss raises excitability in the auditory cortex. J Neurosci 25:3908–3918.

Kreczko A, Goel A, Song L, Lee H-K (2009) Visual deprivation decreases somatic GAD65 puncta number on layer 2/3 pyramidal neurons in mouse visual cortex. Neural Plast 2009:415135.

Krukowski a E, Miller KD (2001) Thalamocortical NMDA conductances and intracortical inhibition can explain cortical temporal tuning. Nat Neurosci 4:424–430.

Laird FM, Cai H, Savonenko A V, Farah MH, He K, Melnikova T, Wen H, Chiang H-C, Xu G, Koliatsos VE, Borchelt DR, Price DL, Lee H-K, Wong PC (2005) BACE1, a major determinant of selective vulnerability of the brain to amyloid-beta amyloidogenesis, is essential for cognitive, emotional, and synaptic functions. J Neurosci 25:11693–11709.

Lakatos P, Chen CM, O'Connel MN, Mills A, Schroeder CE (2007) Neuronal Oscillations and Multisensory Interaction in Primary Auditory Cortex. Neuron 53:279–292.

Lee AG, Martin CO (2004) Neuro-ophthalmic findings in the visual variant of Alzheimer's disease. Ophthalmology 111:376–80; discussion 380–1.

Lee DS, Lee JS, Oh SH, Kim S-K, Kim J-W, Chung J-K, Lee M., Kim CS (2001) Cross-modal plasticity and cochlear implants. Nature 409:149.

Lee H-K (2012) Ca-permeable AMPA receptors in homeostatic synaptic plasticity. Front Mol Neurosci 5:17.

Lee H-K, Kirkwood A (2011) AMPA receptor regulation during during synaptic plasticity in hippocampus and neocortex. Semin Cell Dev Biol 22:514–520.

Lee S, Hjerling-Leffler J, Zagha E, Fishell G, Rudy B (2010) The largest group of superficial neocortical GABAergic interneurons expresses ionotropic serotonin receptors. J Neurosci 30:16796–16808 Available at: http://www.pubmedcentral.nih.gov/articlerender.fcgi?artid=3025500&tool=pmcentrez&rendertype=abstract [Accessed April 29, 2014].

Lessard N, Paré M, Lepore F, Lassonde M (1998) Early-blind human subjects localize sound sources better than sighted subjects. Nature 395:278–280.

Levanen S (1998) Neuromagnetic studies of human auditory cortex function and reorganization. Scandanavian Audiol 27:1–6.

Levänen S, Hamdorf D (2001) Feeling vibrations: enhanced tactile sensitivity in congenitally deaf humans. Neurosci Lett 301:75–77.

Levay S, Gilbert CD (1976) LAMINAR PATTERNS OF GENICULCORTICAL PROJECTION IN THE CAT. Brain Res 113:1–19.

Li L, Li Y, Zhou M, Tao HW, Zhang LI (2013) Intracortical multiplication of thalamocortical signals in mouse auditory cortex. Nat Neurosci 16:1179–1181.

Linden ML, Heynen AJ, Haslinger RH, Bear MF (2009) Thalamic activity that drives visual cortical plasticity. Nat Neurosci 12:390–392.

Link W, Konietzko U, Kauselmann G, Krug M, Schwanke B, Frey U, Kuhl D (1995) Somatodendritic expression of an immediate early gene is regulated by synaptic activity. Proc Natl Acad Sci U S A 92:5734–5738.

Liu B, Li P, Li Y, Sun YJ, Yanagawa Y, Obata K, Zhang LI, Tao HW (2009) Visual receptive field structure of cortical inhibitory neurons revealed by two-photon imaging guided recording. J Neurosci 29:10520–10532.

Liu B-H, Li P, Sun YJ, Li Y-Y, Zhang L., Tao HW (2010) Intervening Inhibition Underlies Simple-Cell Receptive Field Structure in Visual Cortex. Nat Neurosci 13:89–96.

Liu B-H, Li Y-T, Ma W-P, Pan C-J, Zhang LI, Tao HW (2012) Broad Inhibition Sharpens Orientation Selectivity By Expanding Input Dynamic Range in Mouse Simple Cells. Neuron 71:542–554.

Liu B-H, Wu GK, Arbuckle R, Tao HW, Zhang L. (2007) Defining cortical frequency tuning with recurrent excitatory circuitry. Nat Neurosci 10:1594–1600.

Liu SJ, Zukin RS (2007) Ca2+-permeable AMPA receptors in synaptic plasticity and neuronal death. Trends Neurosci 30:126–134.

Livingstone S, Hubel H (1984) ANATOMY AND PHYSIOLOGY OF A COLOR SYSTEM IN THE PRIMATE VISUAL CORTEX. J Neurosci 4:309–356.

Lomber SG, Meredith MA, Kral A (2011) Adaptive crossmodal plasticity in deaf auditory cortex: areal and laminar contributions to supranormal vision in the deaf., 1st ed. Elsevier B.V.

Lund JS, Yoshioka T, Levitt JB (1993) Comparison of intrinsic connectivity in different areas of macaque monkey cerebral cortex. Cereb cortex 3:148–162.

Luo Y, Bolon B, Kahn S, Bennett BD, Babu-khan S, Denis P, Fan W, Kha H, Zhang J, Gong Y, Martin L, Louis J, Yan Q, Richards WG, Citron M, Vassar R (2001) Mice deficient in BACE1 , the Alzheimer ' s β -secretase , have normal phenotype and abolished β -amyloid generation. Nat Commun 4:231 –232.

Lyford GL, Yamagata K, Kaufmann WE, Barnes C a, Sanders LK, Copeland NG, Gilbert DJ, Jenkins N a, Lanahan a a, Worley PF (1995) Arc, a growth factor and activity-regulated gene, encodes a novel cytoskeleton-associated protein that is enriched in neuronal dendrites. Neuron 14:433–445.

Maffei A, Nataraj K, Nelson SB, Turrigiano GG (2006) Potentiation of cortical inhibition by visual deprivation. Nature 443:81–84.

Maffei A, Nelson SB, Turrigiano GG (2004) Selective reconfiguration of layer 4 visual cortical circuitry by visual deprivation. Nat Neurosci 7:1353–1359.

Maffei A, Turrigiano GG (2008) Multiple modes of network homeostasis in visual cortical layer 2/3. J Neurosci 28:4377–4384.

Malach R, Amir Y, Harel M, Grinvald A (1993) Relationship between intrinsic connections and functional architecture revealed by optical imaging and in vivo targeted biocytin injections in primate striate cortex. Proc Natl Acad Sci U S A 90:10469–10473.

Mariño J, Schummers J, Lyon DC, Schwabe L, Beck O, Wiesing P, Obermayer K, Sur M (2005) Invariant computations in local cortical networks with balanced excitation and inhibition. Nat Neurosci 8:194–201.

Marrocco RT, McClurkin JW, Alkire MT (1996) The influence of the visual cortex on the spatiotemporal response properties of lateral geniculate nucleus cells. Brain Res 737:110–118.

Matsubara J a, Phillips DP (1988) Intracortical connections and their physiological correlates in the primary auditory cortex (AI) of the cat. J Comp Neurol 268:38–48.

Mcbain CJ (1998) A Short-term mechanism of plasticity for interneurones? J Physiol 511:1998.

McClurkin JW, Marrocco RT (1984) Visual Cortical Input Alters Spatial Tuning in Monkey Lateral Geniculate Nucleus Cells. J Physiol 348:135–152.

McCullough S, Emmorey K (1997) Face processing by deaf ASL signers: evidence for expertise in distinguished local features. J Deaf Stud Deaf Educ 2:212–222.

McCurry CL, Shepherd JD, Tropea D, Wang KH, Bear MF, Sur M (2010) Loss of Arc renders the visual cortex impervious to the effects of sensory experience or deprivation. Nat Neurosci 13:450–457.

Melom JE, Akbergenova Y, Gavornik JP, Littleton JT (2013) Spontaneous and evoked release are independently regulated at individual active zones. J Neurosci 33:17253–17263.

Merabet LB, Hamilton R, Schlaug G, Swisher JD, Kiriakopoulos ET, Pitskel NB, Kauffman T, Pascual-Leone A (2008) Rapid and reversible recruitment of early visual cortex for touch. PLoS One 3:e3046.

Merzenich M, Linn G (1975) Representation of Cochlea within Primary Auditory Cortex in the Cat. J Neurophysiol 38:231–249.

Merzenich MM, Brugge JF (1973) Representation of the Cochlear Partition on the Superior Temporal Plane of the Macaque Monkey. Brain Res 50:275–296.

Meskenaite V (1997) Calretinin-immunoreactive local circuit neurons in area 17 of the cynomolgus monkey, Macaca fascicularis. J Comp Neurol 379:113–132.

Metherate R, Aramakis VB (1999) Intrinsic electrophysiology of neurons in thalamorecipient layers of developing rat auditory cortex. Brain Res Dev Brain Res 115:131–144.

Mevel K, Chételat G, Eustache F, Desgranges B (2011) The default mode network in healthy aging and Alzheimer's disease. Int J Alzheimers Dis 2011:535816 Available at: http://www.pubmedcentral.nih.gov/articlerender.fcgi?artid=3132539&tool=pmcentrez&rendertype=abstract [Accessed May 1, 2014].

Miller KD, Pinto DJ, Simons DJ (2001a) Processing in layer 4 of the neocortical circuit: new insights from visual and somatosensory cortex. Curr Opin Neurobiol 11:488–497.

Miller LM, Escabí M a, Read HL, Schreiner CE (2002) Spectrotemporal receptive fields in the lemniscal auditory thalamus and cortex. J Neurophysiol 87:516–527.

Miller LM, Escabí M a, Schreiner CE (2001b) Feature selectivity and interneuronal cooperation in the thalamocortical system. J Neurosci 21:8136–8144.

Mitani a, Shimokouchi M, Itoh K, Nomura S, Kudo M, Mizuno N (1985) Morphology and laminar organization of electrophysiologically identified neurons in the primary auditory cortex in the cat. J Comp Neurol 235:430–447.

Miyashita T, Kubik S, Lewandowski G, Guzowski JF (2008) Networks of Neurons, Networks of Genes: An Integrated View of Memory Consolidation. Neurobiol Learn Mem 89:269–284.

Montey KL, Quinlan EM (2011) Recovery from chronic monocular deprivation following reactivation of thalamocortical plasticity by dark exposure. Nat Commun 2:317.

Morales B, Choi S-Y, Kirkwood A (2002) Dark rearing alters the development of GABAergic transmission in visual cortex. J Neurosci 22:8084–8090.

Morel a, Garraghty PE, Kaas JH (1993) Tonotopic organization, architectonic fields, and connections of auditory cortex in macaque monkeys. J Comp Neurol 335:437–459.

Mosbacher AJ, Schoepfer R, Monyer H, Burnashev N, Seeburg PH, Ruppersberg JP (1994) A Molecular Determinant for Submillisecond Desensitization in Glutamate Receptors. Science (80-) 266:1059–1062.

Mountcastle VB (1957) Modality and Topographic Properties of Single Neurons of Cat's Somatic Sensory Cortex. J Neurophysiol 20:408–434.

Mrsic-Flogel TD, Hofer SB, Ohki K, Reid RC, Bonhoeffer T, Hübener M (2007a) Homeostatic regulation of eye-specific responses in visual cortex during ocular dominance plasticity. Neuron 54:961–972.

Mrsic-Flogel TD, Hofer SB, Ohki K, Reid RC, Bonhoeffer T, Hübener M (2007b) Homeostatic regulation of eye-specific responses in visual cortex during ocular dominance plasticity. Neuron 54:961–972.

Murphy PC (1999) Feedback Connections to the Lateral Geniculate Nucleus and Cortical Response Properties. Science (80-) 286:1552–1554.

Nataraj K, Le Roux N, Nahmani M, Lefort S, Turrigiano G (2010) Visual deprivation suppresses L5 pyramidal neuron excitability by preventing the induction of intrinsic plasticity. Neuron 68:750–762.

Neville HJ, Lawson D (1987) Attention to central and peripheral visual space in a movement detection task. III. Separate effects of auditory deprivation and acquisition of a visual language. Brain Res 405:284–294.

Ni H, Huang L, Chen N, Zhang F, Liu D, Ge M, Guan S, Zhu Y, Wang J-H (2010) Upregulation of barrel GABAergic neurons is associated with cross-modal plasticity in olfactory deficit. PLoS One 5:e13736.

Noudoost B, Moore T (2011) The role of neuromodulators in selective attention. Trends Cogn Sci 15:585–591 Available at: http://www.pubmedcentral.nih.gov/articlerender.fcgi?artid=3351278&tool=pmcentrez&rendertype=abstract [Accessed April 8, 2014].

O'Brien RJ, Kamboj S, Ehlers MD, Rosen KR, Fischbach GD, Huganir RL (1998) Activity-dependent modulation of synaptic AMPA receptor accumulation. Neuron 21:1067–1078.

Oberlaender M, Ramirez A, Bruno RM (2012) Sensory experience restructures thalamocortical axons during adulthood. Neuron 74:648–655.

Oh MC, Derkach V a, Guire ES, Soderling TR (2006) Extrasynaptic membrane trafficking regulated by GluR1 serine 845 phosphorylation primes AMPA receptors for long-term potentiation. J Biol Chem 281:752–758.

Ohki K, Chung S, Ch'ng YH, Kara P, Reid RC (2005) Functional imaging with cellular resolution reveals precise micro-architecture in visual cortex. Nature 433:597–603.

Ohki K, Chung S, Kara P, Hübener M, Bonhoeffer T, Reid RC (2006) Highly ordered arrangement of single neurons in orientation pinwheels. Nature 442:925–928.

Ojima H (1994) Terminal morphology and distribution of corticothalamic fibers originating from layers 5 and 6 of cat primary auditory cortex. Cereb Cortex 4:646–663.

Olsen SR, Bortone DS, Adesnik H, Scanziani M (2012) Gain control by layer six in cortical circuits of vision. Nature 483:47–52.

Otis TS, Raman IM, Trussell LO (1995) AMPA receptors with high Ca2+ permeability mediate synaptic transmission in the avian auditory pathway. J Physiol 482 (Pt 2:309–315.

Petrus E, Anguh TT, Pho H, Lee A, Gammon N, Lee H-K (2011) Developmental switch in the polarity of experience-dependent synaptic changes in layer 6 of mouse visual cortex. J Neurophysiol 106:2499–2505.

Petrus E, Isaiah A, Jones AP, Li D, Wang H, Lee H-K, Kanold PO (2014) Crossmodal Induction of Thalamocortical Potentiation Leads to Enhanced Information Processing in the Auditory Cortex. Neuron 81:664–673.

Petrus E, Lee H-K (2014) BACE1 is necessary for experience-dependent homeostatic synaptic plasticity in visual cortex. Neural Plast in press.

Pfeffer CK, Xue M, He M, Huang ZJ, Scanziani M (2013) Inhibition of inhibition in visual cortex: the logic of connections between molecularly distinct interneurons. Nat Neurosci 16:1068–1076.

Pi H-J, Hangya B, Kvitsiani D, Sanders JI, Huang ZJ, Kepecs A (2013) Cortical interneurons that specialize in disinhibitory control. Nature 503:521–524 Available at: http://www.ncbi.nlm.nih.gov/pubmed/24097352 [Accessed March 23, 2014].

Plant K, Pelkey KA, Bortolotto ZA, Morita D, Terashima A, McBain CJ, Collingridge GL, Isaac JT (2006) Transient incorporation of native GluR2-lacking AMPA receptors during hippocampal long-term potentiation. Nat Neurosci 9.

Plath N et al. (2006) Arc/Arg3.1 is essential for the consolidation of synaptic plasticity and memories. Neuron 52:437–444.

Ploski JE, Pierre VJ, Smucny J, Park K, Monsey MS, Overeem K a, Schafe GE (2008) The activity-regulated cytoskeletal-associated protein (Arc/Arg3.1) is required for memory consolidation of pavlovian fear conditioning in the lateral amygdala. J Neurosci 28:12383–12395.

Popescu M V, Ebner FF (2010) Neonatal sensory deprivation and the development of cortical function: unilateral and bilateral sensory deprivation result in different functional outcomes. J Neurophysiol 104:98–107.

Porter JT, Cauli B, Tsuzuki K, Lambolez B, Rossier J, Audinat E (1999) Selective excitation of subtypes of neocortical interneurons by nicotinic receptors. J Neurosci 19:5228–5235 Available at: http://www.ncbi.nlm.nih.gov/pubmed/10377334.

Pouille F, Scanziani M (2001) Enforcement of temporal fidelity in pyramidal cells by somatic feed-forward inhibition. Science (80-) 293:1159–1163.

Prieto JJ, Winer JA (1999) Layer VI in Cat Primary Auditory Cortex: Golgi Study and Sublaminar Origins. J Comp Neurol 404:332–358.

Prvulovic D, Van de Ven V, Sack AT, Maurer K, Linden DEJ (2005) Functional activation imaging in aging and dementia. Psychiatry Res 140:97–113 Available at: http://www.ncbi.nlm.nih.gov/pubmed/16257186 [Accessed April 30, 2014].

Qian H, Matt L, Zhang M, Nguyen M, Patriarchi T, Koval OM, Anderson ME, He K, Lee H-K, Hell JW (2012) β2-Adrenergic receptor supports prolonged theta tetanus-induced LTP. J Neurophysiol 107:2703–2712.

Rall W (1969) Distributions of potential in cylindrical coordinates and time constants for a membrane cylinder. Biophys J 9:1509–1541.

Rannals MD, Kapur J (2012) Homeostatic Strengthening of Inhibitory Synapses is Mediated by the Accumulation of GABAa receptors. Neurosci J 31:17701–17712.

Ranson A, Cheetham CEJ, Fox K, Sengpiel F (2012) Homeostatic plasticity mechanisms are required for juvenile, but not adult, ocular dominance plasticity. Proc Natl Acad Sci U S A 109:1311–1316.

Rao Y, Daw NW (2004) Layer variations of long-term depression in rat visual cortex. J Neurophysiol 92:2652–2658.

Read HL, Winer J a, Schreiner CE (2001) Modular organization of intrinsic connections associated with spectral tuning in cat auditory cortex. Proc Natl Acad Sci U S A 98:8042–8047.

Reale R a, Imig TJ (1980) Tonotopic organization in auditory cortex of the cat. J Comp Neurol 192:265–291.

Rial Verde EM, Lee-Osbourne J, Worley PF, Malinow R, Cline HT (2006) Increased expression of the immediate-early gene arc/arg3.1 reduces AMPA receptor-mediated synaptic transmission. Neuron 52:461–474.

Ribak CE, Peters A (1975) AN AUTORADIOGRAPHIC STUDY OF THE PROJECTIONS FROM THE LATERAL GENICULATE BODY OF THE RAT. Brain Res 92:341–368.

Rittenhouse CD, Shouval HZ, Paradiso MA, Bear MF (1999) Monocular deprivation induces homosynaptic long-term depression in visual cortex Ocular dominance. Nature 397:347–350.

Rittenhouse CD, Siegler B a, Voelker CC, Voelker C a, Shouval HZ, Paradiso M a, Bear MF (2006) Stimulus for rapid ocular dominance plasticity in visual cortex. J Neurophysiol 95:2947–2950.

Roberds SL et al. (2001) BACE knockout mice are healthy despite lacking the primary β -secretase activity in brain : implications for Alzheimer ' s disease therapeutics. Hum Mol Genet 10:1317–1324.

Roche KW, O'Brien RJ, Mammen a L, Bernhardt J, Huganir RL (1996) Characterization of multiple phosphorylation sites on the AMPA receptor GluR1 subunit. Neuron 16:1179–1188.

Rockland KS, Pandya DN (1979) Laminar Origins and Terminations of Cortical Connections of the Occipital Lobe in the Rhesus Monkey. Brain Res 179:3–20.

Röder B, Rösler F, Neville HJ (2001) Auditory memory in congenitally blind adults: a behavioral-electrophysiological investigation. Brain Res Cogn Brain Res 11:289–303.

Roder B, Teder-Salejarvi W, Sterr A, Rosler F, Hillyard SA, Neville HJ (1999) Improved auditory spatial tuning in blind humans. Nature 400:162–166.

Roe AW, Pallas SL, Hahm J, Sur M (1990) A Map of Visual Space Induced in Primary Auditory Cortex. Science (80-) 250:818–820.

Romanski LM, LeDoux JE (1993) Organization of rodent auditory cortex: anterograde transport of PHA-L from MGv to temporal neocortex. Cereb cortex 3:499–514.

Rose JE, Woolsey CN (1949) The Relations of Thalamic Connections, Cellular Structure and Evocable Electrical Activity in the Auditory Region of the Cat. J Comp Physiol 91:441–466.

Rothschild G, Nelken I, Mizrahi A (2010) Functional organization and population dynamics in the mouse primary auditory cortex. Nat Neurosci 13:353–360.

Rouger J, Lagleyre S, Fraysse B, Deneve S, Deguine O, Barone P (2007) Evidence that cochlear-implanted deaf patients are better multisensory integrators. Proc Natl Acad Sci U S A 104:7295–7300.

Rudy B, Fishell G, Lee S, Hjerling-Leffler J (2010) Three groups of interneurons account for nearly 100% of neocortical GABAergic neurons. Dev Neurobiol 71:45–61 Available at: http://www.pubmedcentral.nih.gov/articlerender.fcgi?artid=3556905&tool=pmcentrez&rendertype=abstract [Accessed March 21, 2014].

Rutherford LC, Nelson SB, Turrigiano GG (1998) BDNF has opposite effects on the quantal amplitude of pyramidal neuron and interneuron excitatory synapses. Neuron 21:521–530.

Sadato N, Pascual-Leone A, Grafman J, Deiber MP, Ibañez V, Hallett M (1998) Neural networks for Braille reading by the blind. Brain 121 (Pt 7:1213–1229.

Sadato N, Pascual-Leone A, Grafman J, Ibanez V, Deiber M-P, Dold G, Hallett M (1996) Activation of the primary visual cortex by Braille reading in blind subjects. Nature 380:526–528.

Sale A, Berardi N, Spolidoro M, Baroncelli L, Maffei L (2010) GABAergic inhibition in visual cortical plasticity. Front Cell Neurosci 4:10.

Sale A, Maya Vetencourt JF, Medini P, Cenni MC, Baroncelli L, De Pasquale R, Maffei L (2007) Environmental enrichment in adulthood promotes amblyopia recovery through a reduction of intracortical inhibition. Nat Neurosci 10:679–681.

Sanes DH, Bao S (2009) Tuning up the developing auditory CNS. Curr Opin Neurobiol 19:188–199.

Sawtell NB, Frenkel MY, Philpot BD, Nakazawa K, Tonegawa S, Bear MF (2003) NMDA receptor-dependent ocular dominance plasticity in adult visual cortex. Neuron 38:977–985.

Schreiner CE, Kanold PO, Lomber SG (2012) AUDITORY CORTICAL FUNCTION : INSIGHTS FROM CURRENT APPROACHES. Acoust Today:42–50.

Schreiner CE, Read HL, Sutter ML (2000) MODULAR ORGANIZATION OF FREQUENCY INTEGRATION IN PRIMARY AUDITORY CORTEX. Annu Rev Neurosci 23:501–529.

Senden M V. (1960) Space and Sight: The Perception of Space and Shape in the Congenitally Blind before and after Operation.

Seol GH, Ziburkus J, Huang S, Song L, Kim IT, Takamiya K, Huganir RL, Lee H, Kirkwood A (2007) Neuromodulators Control the Polarity of Spike-Timing-Dependent Synaptic Plasticity. Neuron 55:919–929.

Sharma J, Angelucci A, Sur M (2000) Induction of visual orientation modules in auditory cortex. Nature 404:841–847.

Shepherd JD, Bear MF (2011) New views of Arc, a master regulator of synaptic plasticity. Nat Neurosci 14:279–284.

Shepherd JD, Rumbaugh G, Wu J, Chowdhury S, Plath N, Kuhl D, Huganir RL, Worley PF (2006) Arc/Arg3.1 mediates homeostatic synaptic scaling of AMPA receptors. Neuron 52:475–484.

Sherman, S.M. KC (1986) Overview The control of retinogeniculate transmission in the mammalian lateral geniculate nucleus. Exp brain Res 63:1–20.

Silverman DHS, Small GW, Chang CY, Lu CS, Aburto MAK De, Czernin J, Rapoport SI, Alexander GE, Schapiro MB, Jagust WJ, Hoffman JM, Welsh-bohmer KA, Clark CM, Leon MJ De, Phelps ME, Page P (2001) Positron Emission Tomography in Evaluation of Dementia. JAMA 286:2120–2127.

Simons DJ, Carvell GE (1989) Thalamocortical response transformation in the rat vibrissa/barrel system. J Neurophysiol 61:311–330.

Singer W, Tretter F, Cynader M (1975) Organization of cat striate cortex: a correlation of receptive-field properties with afferent and efferent connections. J Neurophysiol 38:1080–1098.

Smith PH, Populin LC (2001) Fundamental differences between the thalamocortical recipient layers of the cat auditory and visual cortices. J Comp Neurol 436:508–519.

Smith PH, Uhlrich DJ, Manning K a, Banks MI (2012) Thalamocortical projections to rat auditory cortex from the ventral and dorsal divisions of the medial geniculate nucleus. J Comp Neurol 520:34–51.

Somers DC, Nelson SB, Sur M (1995) AN EMERGENT MODEL OF ORIENTATION SELECTIVITY IN CAT VISUAL CORTICAL SIMPLE CELLS. J Neurosci 15:5448–5465.

Sommer B, Kohler M, Sprengel F, Seeburg PH (1991) RNA Editing in Brain Controls of Ion Flow in Glutamate-Gated a Determinant Channels. Cell 67:11–19.

Staiger JF, Flagmeyer I, Schubert D, Zilles K, Kötter R, Luhmann HJ (2004) Functional diversity of layer IV spiny neurons in rat somatosensory cortex: quantitative morphology of electrophysiologically characterized and biocytin labeled cells. Cereb Cortex 14:690–701 Available at: http://www.ncbi.nlm.nih.gov/pubmed/15054049 [Accessed April 28, 2014].

Stellwagen D, Malenka RC (2006) Synaptic scaling mediated by glial TNF-alpha. Nature 440:1054–1059.

Steward O, Wallace CS, Lyford GL, Worley PF (1998) Synaptic activation causes the mRNA for the IEG Arc to localize selectively near activated postsynaptic sites on dendrites. Neuron 21:741–751.

Stickgold R, Hobson J a, Fosse R, Fosse M (2001) Sleep, learning, and dreams: off-line memory reprocessing. Science (80-) 294:1052–1057.

Stiebler I, Neulist R, Fichtel I, Ehret G (1997) The auditory cortex of the house mouse: left-right differences, tonotopic organization and quantitative analysis of frequency representation. J Comp Physiol A 181:559–571.

Stratford KJ, Tarczy-Hornoch K, Martin KAC, Bannister NJ, Jack JJB (1996) Excitatory synaptic inputs to spiny stellate cells in cat visual cortex. Lett to Nat 382:258–261.

Suga N, Zhang Y, Yan J (1997) Sharpening of frequency tuning by inhibition in the thalamic auditory nucleus of the mustached bat. J Neurophysiol 77:2098–2114.

Sun X, Zhao Y, Wolf ME (2005) Dopamine receptor stimulation modulates AMPA receptor synaptic insertion in prefrontal cortex neurons. J Neurosci 25:7342–7351.

Sur M, Garraghty PE, Roe A. (1986) Experimentally Induced Visual Projections into Auditory Thalamus and Cortex. Science (80-) 242:1437–1441.

Tagawa Y, Kanold PO, Majdan M, Shatz CJ (2005) Multiple periods of functional ocular dominance plasticity in mouse visual cortex. Nat Neurosci 8:380–388 Available at: http://www.ncbi.nlm.nih.gov/pubmed/15723060 [Accessed April 29, 2014].

Tan a YY, Atencio C a, Polley DB, Merzenich MM, Schreiner CE (2007) Unbalanced synaptic inhibition can create intensity-tuned auditory cortex neurons. Neuroscience 146:449–462.

Tan AYY, Brown BD, Scholl B, Mohanty D, Priebe NJ (2012) Orientation Selectivity of Synaptic Input to Neurons in Mouse and Cat Primary Visual Cortex. J Neurosci 31:12339–12350.

Tan, Andrew Y YZhang LI, Merzenich MM, Schreiner CE (2004) Tone-evoked excitatory and inhibitory synaptic conductances of primary auditory cortex neurons. J Neurophysiol 92:630–643.

Thomson AM (2010) Neocortical layer 6, a review. Front Neuroanat 4:13.

Tononi G, Cirelli C (2003) Sleep and synaptic homeostasis: a hypothesis. Brain Res Bull 62:143–150.

Tononi G, Cirelli C (2006) Sleep function and synaptic homeostasis. Sleep Med Rev 10:49–62 Available at: http://www.ncbi.nlm.nih.gov/pubmed/16376591 [Accessed April 29, 2014].

Traynelis SF, Wollmuth LP, Mcbain CJ, Menniti FS, Vance KM, Ogden KK, Hansen KB, Yuan H, Myers SJ, Dingledine R (2010) Glutamate Receptor Ion Channels : Structure , Regulation , and Function. Pharmacol Rev 62:405–496.

Troyer TW, Krukowski a E, Priebe NJ, Miller KD (1998) Contrast-invariant orientation tuning in cat visual cortex: thalamocortical input tuning and correlation-based intracortical connectivity. J Neurosci 18:5908–5927.

Tsumoto T, Suda K (1980) Three groups of cortico-geniculate neurons and their distribution in binocular and monocular segments of cat striate cortex. J Comp Neurol 193:223–236.

Turrigiano GG (2008) The self-tuning neuron: synaptic scaling of excitatory synapses. Cell 135:422–435.

Turrigiano GG, Leslie KR, Desai NS, Rutherford LC, Nelson SB (1998) Activity-dependent scaling of quantal amplitude in neocortical neurons. Nature 391:892–896.

Turrigiano GG, Nelson SB (2004) Homeostatic plasticity in the developing nervous system. Nat Rev Neurosci 5:97–107.

Venkitaramani D V, Chin J, Netzer WJ, Gouras GK, Malinow R, Lombroso PJ (2007) Beta-amyloid modulation of Synaptic Transmission and Plasticity. J Neurosci 27:11832–11837.

Villa a E, Rouiller EM, Simm GM, Zurita P, de Ribaupierre Y, de Ribaupierre F (1991) Corticofugal modulation of the information processing in the auditory thalamus of the cat. Exp brain Res 86:506–517.

Voss P, Gougoux F, Zatorre RJ, Lassonde M, Lepore F (2008) Differential occipital responses in early- and late-blind individuals during a sound-source discrimination task. Neuroimage 40:746–758.

Voss P, Lassonde M, Gougoux F, Fortin M, Guillemot J, Lepore F, Postale C (2004) Early- and Late-Onset Blind Individuals Show Supra-Normal Auditory Abilities in Far-Space. Current 14:1734–1738.

Vyazovskiy VV, Cirelli C, Pfister-Genskow M, Faraguna U, Tononi G (2008) Molecular and electrophysiological evidence for net synaptic potentiation in wake and depression in sleep. Nat Neurosci 11:200–208.

Wallace MN, Kitzes LM, Jones EG (1991) Intrinsic inter-and intralaminar connections and their relationship to the tonotopic map in cat primary auditory cortex. Exp brain Res 86:527–544.

Wang H, Megill A, He K, Kirkwood A, Lee H-K (2012) Consequences of inhibiting amyloid precursor protein processing enzymes on synaptic function and plasticity. Neural Plast 2012:272374.

Wang H, Song L, Laird F, Wong PC, Lee H-K (2008) BACE1 knock-outs display deficits in activity-dependent potentiation of synaptic transmission at mossy fiber to CA3 synapses in the hippocampus. J Neurosci 28:8677–8681.

Wang H, Song L, Lee A, Laird F, Wong PC, Lee H-K (2010) Mossy fiber long-term potentiation deficits in BACE1 knock-outs can be rescued by activation of alpha7 nicotinic acetylcholine receptors. J Neurosci 30:13808–13813.

Wang KH, Majewska A, Schummers J, Farley B, Hu C, Sur M, Tonegawa S (2006) In vivo two-photon imaging reveals a role of arc in enhancing orientation specificity in visual cortex. Cell 126:389–402.

Washburn MS, Numberger M, Zhang S, Dingledine R (1997) Differential dependence on GluR2 expression of three characteristic features of AMPA receptors. J Neurosci 17:9393–9406.

Wehr M, Zador AM (2003) Balanced inhibition underlies tuning and sharpens spike timing in auditory cortex. Nature 426:442–446.

Whitt JL, Petrus E, Lee H-K (2013) Experience-dependent homeostatic synaptic plasticity in neocortex. Neuropharmacology 78:45–54.

Wiesel TN, Hubel DH (1965a) EXTENT OF RECOVERY FROM THE EFFECTS VISUAL DEPRIVATION IN KITTENS. J Physiol 28:1060–1072.

Wiesel TN, Hubel DH (1965b) Comparison of the effects of unilateral and bilateral eye closure on cortical unit responses in kittens. J Neurophysiol 28:1029–1040.

William CM, Andermann ML, Goldey GJ, Roumis DK, Reid C, Shatz CJ, Albers MW, Frosch MP, Hyman BT, Service N, Hospital MG (2012) Synaptic plasticity defect following visual deprivation in Alzheimer disease model transgenic mice. J Neurosci 32:8004–8011.

Williams SR, Mitchell SJ (2008) Direct measurement of somatic voltage clamp errors in central neurons. Nat Neurosci 11:790–798.

Winer J a (1984) Anatomy of layer IV in cat primary auditory cortex (AI). J Comp Neurol 224:535–567.

Winer J a, Miller LM, Lee CC, Schreiner CE (2005) Auditory thalamocortical transformation: structure and function. Trends Neurosci 28:255–263.

Winer JA, Prieto JJ (2001) Layer V in cat primary auditory cortex (AI): cellular architecture and identification of projection neurons. J Comp Neurol 434:379–412.

Winkowski DE, Kanold PO (2013) Laminar transformation of frequency organization in auditory cortex. J Neurosci 33:1498–1508.

Woolsey T., Van der Loos H (1970) The Structural Organization ofLayer IV in the Somatosensory Region of S1 of Mouse Cerebral Cortex. Brain Res 17:205–242.

Wu GK, Arbuckle R, Liu B-H, Tao HW, Zhang LI (2008) Lateral sharpening of cortical frequency tuning by approximately balanced inhibition. Neuron 58:132–143.

Wu GK, Li P, Tao HW, Zhang LI (2006) Nonmonotonic synaptic excitation and imbalanced inhibition underlying cortical intensity tuning. Neuron 52:705–715.

Wu GK, Tao HW, Zhang LI (2011a) From elementary synaptic circuits to information processing in primary auditory cortex. Neurosci Biobehav Rev 35:2094–2104.

Wu J, Petralia RS, Kurushima H, Patel H, Jung M, Volk L, Chowdhury S, Shepherd JD, Dehoff M, Li Y, Kuhl D, Huganir RL, Price DL, Scannevin R, Troncoso JC, Wong PC, Worley PF (2011b) Arc/Arg3.1 regulates an endosomal pathway essential for activity-dependent β-amyloid generation. Cell 147:615–628.

Xu H, Jeong H-Y, Tremblay R, Rudy B (2013) Neocortical somatostatin-expressing GABAergic Interneurons Disinhibit the Thalamorecipient Layer 4. Neuron 77:155–167.

Xu J, Pang ZP, Shin O-H, Südhof TC (2009) Synaptotagmin-1 functions as a Ca2+ sensor for spontaneous release. Nat Neurosci 12:759–766.

Xu X, Callaway EM (2009) Laminar specificity of functional input to distinct types of inhibitory cortical neurons. J Neurosci 29:70–85 Available at: http://www.pubmedcentral.nih.gov/articlerender.fcgi?artid=2656387&tool=pmcentrez&rendertype=abstract [Accessed April 28, 2014].

Yang L-B, Lindholm K, Yan R, Citron M, Xia W, Yang X-L, Beach T, Sue L, Wong P, Price D, Li R, Shen Y (2003) Elevated β -secretase expression and enzymatic activity detected in sporadic Alzheimer disease. Nat Lett to Ed 9:3–4.

Yang W, Carrasquillo Y, Hooks BM, Nerbonne JM, Burkhalter A (2013) Distinct balance of excitation and inhibition in an interareal feedforward and feedback circuit of mouse visual cortex. J Neurosci 33:17373–17384 Available at: http://www.pubmedcentral.nih.gov/articlerender.fcgi?artid=3812505&tool=pmcentrez&rendertype=abstract [Accessed May 1, 2014].

Yoon B-J, Smith GB, Heynen AJ, Neve RL, Bear MF (2009) Essential role for a long-term depression mechanism in ocular dominance plasticity. Proc Natl Acad Sci U S A 106:9860–9865.

Yoshioka T, Blasdel GG, Levitt JB, Lund JS (1996) Relation between patterns of intrinsic lateral connectivity, ocular dominance, and cytochrome oxidase-reactive regions in macaque monkey striate cortex. Cereb Cortex 6:297–310.

Yousef T, Bonhoeffer T, Kim DS, Eysel UT, Tóth E, Kisvárday ZF (1999) Orientation topography of layer 4 lateral networks revealed by optical imaging in cat visual cortex (area 18). Eur J Neurosci 11:4291–4308.

Yu X, Chung S, Chen D-Y, Wang S, Dodd SJ, Walters JR, Isaac JTR, Koretsky AP (2012) Thalamocortical inputs show post-critical-period plasticity. Neuron 74:731–742.

Zarrinpar A, Callaway EM (2006) Local Connections to Specific Types of Layer 6 Neurons in the Rat Visual Cortex. J Neurophysiol 95:1751–1761.

Zhang LI, Tan AYY, Schreiner CE (2003) Topography and synaptic shaping of direction selectivity in primary auditory cortex. Nature 424:201–205.

Zhang LI, Zhou Y, Tao HW (2011) Perspectives on: information and coding in mammalian sensory physiology: inhibitory synaptic mechanisms underlying functional diversity in auditory cortex. J Gen Physiol 138:311–320.

Zheng J-J, Li S-J, Zhang X-D, Miao W-Y, Zhang D, Yao H, Yu X (2014) Oxytocin mediates early experience-dependent cross-modal plasticity in the sensory cortices. Nat Neurosci 17:391–399.

Zhou X, Merzenich MM (2007) Intensive training in adults refines A1 representations degraded in an early postnatal critical period. Proc Natl Acad Sci U S A 104:15935–15940.

Zhou X, Merzenich MM (2009) Developmentaly degraded cortical temporal processing restored by training. Nat Neurosci 12:26–28.

Zhou Y, Liu B, Wu GK, Kim Y-J, Xiao Z, Tao HW, Zhang LI (2010) Preceding inhibition silences layer 6 neurons in auditory cortex. Neuron 65:706–717.

Appendix

Table 3.1. Layer 6 Neuronal Properties

Age (postnatal day)	Conditions	Rise Time (ms)	Decay Time Constant (τ, ms)	R_{in} (MΩ)	R_{ser} (MΩ)
16	NR *(n = 10)*	1.7 ± 0.08	3.9 ± 0.3	439 ± 70	22.6 ± 1.1
	2d-DE *(n = 10)*	1.4 ± 0.11	3.5 ± 0.4	487 ± 93	23.5 ± 0.6
	1d-LE *(n = 9)*	2.0 ± 0.06 #	4.8 ± 0.2 ¶	518 ± 72	23.8 ± 0.7
23	NR *(n = 10)*	1.8 ± 0.07	3.7 ± 0.3	362 ± 31	20.5 ± 0.9
	2d-DE *(n = 10)*	1.8 ± 0.02	4.5 ± 0.3 *	395 ± 80	21.9 ± 1.3
28	NR *(n = 12)*	1.6 ± 0.07	3.5 ± 0.2	405 ± 62	24.1 ± 0.5
	7d-DE *(n = 14)*	1.7 ± 0.07	4.2 ± 0.3 §	394 ± 58	22.7 ± 0.9
	1d-LE *(n = 13)*	1.7 ± 0.08	3.1 ± 0.2	264 ± 47	23.7 ± 0.4

Age, at recording; R_{in}, Input resistance; R_{ser}, Series resistance.

Statistics: t-test, *: $p < 0.05$; One-way ANOVA, #: $p < 0.002$ (Fisher's PLSD posthoc test: $p < 0.03$ between NR and 1d-LE, $p < 0.001$ between 2d-DE and 1d-LE), ¶: $p < 0.03$ (Fisher's PLSD posthoc test: $p < 0.01$ between 2d-DE and 1d-LE), §: $p < 0.02$ (Fisher's PLSD posthoc test: $p < 0.01$ between 7d-DE and 1d-LE).

Table 4.1. Comparison of thalamocortical Sr^{2+}-mEPSC parameters.

Area	Conditions	Paradigm	Amplitude (pA)	Frequency (Hz)	Rise Time (ms)	Decay τ (ms)	Series R (MΩ)	Input R (MΩ)	RMS Noise
A1	PreLED	NR	10.0 ± 0.46	2.8 ± 0.25	1.9 ± 0.06	2.5 ± 0.28	19.1 ± 1.2	238 ± 41	1.4 ± 0.06
		7d-DE	11.6 ± 1.27	2.9 ± 0.25	1.9 ± 0.04	2.6 ± 0.25	22.4 ± 0.8	175 ± 20	1.4 ± 0.07
		7d-LE	10.1 ± 0.45	4.0 ± 0.42	1.7 ± 0.06	2.9 ± 0.20	19.4 ± 1.0	182 ± 18	1.6 ± 0.05
	PostLED	NR	10.2 ± 0.40	3.5 ± 0.29	1.8 ± 0.06	2.2 ± 0.14	19.1 ± 1.2	238 ± 41	1.4 ± 0.05
		7d-DE	14.6 ± 1.3*	5.0 ± 0.31	1.8 ± 0.05	2.7 ± 0.20	22.4 ± 0.8	175 ± 20	1.4 ± 0.07
		7d-LE	10.9 ± 0.56	6.3 ± 0.76	1.7 ± 0.04	2.8 ± 0.22	19.4 ± 1.0	182 ± 18	1.6 ± 0.05
	Calculated TC-mEPSCs	NR (n = 14)	12.8 ± 1.3	–	–	–	–	–	–
		7d-DE (n = 12)	25.7 ± 4.4*	–	–	–	–	–	–
		7d-LE (n = 14)	13.7 ± 1.4	–	–	–	–	–	–
V1	PreLED	NR	11.4 ± 0.52	3.6 ± 0.37	1.7 ± 0.06	3.1 ± 0.20	18.9 ± 1.4	283 ± 52	1.6 ± 0.07
		7d-DE	10.5 ± 0.77	3.5 ± 0.23	1.8 ± 0.04	3.3 ± 0.17	19.0 ± 1.4	175 ± 24	1.4 ± 0.07
	PostLED	NR	11.6 ± 0.46	5.0 ± 0.44	1.7 ± 0.07	3.2 ± 0.19	18.9 ± 1.4	283 ± 52	1.6 ± 0.07
		7d-DE	11.7 ± 0.97	5.6 ± 0.43	1.8 ± 0.06	3.1 ± 0.18	19.0 ± 1.4	175 ± 24	1.4 ± 0.07
	Calculated TC-mEPSCs	NR (n = 11)	11.3 ± 0.93	–	–	–	–	–	–
		7d-DE (n = 12)	13.4 ± 1.43	–	–	–	–	–	–

*Denotes statistically significant difference from corresponding NR; $P < 0.05$ for one-factor ANOVA followed by Fisher's PLSD post-hoc test.

Table 4.2. Comparison of L4 mEPSC parameters.

Area	Age	Paradigm	n	Amplitude (pA)	Frequency (Hz)	Rise Time (ms)	Decay τ (ms)	Series R (MΩ)	Input R (MΩ)	RMS Noise
A1	P28	NR	15	10.9 ± 0.67	3.0 ± 0.44	1.8 ± 0.05	3.1 ± 0.12	18.5 ± 1.3	161 ± 10	1.7 ± 0.04
		7d-DE	19	13.4 ± 0.70*	3.7 ± 0.34	1.7 ± 0.03	3.1 ± 0.1	19.2 ± 2	224 ± 21	1.7 ± 0.04
		7d-LE	15	10.7 ± 0.50	2.5 ± 0.25	1.8 ± 0.03	3.1 ± 0.1	20.0 ± 0.7	193 ± 20	1.6 ± 0.05
	P90	NR	17	10.7 ± 0.41	2.8 ± 0.24	1.8 ± 0.03	3.1 ± 0.1	21.1 ± 0.9	174 ± 13	1.7 ± 0.03
		7d-DE	13	12.9 ± 0.75*	1.5 ± 0.17	1.9 ± 0.04	3.2 ± 0.1	21.7 ± 0.6	200 ± 19	1.6 ± 0.04
		7d-LE	14	10.8 ± 0.40	2.4 ± 0.26	1.8 ± 0.03	3.1 ± 0.1	21.6 ± 0.7	234 ± 27	1.6 ± 0.04
	CBA P90	NR	12	10.2 ± 0.49	5.0 ± 0.35	1.6 ± 0.05	2.8 ± 0.1	18.6 ± 0.8	160 ± 18	1.7 ± 0.06
		7d-DE	16	11.7 ± 0.32*	5.1 ± 0.41	1.6 ± 0.02	2.8 ± 0.1	22.3 ± 0.8	197 ± 21	1.7 ± 0.4
V1	P90	NR	15	9.4 ± 0.43	2.1 ± 0.24	1.8 ± 0.04	3.3 ± 0.1	19.0 ± 0.9	208 ± 19	1.6 ± 0.05
		7d-DE	13	10.2 ± 0.56	1.6 ± 0.24	1.8 ± 0.03	3.4 ± 0.1	19.2 ± 1	184 ± 20	1.6 ± 0.04

*Denotes statistically significant difference from corresponding NR; $P < 0.05$ for one-factor ANOVA followed by Fisher's PLSD post-hoc test.

Table 5.1: mEPSC and mIPSC parameters in A1 and V1

Area	Layer	Group	n	Amplitude (pA)	Frequency (Hz)	Rise Time (ms)	Decay τ (ms)	Series R (MΩ)	Input R (MΩ)	RMS Noise
A1	m-EPSC L2/3	NR	11	12.7 ± 0.6	3.4 ± 0.5	1.6 ± 0.04	2.9 ± 0.2	23 ± 0.7	274 ± 44	1.6 ± 0.07
		DE	10	10.3 ±0.7*	4.3 ± 0.6	1.7 ± 0.04	3.2 ± 0.1	22 ± 1.2	237 ± 46	1.7 ± 0.04
		LE	13	13.1 ± 1.0	3.4 ± 0.4	1.7 ± 0.04	2.9 ± 0.1	21 ± 1.0	229 ± 42	1.8 ± 0.03
	mIPSC L2/3	NR	16	37.5 ± 1.9	7.1 ± 0.8	1.6 ± 0.1	6.4 ± 0.5	20 ± 1	215 ± 19	2.6 ± 0.1
		DE	11	41.1 ± 3.3	12.6±1.9*	1.7 ± 0.1	5.9 ± 0.5	19 ± 1.1	189 ± 15	2.5 ± 0.1
	mIPSC L4	NR	16	49.7 ± 2.9	9.2 ± 0.9	1.2 ± 0.1	6.8 ± 0.5	20 ± 0.7	287 ± 34	2.6 ± 0.1
		DE	11	54.1 ± 4.1	8.1 ± 1.5	1.4 ± 0.1	7.2 ± 0.8	19 ± 1.3	312 ± 56	2.4 ± 0.2
V1	m-EPSC L2/3	NR	14	10.3 ± 0.3	3.4 ± 0.5	1.7 ± 0.05	3.3 ± 0.2	21.5 ± 0.8	225 ± 31	1.7 ± 0.04
		DE	11	11.3 ±0.2*	2.6 ± 0.4	1.7 ± 0.03	3.3 ± 0.1	22.5 ± 0.8	188 ± 24	1.6 ± 0.04
		LE	10	9.8 ± 0.4	3.2 ± 0.4	1.5 ± 0.09	2.5 ± 0.1	21.5 ± 0.9	254 ± 43	1.6 ± 0.07

*Denotes statistically significant difference from corresponding NR; $P < 0.05$ for one-factor ANOVA followed by Fisher's PLSD post-hoc test for three group measurements, student's T-test for two group measurements. n = number of cells, 2-3 slices per animal, 4-6 animals per group. Maximum of 3 cells per animal were used, maximum of 2 cells per slice.

Table 5.2: Sr^{2+} evoked mEPSCs in A1

Conditions	Paradigm	Amplitude (pA)	Frequency (Hz)	Rise Time (ms)	Decay τ (ms)	Series R (MΩ)	Input R (MΩ)	RMS Noise
L4 -> L2/3 PreLED	NR	11.6 ± 0.7	4.7 ± 0.3	1.6 ± 0.1	3.0 ± 0.1	22 ± 0.4	184 ± 29	1.6 ± 0.1
	DE	11.6 ± 0.8	4.8 ± 0.6	1.7 ± 0.1	3.1 ± 0.2	21 ± 0.8	242 ± 20	1.6 ± 0.1
L4 -> L2/3 PostLED	NR	10.8 ± 0.5	9.6 ± 0.8	1.6 ± 0.1	2.9 ± 0.1	22 ± 0.4	184 ± 29	1.6 ± 0.1
	DE	12.9 ± 1.0	9.2 ± 1.2	1.6 ± 0.1	3.2 ± 0.2	21 ± 0.8	242 ± 20	1.6 ± 0.1
Calculated A1 FF-mEPSCs	NR (n = 9)	**10.0 ± 0.5**	–	–	–	–	–	–
	DE (n = 10)	**14.2 ± 1.4***	–	–	–	–	–	–
L2/3 -> L2/3 PreLED	NR	11.6 ± 1.2	3.5 ± 0.6	1.7 ± 0.1	3.5 ± 0.3	18 ± 1.6	229 ± 55	1.7 ± 0.1
	DE	10.9 ± 0.6	3.6 ± 0.2	1.5 ± 0.1	3.3 ± 0.4	20 ± 1.3	278 ± 55	1.6 ± 0.1
L2/3 -> L2/3 Post LED	NR	12.7 ± 1.0	8.9 ± 1.2	1.6 ± 0.1	3.5 ± 0.3	18 ± 1.6	229 ± 55	1.7 ± 0.1
	DE	10.5 ± 0.4	11.3 ± 0.9	1.5 ± 0.1	3.3 ± 0.4	20 ± 1.3	278 ± 55	1.6 ± 0.1
Calculated A1 L2/3 lateral	NR (n = 10)	**13.0 ± 1.1**	–	–	–	–	–	–
	DE (n =12)	**10.3 ± 0.5***	–	–	–	–	–	–
L4 -> L4 PreLED	NR	10.6 ± 0.4	4.5 ± 0.6	1.8 ± 0.1	3.8 ± 0.2	22 ± 0.5	202 ± 21	1.6 ± 0.1
	DE	10.8 ± 1.0	4.2 ± 0.5	1.6 ± 0.1	3.0 ± 0.3	19 ± 1.4	231 ± 31	1.4 ± 0.1
L4 -> L4 Post LED	NR	10.1 ± 0.5	9.4 ± 0.9	1.8 ± 0.1	3.6 ± 0.2	22 ± 0.5	202 ± 21	1.6 ± 0.1
	DE	15.1 ± 2.5	9.7 ± 1.2	1.6 ± 0.1	3.0 ± 0.3	19 ± 1.4	231 ± 31	1.4 ± 0.1
Calculated A1 L4 lateral	NR (n = 12)	**9.9 ± 0.7**	–	–	–	–	–	–
	DE (n = 9)	**18.0 ± 3.1***	–	–	–	–	–	–

Table 5.3: Sr^{2+} evoked mEPSCs in V1

Conditions	Paradigm	Amplitude (pA)	Frequency (Hz)	Rise Time (ms)	Decay τ (ms)	Series R (MΩ)	Input R (MΩ)	RMS Noise
L4 -> L2/3 PreLED	NR	14.6 ± 1.3	5.3 ± 0.4	1.7 ± 0.1	3.6 ± 0.2	18 ± 1.4	188 ± 14	1.7 ± 0.1
	DE	12.7 ± 1.0	5.3 ± 0.5	1.5 ± 0.1	3.3 ± 0.2	18 ± 1.3	158 ± 16	1.7 ± 0.1
L4 -> L2/3 PostLED	NR	14.4 ± 0.7	9.6 ± 0.7	1.6 ± 0.1	3.5 ± 0.2	18 ± 1.4	188 ± 14	1.7 ± 0.1
	DE	13.9 ± 0.9	10.9 ± 0.6	1.5 ± 0.1	3.1 ± 0.2	18 ± 1.3	158 ± 16	1.7 ± 0.1
Calculated V1 FF-mEPSCs	NR (n = 14)	**13.9 ± 1.6**	–	–	–	–	–	–
	DE (n = 10)	**14.5 ± 1.1**	–	–	–	–	–	–
L2/3 -> L2/3 PreLED	NR	11.2 ± 0.9	3.9 ± 0.5	1.6 ± 0.1	3.2 ± 0.2	20 ± 1.3	282 ± 52	1.7 ± 0.1
	DE	12.6 ± 0.9	4.4 ± 0.5	1.6 ± 0.1	3.3 ± 0.2	20 ± 1.4	188 ± 15	1.7 ± 0.1
L2/3 -> L2/3 Post LED	NR	11.7 ± 0.6	10.1 ± 1.2	1.7 ± 0.1	3.2 ± 0.2	20 ± 1.3	282 ± 52	1.7 ± 0.1
	DE	16.4 ± 1.6	13.4 ± 2	1.6 ± 0.1	3.3 ± 0.2	20 ± 1.4	188 ± 15	1.7 ± 0.1
Calculated V1 L2/3 lateral	NR (n = 10)	**11.7 ± 0.4**	–	–	–	–	–	–
	DE (n = 10)	**18.2 ± 2.0***	–	–	–	–	–	–

Table 5.4: Sr^{2+} evoked mIPSCs in from PV^{+} neurons A1

Conditions	Paradigm	Amplitude (pA)	Frequency (Hz)	Rise Time (ms)	Decay τ (ms)	Series R (MΩ)	Input R (MΩ)	RMS Noise
PV -> L2/3 PreLED	NR	51.9 ± 3.7	5.9 ± 0.7	1.0 ± 0.1	6.7 ± 0.8	18 ± 1.2	198 ± 21	2.9 ± 0.1
	DE	40.4 ± 4.5	5.6 ± 0.6	1.0 ± 0.1	5.9 ± 0.6	19 ± 0.9	248 ± 48	2.8 ± 0.2
PV -> L2/3 PostLED	NR	53.7 ± 3.4	12.7 ± 2.4	0.9 ± 0.1	6.0 ± 0.8	18 ± 1.2	198 ± 21	2.9 ± 0.1
	DE	43.0 ± 4.8	9.5 ± 0.7	1.0 ± 0.1	5.6 ± 0.5	19 ± 0.9	248 ± 48	2.8 ± 0.2
Calculated PV to L2/3 mIPSCs	NR (n = 10)	**55.6 ± 4.9**	–	–	–	–	–	–
	DE (n = 10)	**46.1 ± 6.8**	–	–	–	–	–	–
PV -> L4 PreLED	NR	49.8 ± 6.7	5.8 ± 0.8	1.2 ± 0.1	8.1 ± 1.0	22 ± 0.9	254 ± 32	2.8 ± .3
	DE	44.8 ± 3.5	6.5 ± 0.6	1.2 ± 0.1	8.2 ± 0.6	20 ± 1.2	250 ± 36	2.7 ± 0.1
PV -> L4 Post LED	NR	48.3 ± 6.4	12.2 ± 1.3	1.2 ± 0.1	7.5 ± 0.9	22 ± 0.9	254 ± 32	2.8 ± .3
	DE	53.2 ± 3.3	10.6 ± 0.7	1.1 ± 0.1	8.0 ± 0.6	20 ± 1.2	250 ± 36	2.7 ± 0.1
Calculated PV to L4	NR (n = 11)	**46.5 ± 6.6**	–	–	–	–	–	–
	DE (n = 11)	**65.5 ± 4.7***	–	–	–	–	–	–

Table 6.2: Comparison of mEPSC and neuronal parameters across between BACE1 WT and KO mice

Genotype	Group	Frequency (Hz)	Amplitude (pA)	Rise time (ms)	Decay (τ, ms)	Series R (MΩ)	Input R (MΩ)	RMS Noise
WT	NR *(n = 3;9)*	3.3 ± 0.6	9.2 ± 0.4	1.7 ± 0.05	3.1 ± 0.1	23.2 ± 0.6	179 ± 18	1.6 ± 0.05
	DE *(n= 4;10)*	2.4 ± 0.2	13.9 ± 1.0*	1.6 ± 0.04	3.1 ± 0.1	20.8 ± 1.3	346 ± 83	1.7 ± 0.04
	LE *(n = 3;9)*	3.2 ± 0.4	10.4 ± 0.3	1.6 ± 0.09	3.0 ± 0.2	21.2 ± 1.6	238 ± 39	1.6 ± 0.06
KO	NR *(n = 3;9)*	2.5 ± 0.3	11.7 ± 0.6	1.5 ± 0.09	3.1 ± 0.2	22.9 ± 0.7	192 ± 36	1.6 ± 0.06
	DE *(n= 4;11)*	3.3 ± 0.5	12.8 ± 0.8	1.6 ± 0.06	3.2 ± 0.1	21.2 ± 0.9	220 ± 26	1.6 ± 0.06
	LE *(n = 3;9)*	4.5 ± 0.8	12.4 ± 1.1	1.6 ± 0.05	3.0 ± 0.3	19.4 ± 1.2	244 ± 39	1.6 ± 0.09

Values represents mean ± standard error of each measured parameter from neurons (*n*, number of neurons). R, resistance. *: Indicates statistically significant difference from other groups within a genotype as determined by $p < 0.05$ from one-factor ANOVA followed by Newman-Keuls Multiple Comparison *post hoc* test. *n* = number of animals; number of cells, 1-2 cells recorded per slice, 2-3 slices per mouse.

Table 6.3: Comparison of confocal analysis of Arc protein expression

Area	Condition	n (slices: mice)	Cell Density	ARC % of NR	Overlap Coefficient
V1	NR	30:3	22.3 ± 0.25	100 ± 13.0%	0.03 ± 0.01
	2d-DE	30:3	22.2 ± 0.25	119 ± 5.9%	0.07 ± 0.02
	7d-DE	30:3	22.2 ± 0.23	127 ± 6.5 %	0.04 ± 0.02
A1	NR	30:3	22.4 ± 0.21	100 ± 3.5%	0.1 ± 0.03
	2d-DE	30:3	22.4 ± 0.45	108 ± 5.1%	0.1 ± 0.03
	7d-DE	30:3	22.1 ± 0.22	207 ± 5.5%*	0.09 ± 0.03
S1	NR	30:3	21.3 ± 0.38	100 ± 3.0%	0.1 ± 0.03
	2d-DE	30:3	21.5 ± 0.15	89 ± 2.8%	0.1 ± 0.03
	7d-DE	30:3	21.4 ± 0.36	153 ± 5.3%*	0.12 ± 0.04

ANOVA tests performed between NR, DE and LE groups of each cortical area. * denotes a significant p value ($p < 0.05$) within cortical area, between experimental paradigm.

Cell Density indicates number of cells per 10,000 μm^2

Overlap Coefficient refers to Pearson's overlap coefficient of ARC to NeuN coexpression.

Table 6.4: Comparison of mEPSC and neuronal parameters across between Arc WT and KO mice

WT	Freq (Hz)	Amp (pA)	Rise (ms)	Decay (tau)	Series R (MΩ)	Input R(MΩ)	RMS Noise
NR (n =10)	3.7 ± 0.6	12.6 ± 0.7	1.8 ± 0.1	3.1 ± 0.2	22 ± 1.2	153 ± 15	1.7 ± 0.04
DE (n = 9)	2.1 ± 0.4	10.1 ± 0.7*	2.0 ± 0.03	3.2 ± 0.2	21 ± 1.2	204 ± 29	1.7 ± 0.1
LE (n = 10)	2.2 ± 0.7	13.1 ± 1.0	1.9 ± 0.1	3.3 ± 0.1	20 ± 1.3	193 ± 35	1.6 ± 0.07
KO							
NR (n = 13)	2.8 ± 0.3	12.1 ± 0.6	1.7 ± 0.04	3.2 ± 0.1	20 ± 1.0	203 ± 20	1.6 ± 0.05
DE (n = 14)	3.1 ± 0.3	11.1 ± 0.9	1.7 ± 0.1	3.1 ± 0.2	21 ± 1.2	163 ± 17	1.7 ± 0.04
LE (n = 13)	3.1 ± 0.6	12.2 ± 0.9	1.7 ± 0.1	3.1 ± 0.1	18 ± 0.8	164 ± 11	1.6 ± 0.07

ANOVA tests performed between NR, DE and LE groups of each genotype. * denotes a significant p value ($p < 0.05$) within genotype, between experimental paradigm.

Curriculum Vitae

Emily Rose Petrus

Education

Expected Graduation May 2014	Ph.D. Neuroscience, Johns Hopkins University, Baltimore MD
2007-2008	M.S. University of Bucharest, Romania
2003-2007	B.S. Biology, Wagner College, Staten Island, NY

Grants & Honors

2012- 2014: NIH Ruth L. Kirchstein National Research Service Award Predoctoral Fellow
2010: NSF Graduate Research Fellowship Program Honorable Mention
2007: Baccalaureate Speaker for Biological Sciences Department at Wagner College
2006: Inducted into TriBeta (Biological Honors Society)
2003-2007: Wagner College Dean's List

Publications

Petrus E, Lee, HK. BACE1 is necessary for experience-dependent homeostatic synaptic plasticity in visual cortex. (2014). Neural Plasticity, *In Press.*

Petrus E*, Isaiah A*, Jones AP, Wang H, Lee HK, Kanold PO. Cross-modal plasticity of thalamocortical transmission leads to enhanced information processing in the auditory cortex. (2014) Neuron 81, 664-73. PMID 24507.

Whitt JL*, **Petrus E***, Lee HK. Experience-dependent homeostatic synaptic plasticity in neocortex. (2013). Neuropharmacology. 02(16) Epub. PMID 23466332.

He K, **Petrus E**, Gammon N, Lee HK. Distinct sensory requirements for unimodal and cross-modal homeostatic synaptic plasticity. (2012). J. Neuroscience. 32(25):8469-74. PMID: 22723686

Petrus E*, Anguh TT*, Pho H, Lee A, Gammon, N, Lee HK. Developmental switch in the polarity of experience-dependent synaptic changes in layer 6 of mouse visual cortex. (2011). J. Neurophysiology. 106(5):2499 – 505. PMID: 21813745.

Dimitrov E; **Petrus E**; Usdin T. Tuberoinfundibular peptide of 39 resides (TIP29) signaling modulates acute and tonic nociception. (2010). Experimental Neurology. 226(1): 68-83. PMID 20696160.

Abstracts Presented

Petrus E. & Lee HK Potentiation of Feed-forward Inputs in Auditory Cortex After Visual Deprivation

2014 Society for Neuroscience, San Diego, CA

Petrus E. & Lee HK. Cross-modal plasticity of excitatory synapses in auditory cortex following visual deprivation

2013 Cold Spring Harbor Laboratory Meeting on Synapses: From Molecules to Circuits and Behavior

2013 Winter Brain Conference, Breckenridge, CO.

2012 Society for Neuroscience, New Orleans, LA.

Petrus E. & Lee H-K. Visual deprivation produces lamina-specific changes in excitatory synaptic transmission of mouse primary auditory cortex.

2011 Society for Neuroscience, Washington DC

Petrus E., Jacobs, C., Lee, H.K. Visual Deprivation drives cross-modal synaptic plasticity in primary auditory cortex.

2010 Society for Neuroscience San Diego, CA.

2010 University of Maryland Bioscience Day

Petrus E., Dimitrov E., Usdin, T. PTH2 Receptor Blockade Inhibits Pain Response Behavior.

2009 NIMH Retreat & NIH Post-baccalaureate Poster day, Bethesda, MD

Research Experience

2011-present **Graduate Student: Johns Hopkins University, Baltimore MD**

Visual deprivation induced cross modal plasticity in visual and auditory cortices

Principle Investigator - Dr. Hey-Kyoung Lee

2009-2011 **Graduate Student: University of Maryland, College Park, MD**

Transferred to Johns Hopkins University with Dr. Hey-Kyoung Lee

2008-2009 **Post-Baccalaureate Research Fellow: National Institute of Mental Health, Bethesda MD**

Function and location of TIP39 and PTH2R in mouse brain

Principle Investigator - Dr. Ted Usdin

2007-2008 **Research Assistant: University of Bucharest, Romania**

Traumatic injury of adult rat DRGs and its affect on neuropathic pain

Principle Investigator - Dr. Maria-Luiza Flonta

2006-2007 **Research Assistant: Institute for Basic Research, Staten Island, NY**

Glial cell response to beta-amyloid by exposure to toll-like receptor agonists

Principle Investigator - Dr. Daryl Spinner

2005-2007 **Laboratory Assistant: Wagner College, Staten Island, NY**
Regenerative capabilities of zebrafish nervous tissue
Principle Investigator - Dr. Zoltan Fulop

Teaching Experience

2009-present **Mentor: Johns Hopkins University & University of Maryland**
Lead undergraduate students in hypothesis driven research projects

2010 **Teaching Assistant: University of Maryland**
Co-taught Principles of Human Physiology for undergraduates

2009-2010 **Biology Supplemental Instructor: University of Maryland**
Taught biology to undergraduate University of Maryland students from disadvantaged backgrounds for the Academic Achievement Programs

2007-2008 **English as a Second Language**: **Bucharest, Romania**
Private tutoring and classroom instruction for adults and children

Community Involvement

2013 Johns Hopkins VEX Robotics Tournament volunteer: Baltimore, MD
2013 Community Science Day volunteer: Baltimore, MD
2013 Member of Association for Women in Science
2008-2010 Volunteer science fair judge for local high schools in Arlington, VA and Hyattsville, MD.
2008-present Member of Society for Neuroscience

Computer Skills & Languages

Microsoft Office (Word, Excel, PowerPoint), Volocity, Prism, Adobe Photoshop, Image-Pro Plus
Conversational in Romanian & Spanish